2011

[Pi]-[Pi] molecular interactions between intercalating antitumor agents and caffeine

Gabrielle Hill

π-π MOLECULAR INTERACTIONS BETWEEN INTERCALATING ANTITUMOR AGENTS AND CAFFEINE

by

GABRIELLE HILL

A THESIS

Submitted in partial fulfillment of the requirements
for the degree of Master of Science
in
The Department of Chemistry
to
The School of Graduate Studies
of
The University of Alabama in Huntsville

HUNTSVILLE, ALABAMA
2011

In presenting this thesis in partial fulfillment of the requirements for a master's degree from The University of Alabama in Huntsville, I agree that the Library of this University shall make it freely available for inspection. I further agree that permission for extensive copying for scholarly purposes may be granted by my advisor or, in his/her absence, by the Chair of the Department or the Dean of the School of Graduate Studies. It is also understood that due recognition shall be given to me and to The University of Alabama in Huntsville in any scholarly use which may be made of any material in this thesis.

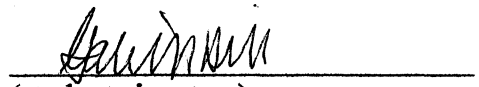

(student signature)

8.8.11

(date)

THESIS APPROVAL FORM

Submitted by Gabrielle M. Hill in partial fulfillment of the requirements for the degree of Master of Science in Chemistry and accepted on behalf of the Faculty of the School of Graduate Studies by the thesis committee.

We the undersigned members of the Graduate Faculty of the University of Alabama in Huntsville, certify that we have advised and/or supervised the candidate on the work described in this thesis. We further certify that we have reviewed the thesis manuscript and approve it in partial fulfillment of the requirements of the degree of Master of Science in Chemistry.

6-30-11 Committee Chair
(Date)

6/30/11

Department Chair

6/30/11 College Dean

8/8/11 Graduate Dean

ABSTRACT
The School of Graduate Studies
The University of Alabama in Huntsville

Degree Master of Science College/Dept. Science/Chemistry

Name of Candidate Gabrielle M. Hill

Title π-π Molecular Interactions between Intercalating Antitumor Agents and Caffeine

Many antitumor drugs function by intercalating into DNA and forming π-π molecular complexes. The drugs can also form these bonds with other planar aromatic structures such as the xanthine alkaloid caffeine, which may block the drug from intercalating into the DNA, thereby lowering the toxicity of the drug to the cancer cells. The IC_{50} values of several known DNA intercalators were determined by testing for cytotoxicity on MCF-7 breast cancer cells both in the presence and absence of caffeine to test for attenuation in cytotoxicity of each drug. Computational molecular modeling studies involving several intercalating antitumor drugs with caffeine were also performed using the density functional theory and the recently developed M06 functional to discover the most probable configuration of the two interacting molecules determined by their interaction energies.

Abstract Approval: Committee Chair

Department Chair

Graduate Dean Rhonda Kay Deede 8/8/11

ACKNOWLEDGMENTS

I would like to offer a special thank you to Dr. William Setzer for extending this graduate degree opportunity to me. This body of work could not have been possible without his unending support, advice and extreme patience. I would also like to extend my appreciation to my other committee members, Dr. Bernhard Vogler and Dr. Debra Moriarity, who made themselves readily available for help and advice, and to Dr. Moriarity especially who allowed me to work independently in her laboratory.

I must also thank those who provided their support either directly or indirectly. Thank you to Brenda Wright who taught me everything I needed to know about growing cancer cells. Thanks also to my UAH friends Mary Setzer, Victor Ogungbe, Rebecca Crouch, Tameka Walker, Mary Mays and Caitlin Deskins for their guidance and endless "question answering," both in the laboratory and out of the laboratory.

Also, this graduate opportunity could not have come at a more opportune time, and this I must acknowledge as God's perfect timing. Also a big thank you to my sweet husband Joseph, who has shown me unending patience and moral support throughout this whole process. Without his patience and support, this accomplishment could not have been possible.

TABLE OF CONTENTS

LIST OF FIGURES

LIST OF TABLES

CHAPTER ONE

INTRODUCTION

1.1 Cancer and Chemotherapy

Cancer is a disease that is characterized by groups of cells that exhibit uncontrolled growth and differentiation, leading to metastasis and in some cases, tumor formation. There are many types of cancers, of which the leading types are lung, breast, and colon. One in four deaths in the United States is due to cancer (American Cancer Society, 2010), and roughly 13% of the worlds deaths in 2007 were attributed to some kind of cancer (Shewach, 2009).

Chemotherapy refers to the treatment of cancer by a chemical or drug used either by itself or in combination with another drug. Many of these drugs are isolated from natural products and can then be replicated synthetically in order to more easily market them. There are many different types of chemotherapy drugs and each type attacks the cancer in different ways, including inhibiting cellular topoisomerases, cyclin-dependent kinases, and preventing new blood vessel formation (angiogenesis) around a tumor (Shewach, 2009). Some of these drugs inhibit cancer cells from dividing and replicating by intercalating directly into the helix of the DNA.

1.2 Intercalation

Intercalation is a specific interaction between certain types of molecules with DNA. This interaction is a reversible binding that mainly occurs between planar aromatic molecules and the double helix of a DNA molecule. The planar geometry of the

molecule allows it to, in a sense, lodge itself between parallel DNA base pairs (Rozmus, 2005).

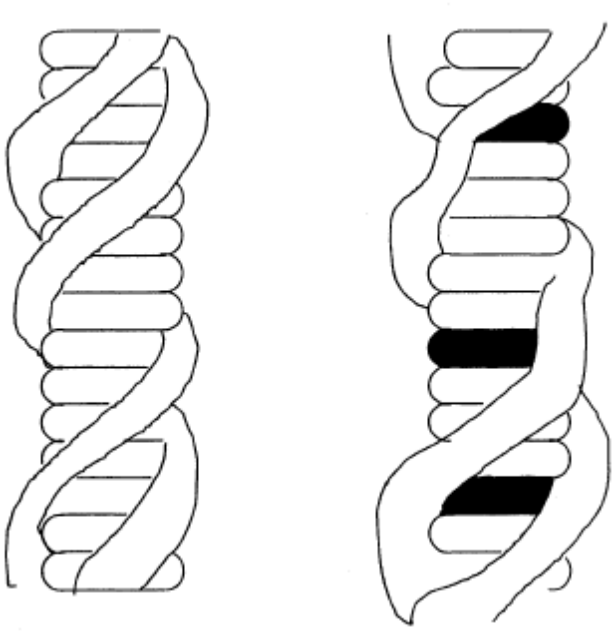

Figure 1.1 Intercalation Model

The molecule in question must also be of appropriate size to fit between the DNA base pairs, which are also planar, cyclic structures. The structure on the right in Figure 1.1 illustrates the intercalation model, with the drug shown as a dark band that has fitted itself into the DNA helix. Upon intercalation, the presence of the molecule physically inhibits replication of the DNA, ultimately leading to cell death (Burghardt, et al., 2009). The process of intercalation is thought to happen by the molecule inserting itself between two base pairs, with the helix partially unwinding at this site which decreases the natural 36˚ of rotation to less from the base pair closest to the intercalator to its neighboring base pair. The strand of DNA is actually lengthened by around 3.4 Å which is the width of a general intercalator, the length of which can be detected by

sedimentation methods (Brana, et al., 2001). Several cancer drugs currently on the market function by intercalation.

1.3 Intercalating cancer drugs

1.3.1 Daunorubicin and Doxorubicin

Many cancer drugs, including the anthracycline antibiotics daunorubicin and doxorubicin, function by intercalation. The anthracyclines possess a planar anthraquinone ring structure which allows for the intercalation and have been shown to be drawn to B-DNA sites that are G-C rich (Brana, et al., 2001). Daunorubicin was first isolated from the bacteria *Streptomyces peucetius*, and is most prevalently used for the treatment of lymphomas and leukemias, though it does pose toxicity to cardiac tissue.

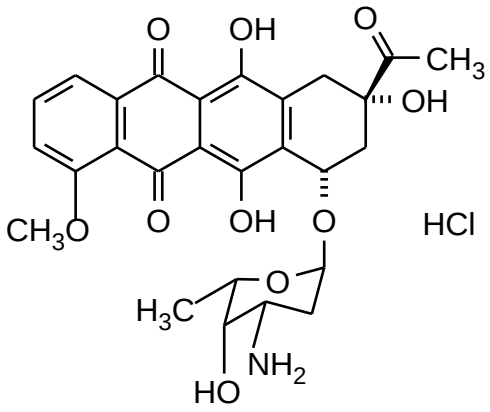

Figure 1.2 Daunorubicin

The structure of daunorubicin is shown in Figure 1.2, illustrating its planar ring structure that allows it to effectively intercalate into DNA. In an effort to lessen its toxicity to normal body cells and to more specifically target cancer cells, the daunorubicin molecule was slightly altered to include a hydroxyl group. The altered molecule was named doxorubicin, and is currently used against a variety of malignant tumors including lymphomas, breast, ovarian and thyroid.

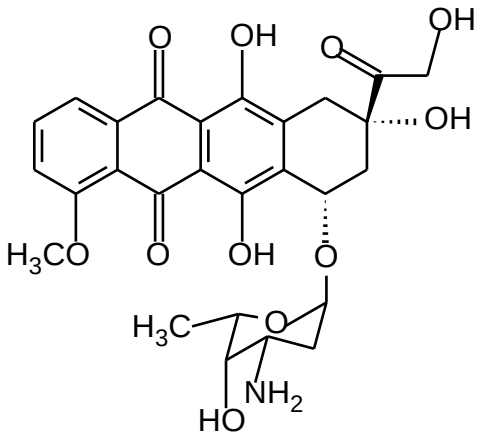

Figure 1.3 Doxorubicin

Figure 1.3 illustrates the structure of doxorubicin. Doxorubicin is currently in use for the afore-mentioned cancers, but the toxicities associated with anthracycline antibiotics, such as cardiotoxicity, still exist even with the group substitution (Trnkova, et al., 2009).

Doxorubicin actually binds to B-DNA in the same manner as does daunorubicin. When both daunorubicin and doxorubicin intercalate with DNA, they form complexes with the enzyme topoisomerase II by covalently binding it (Nitiss, 2009). Topoisomerase II is an enzyme whose function is to nick both strands of double-stranded DNA in order to relieve supercoiling associated with transcription and replication. These anthracycline/topoisomerase II complexes themselves cause lesions on the DNA and also attach to certain proteins that further inhibit both transcription and replication (Nitiss, 2009).

1.3.2 Camptothecin

Camptothecin is an anticancer drug isolated from the Chinese tree *Camptotheca acuminata* (Ying, et al., 2007). It showed remarkable cytotoxicity toward cancer cells but also showed toxicity toward normal cells as well as causing leucopenia and diarrhea

(Dexheimer, et al., 2008). Two of its derivatives are currently used in the treatment of leukemia and various other types of cancers. Camptothecin and its derivatives are also DNA intercalators, but intercalate in a different area of the molecule than do the anthracyclines. Camptothecin inhibits the enzyme topoisomerase I, which is responsible for creating single-strand breaks in DNA by covalently binding to the molecule during transcription and replication which relieves the DNA molecule of supercoiling (Dexheimer, et al., 2008). Camptothecin inhibits this enzyme by intercalating between two bases, with preference for the bases thymine and guanine (Punchihewa, et al., 2009), one of which is bound to the topoisomerase I molecule (Nitiss, 2008). This stabilizes the topoisomerase I/DNA complex, preventing the enzyme from performing its nicking action, and thus is cytotoxic to the DNA and ultimately to the cell.

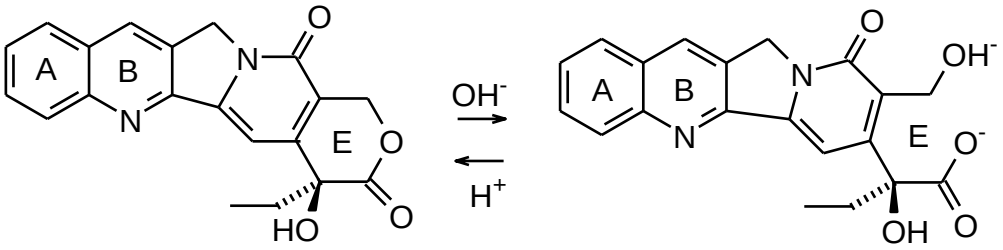

Figure 1.4 Camptothecin

Shown in Figure 1.4 is the structure of camptothecin, with labeled ring structures. The E ring is responsible for the cytotoxicity of the compound, and is inactive against topoisomerase I in its open E ring form, or its carboxylate state (Dexheimer, et al., 2008). The figure on the left shows the camptothecin structure in its active state, the lactone state. The camptothecin structure on the right illustrates the open E ring state, or the carboxylate state which is inactive. Some camptothecin derivatives have been created

with added or subtracted groups associated with the E ring in order to stabilize it. Diflomotecan is traditional camptothecin with an added methylene group to the E ring which prevents the ring from opening; also, a trial molecule has been formed by removal of the lactone group which also provides a very stable E ring.

1.4 Importance of Natural Products

Natural products have been used for hundreds of years for their medicinal and healing qualities and now play major roles in drug discovery for various diseases and ailments. Alkaloids are naturally occurring compounds found in many plants and other organisms as byproducts of metabolism or are purposefully produced specifically for protection of the species from predators. Compounds categorized as alkaloids are generally heterocyclic structures that contain nitrogen and have a basic (alkaline) pH. There are many different classifications of alkaloids, mostly based on common chemical structure and relation of activities on substrates. The isoquinolines make up an important category and contain, among others, protoberberine and benzophenanthridine alkaloids, both of which are isolated from plants. The active compounds found in these groups are cytotoxic and function in different ways and are effective for many different illnesses such as hypertension, inflammation, high cholesterol, respiratory problems, skin lesions, and different types of cancers. Both the protoberberine and benzophenanthridine alkaloids have a planar aromatic structure which allows them to partially or fully intercalate into the DNA molecule, depending on the individual alkaloid.

1.4.1 Protoberberines

Most protoberberines, although considered planar, do possess a slightly buckled structure, which affects its degree of intercalation into DNA. Protoberberine alkaloids are

found in several families of plants, including Papaveraceae, sometimes referred to as the poppy family, to which the genus *Bocconia* belongs. This is a large class of isoquinolines and includes berberine, which can be found among a variety of plant families including Berberidaceae, Ranunculaceae and Menispermaceae (Grycova, et al., 2007). It is most commonly isolated from the plant *Berberis vulgaris,* a plant found primarily in Asia that produces both flowers and fruit, and appears as a yellow extract. There are uses for almost all of the parts of this plant, however, the several alkaloids that it contains are, for the most part, found in the stems and roots (Imanshahidi, et al., 2008).

1.4.2 Berberine

Berberine effects cellular activity in a variety of different ways including effects on bacterial infection, hyperglycemia, hypertension, inflammation and several types of cancers (Imanshahidi, et al., 2008). Like most protoberberines, berberine, shown in Figure 1.5, has a slightly buckled structure.

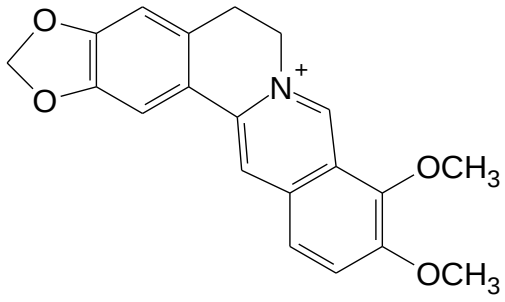

Figure 1.5 Berberine

Berberine's anti-tumor properties remain the most impressive, mostly because cancers are life-threatening and cannot be ignored, and because berberine expresses cytotoxic effects on several different types of tumors and with several different mechanisms of action. These methods of action range from berberine's COX-2 inhibition to a blockage of K^+ channels in cancer cells to intercalation into DNA. One study

reported that berberine induces apoptosis of a tongue carcinoma both *in vitro* and *in vivo*. This was studied by transplanting the tumor cells into the flanks of mice. Three groups of mice were treated with either berberine extract, nothing (control), or doxorubicin, a common cancer drug used to treat carcinomas and sarcomas. After 10 days of treatment, both the tumors treated with doxorubicin and berberine showed significant reduction in size as compared to the control group, with doxorubicin in a 4 mg/kg dosage and berberine with a 10 mg/kg dosage. The doxorubicin was reported as having a slight advantage in tumor reduction with 65% decrease in size compared with the berberine result of 52% reduction of the tumors. Although doxorubicin appeared to have a more toxic effect on the tumors, the effect that berberine had on the tumors is significant when taking into account that doxorubicin is a known chemotherapy drug (Ho, et al., 2009).

Berberine has been shown to have anti-tumor results on many different types of cancer cells by taking advantage of several different cellular processes. One study was conducted to investigate how berberine acts on U2OS (osteosarcoma) cells as compared with its effects on a normal osteoblast cell line (HCO) *in vitro*, with the focus on p53 dependency, general apoptotic activity, and DNA breakage (Liu, et al., 2009). U2OS and HCO cells were treated with berberine for 24 hours and flow cytometry was conducted to determine at what stage in the cell cycle the cells were arrested. Both the U2OS cells and the HCO cells treated with berberine were detained in the G1 phase, and raised suspicion that this result may be p53 related. p53, a cell cycle regulator which often functions as a tumor suppressor, is found in both the U2OS line and the HCO line. Another osteosarcoma cell line, Saos-2, which is known to not express p53, was also treated with berberine and did not show cell cycle arrest in the G1 phase, but did in the G2/M phase.

This indicates that berberine somehow upregulates the expression of p53 in cells that contain it, and is reliant upon it to a certain extent to stop cell growth in the G1 phase. This upregulation of p53 could be related to cyclins such as p21, which, when active, halts the progression of cells out of the G1 cycle. The response by p21 is usually triggered by some sort of DNA damage, which leads to other theories behind the activity of berberine. This theory is also supported by Saos-2 not appearing to be greatly inhibited by berberine in the G1 phase, and a number of these cells proceeded to the S and G2 phases (Liu, et al., 2009).

As mentioned above, the enhancement of p53 by p21 is usually related to some kind of DNA damage. When DNA damage occurs, the histone-related H2AX is phosphorylated on serine 139 by certain kinases to become γ–H2AX which investigates the double stranded DNA for breaks. High levels of γ–H2AX would therefore indicate DNA damage, in this case, resulting from the treatment of cells with berberine. The results of a Western blot showed a dose-dependent relationship on U2OS cells after 48 hours of treatment with berberine, with β actin, being ever-present in cells, as the control (Liu, et al., 2009). This study exposes another method of anti-tumor activity involving berberine in addition to its p53-dependent cell cycle arrest at the G1 phase. How berberine causes this DNA damage is thought to be related to its ability to intercalate with the DNA. The intercalation of berberine into DNA can be investigated by differential pulse voltammetry by using a current and a DNA marker on an double-stranded DNA treated electrode surface. The DNA marker was incubated in a berberine solution for 10, 60 and 120 minutes, at berberine concentrations of 1, 10, 50 and 100 μg/mL for each time. At the highest concentration of berberine and the longer

incubation times of 60 and 120 minutes, DNA damage was detected. The results that the highest concentrations of berberine caused the damage, points to an intercalative process, which has been found to be the binding mechanism found at higher ionic concentrations (Letasiova, et al., 2006). This information led the author to conclude that upon intercalation, berberine most likely caused double-stranded DNA breaks leading to the inference that berberine is a topoisomerase II inhibitor.

1.4.3 Palmatine

Another often-discussed protoberberine is palmatine. Palmatine is found most prevalently in the rhizome of the *Coptis chinensis* plant from the family Ranunculaceae. *C. chinensis* has been used for centuries in traditional Chinese medicine for various ailments including abdominal pain, peptic ulcers and inflammation (Lee, et al., 2010). Upon close observation, palmatine exists as a molecule both structurally and bioactively similar to berberine. It possesses many of the same qualities as berberine including anti-hypertension, anti-inflammation, anti-diarrheal and anti-tumor. It is also very effective in the treatment of liver disorders including jaundice and the promotion of liver metabolism by its active role in blocking K^+ ion channels (Bhadra, et al., 2010) and also for the protection of liver cells (Lee, et al., 2010).

Palmatine's anti-tumor activity is also similar to that of berberine and is thought to partially bind DNA in the same way due to its analogous buckled structure. Its antitumor activity is thought to rely on its inhibition of topoisomerase I and II and also its binding to DNA by intercalation. Not only does palmatine bind to DNA, it does so preferentially. One study shows that palmatine binds specifically to AT base pairs. Several experiments were done, but the most convincing evidence for this was a steady state fluorescence

titration experiment that contrasts the binding of palmatine on AT homopolymers, AT heteropolymers, GC homopolymers and GC heteropolymers (Bhadra, et al., 2007). The results of the fluorescence titrations show that the AT homopolymer showed a large curve leading to the conclusion that palmatine preferentially binds AT sequences (Sabisz, et al., 2008).

1.4.4 Coralyne

Coralyne, a synthetic protoberberine, possesses many of the same qualities that are seemingly general to other protoberberines. It too has anti-tumor capabilities, and works in much the same way as do berberine and palmatine. Structurally, it is related to the previously mentioned protoberberines, but it is totally planar instead of having a slightly buckled conformation as berberine does. It is thought that this planar attribute may allow it to intercalate fully with double-stranded DNA instead of only partially like berberine and palmatine (Bhadra, et al., 2008). Coralyne has been shown to exhibit higher topoisomerase inhibition than berberine and palmatine, most likely because of its complete intercalation with DNA. Recently, coralyne has been the topic of discussion within the matter of DNA photonicking. Photonicking refers to the damage of DNA caused by ultraviolet or infrared radiation. This damage is due to the ability of molecules in the protoberberine family to initiate release of different oxygen species when subjected to radiation. By combining coralyne and UVA treatments, both cells expressing and not expressing p53 would be affected by this type of treatment, as many types of cancer cells are mutated to no longer express p53. Different types of cancer cell lines, some p53 wild types and some p53 mutants were used in this study to test for cell death with coralyne and with coralyne plus UVA treatment (CUVA) (Patro, et al., 2010).

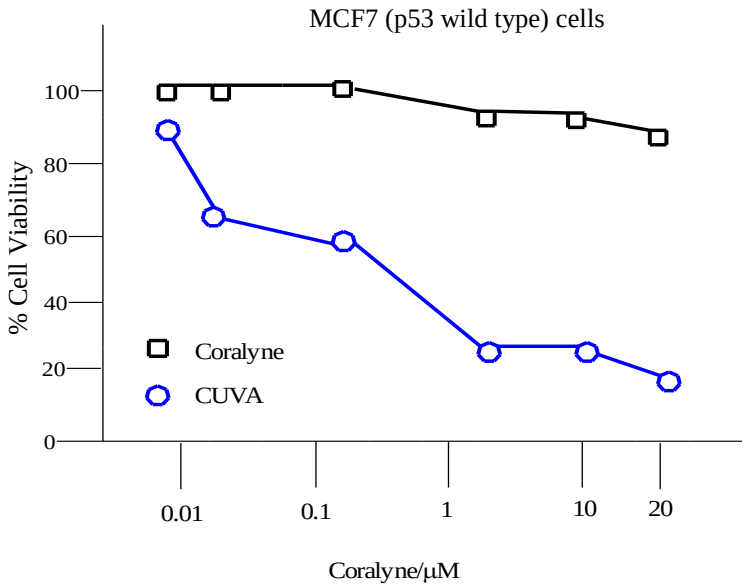

Figure 1.6: Effects of Coralyne and CUVA on MCF-7 Cells

Figure 1.6 shows the MCF-7 breast cancer cell line, which is a p53 wild type (Patro, et al., 2010). By itself, coralyne showed some cytotoxicity with increasing concentrations, but with the CUVA treatment, the graph dramatically shows the enhanced cytotoxicity with increasing concentrations. When tested on the breast cancer cell line MDA-MB-231, a p53 mutant, The results show close to the same results as with the p53 wild type cell line with enhanced cytotoxicity with the CUVA treatment. The results for both cell lines result from MTT assays (Patro, et al., 2010). These findings are significant in that they show the ability of coralyne and CUVA, both separate and together to successfully treat mutant p53 cancer cells. These experiments further show the potency and flexibility of the protoberberine coralyne in its various cancer-treating abilities, both individually and in combination with other treatments.

1.4.5 Protoberberine comparison study

The DNA binding capabilities of the afore-mentioned protoberberines are more easily understood when compared with each other. The intercalation of these compounds

with DNA are crucial for the understanding of their anti-tumor activities, and can be examined in several different ways, being better understood when the results of the studies are compiled. Recalling that berberine and palmatine exist as buckled structures, it has been proposed that these compounds do not fully intercalate with DNA. Coralyne, the synthetic protoberberine, exists as a planar molecule and is thought to fully intercalate with DNA (Giri, et al., 2008).

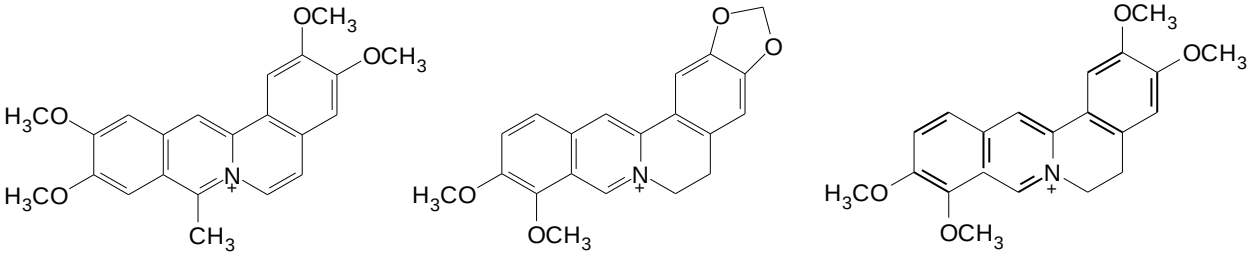

Coralyne Berberine Palmatine

Figure 1.7 The Structures of Coralyne, Berberine and Palmatine

Comparing the three structures in Figure 1.7 makes it easier to visualize the differences in saturation and functional groups attached at different points. Berberine, probably the most intensely studied protoberberine intercalator, is the focus of a study involving excitation-emission fluorescence spectroscopy (Xia, et al., 2007). This study deals with the issue of berberine intercalation of DNA and compares it with that of daunorubicin, an antibiotic that has previously been shown to possess anticancer qualities, and whose intercalative activity with DNA has been previously investigated. A three-way data array using the PARAFAC (a parallel factor analysis) model was obtained by using excitation-emission fluorescence spectroscopy information gathered by use of a fluorescence spectrophotometer. PARAFAC is a decomposition method of condensing a large amount of data. The three factors that make up the PARAFAC model

used in this study are I (excitation), J (emission) and K (constant at equilibrium). This method provides several profiles that fit berberine and DNA, daunorubicin and DNA and berberine, daunorubicin with DNA, based on concentration changes in the two drugs while the concentration of DNA is held constant. The daunorubicin profile appeared as expected from information in previous studies, showing increased fluorescence when combined with DNA than in the absence of DNA. Berberine showed similar fluorescence results compared with those of daunorubicin. A competitive mechanism was also suspected, and the excitation and emission data for the binding of both compounds to DNA was consistent with the theory that both compounds may intercalate into the same sites on the DNA. These data support the theory that berberine is indeed a DNA intercalator (Xia, et al., 2007).

The new research concept of protoberberines binding with RNA has emerged from the previous research conducted on DNA binding of these compounds. Many different proteins and transcription factors are overexpressed in cancer cells, and the molecule PAP (poly rA polymerase) has been identified as one such molecule (Giri, et al., 2008). Normally expressed in cells, PAP oversees the poly-A tail being attached to mRNAs shortly after they are transcribed. The poly-A tail is important because it protects the mRNA from premature degradation, but, with age, it normally gets shorter. Because protoberberines have the ability to intercalate with genetic material, they will most likely be able to bind to the poly-A tail of an mRNA, reducing or stopping mRNA function in cancer cells. The ability of berberine, palmatine and coralyne to induce self-structure with the poly-A tail was investigated by absorption titration which consists of measured amounts of the compounds being titrated into a system with the mRNA and the

absorbance being measured at the end of the titration. By observing the hypochromic and bathochromic effects of these compounds and translating the data by computer software programs, cooperative vs. non-cooperative binding could be observed. Cooperative binding is characterized by the binding of a ligand at one site being either helped or deterred by the binding of another ligand at a separate site; that is, the binding of one ligand is reliant upon the binding of another. Non-cooperative binding refers to the binding of a ligand that is not reliant upon the binding of another; that is, it binds independently. Cooperative binding was suspected as pointing to the ability of the compound tested to induce self-structure in the poly-A tail. Coralyne was determined to be cooperative as the data translated into a Scatchard plot that had a positive slope in comparison with both berberine and palmatine which did not. This is presumably due to the planar structure of coralyne compared with the buckled structure of the other two (Giri, et al., 2008). To further examine whether coralyne fully binds to the poly-A tail, circular dichroism melting experiments and optical melting profiles as determined by an absorption spectrophotometer, were performed. An mRNA poly-A tail was also profiled in this way so the compounds tested could be compared to this. A positive melting profile was observed for coralyne, but not for the other two compounds, probably due to its planar structure.

ITC studies were also conducted to investigate the binding affinity for the compounds. All three compounds were found to have high affinity to bind poly-A, but as determined above, berberine and palmatine cannot fully bind. Again, this is most likely due to their structural differences and only partial intercalation of the poly-A tail.

Nevertheless, this study sheds light on yet another avenue that can be explored for induced cancer cell death (Giri, et al., 2008).

The topoisomerases are enzymes that function to relieve supercoiling of DNA. A normal double-stranded DNA molecule has a coil of 10.4 nucleotide base pairs per turn; however, after processes such as replication or transcription, the DNA molecule supercoils in order to keep its strands in close proximity so that the strands cannot anneal with a neighboring molecule. When supercoiling occurs, the tension in the DNA molecule is released by topoisomerases. Topoisomerase I nicks one strand of the DNA molecule to allow it to relax, and topoisomerase II works in much the same way, but nicks both of the strands. After relieving the tension of the DNA molecule, the topoisomerases also function to help reanneal the DNA. Cancer drugs that target the topoisomerases inhibit their normal cell cycle activities such as replication and transcription because the DNA strands will not be cut and put back together properly (Maiti, et al., 2010). It is thought that the structure of the molecule of most protoberberine alkaloids accounts for the topoisomerase I inhibition. As most of the protoberberine alkaloids have a four-ring structure, the A and D rings appear to be most responsible for diminishing topoisomerase activity, as previous studies have shown that modification of one or both of these rings appears to alter topoisomerase activity. Although berberine and palmatine both show topoisomerase inhibition, coralyne shows the greatest inhibition.

1.4.6 Benzophenanthridines

Another important category of isoquinoline alkaloids are the benzophenanthridines which are mainly found in the family Papaveraceae, but can be

found in other families as well. Two of the main sources of benzophenanthridines are plants from the genera *Bocconia* (*Bocconia frutescens*) and *Sanguinaria* (*Sanguinaria canadensis*). *Sanguinaria canadensis*, commonly called bloodroot due to the reddish liquid that seeps from its rhizomes, has flowers with white petals and yellow stamens, and can be found in a variety of different places in North America (Graf, et al., 2007). Its healing qualities were first discovered by native Americans who used bloodroot for a wide range of ailments from cough suppressants to "cancers;" they also used the reddish fluid for dyes, and as recently as the early 1980s, bloodroot was used for its antimicrobial qualities (Graf, et al., 2007).

The genus *Bocconia* contains several species, the most studied of which is *Bocconia frutescens*. *B. frutescens,* also called plume poppy or parrotweed, is found mainly in tropical areas in places including Mexico, Costa Rica, and Hawaii. Traditionally, all parts of this plant including the leaves, stems and seeds, have been employed for various uses by indigenous peoples; these uses include treatment of respiratory infections, skin infections and gastrointestinal ailments (Arreola, et al., 2006). The seeds are large and are very hearty, as they can survive for long periods of time in the soil, not only due to their tough exterior, but also from the alkaloids they contain, as they are toxic to predators (Veldman, et al., 2007). This species contains two benzophenanthridines, sanguinarine and dihydrosanguinarine, which is a reduced form of sanguinarine, which may be present to reduce the toxicity in the plant tissues.

Currently, alkaloids isolated from *B. frutescens* are used to treat hypertension via the affecting of G-protein coupled receptors and the blocking of angiotensin receptors (George, et al., 2003 and Mackraj, et al., 2008). Certainly, though, their most closely

studied quality is that of anti-cancer by the affecting of several different cell pathways, structures and activities such as tight junction "tightening," loss of mitochondrial membrane potential, induction of apoptosis by over-production of oxygen species, p53 and non-p53 pathways and DNA intercalation.

1.4.7 Sanguinarine

Sanguinarine, a benzophenanthridine alkaloid that is found in *Bocconia frutescens* and *Sanguinaria canadensis*, exists as one of the most toxic alkaloids found in these plants. It has been reported as exhibiting qualities such as anti-hypertensive, antimicrobial, and anti-cancer (George, et al., 2003 and Chaturvedi, et al., 1997).

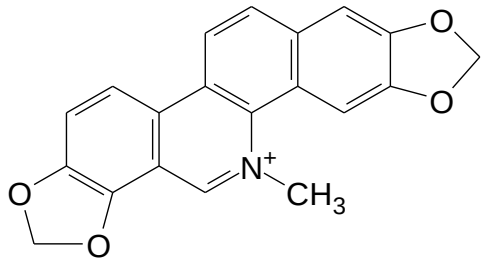

Figure 1.8 Sanguinarine

Figure 1.8 shows the planar aromatic structure of sanguinarine. Because of its planar structure, sanguinarine has been studied for the possibility of its intercalating properties. The theory of sanguinarine intercalation can be better established by examining different characteristics that are displayed by known intercalators upon binding with DNA including changes in enthalpy observed by isothermal titration calorimetry. This was performed by titrating 10 µL of 100 µM sanguinarine into double-stranded calf thymus DNA in four minute increments. The heat of reaction of the addition of sanguinarine into the DNA was measured and subtracted from the heat of reaction from the injection of sanguinarine into a buffer solution, so as to only measure

the correct heat of binding to the DNA. An algorithm was used to predict the K_a and ΔH which then allows for the solving of the Gibbs free energy equation, allowing for the determination of ΔG and ΔS. The enthalpy change was found to be -6.91 kcal/mol and the entropy 1.11 kcal/mol, alluding to an exothermic and enthalpically-driven process (Adhikari, et al., 2008). These numbers point to an intercalative binding scheme based on previous studies with planar intercalating molecules. Isothermal titration calorimetry was also used to address which DNA base pairs sanguinarine binds to the most easily. Two heteropolymers were used- poly(dG-dC)-poly(dG-dC) and poly(dA-dT)-poly (dA-dT) and two homopolymers-poly(dG)poly(dC) and poly(dA)poly(dT). The alternating poly(dG-dC)-poly(dG-dC) had the highest K_a value, followed by the poly (dA-dT)-poly(dA-dT), both of which had negative enthalpy values, which is consistent with intercalative binding. The homopolymer poly(dA)poly(dT) actually had a positive enthalpy which points to it not being the most favorable binding site. From the information presented in this study, sanguinarine does intercalate into DNA and has specificity for alternating G-C sequences followed closely by alternating A-T sequences (Adhikari, et al., 2008).

Another proposition about the anti-cancer tendencies of sanguinarine addresses the theory of oxidation causing DNA damage such as single and double-stranded breaks. Both single and double stranded breaks can be caused by environmental factors such as ultraviolet light, harmful chemicals and oxidation within the molecule, and most breaks can be repaired by different mechanisms within the cell. Single stranded breaks or nicks are the easiest to repair by either base or nucleotide excision repair. Double stranded breaks, however, pose a more difficult challenge, especially if these breaks leave the

DNA with blunt ends. One of the few methods in reattaching these broken strands exists in the action of specific proteins called KU proteins. These proteins bind to the ends of the broken strands and bind them together. However, these KU proteins do not have any specificity of knowledge of how these ends should go together, posing significant problems should there be more than one break. If sanguinarine does induce double stranded breaks by oxidation or otherwise into the DNA, it could be the mechanism or one of the mechanisms by which apoptosis is induced by sanguinarine. Another study was conducted involving three colon cancer cell lines with different p53 expression levels to elucidate whether involvement of the p53 mechanism has any effect on the sanguinarine interaction. All three of the cell lines were subjected to the same dosages of sanguinarine at the same periods of time, and all showed roughly the same results in reference to cell viability, eliminating the question of p53 involvement (Matkar, et al., 2009). Death was verified as the apoptosis pathway by observation of qualities specific to apoptosis such as membrane blebbing and nuclear cleavage. To determine DNA breaks and the extent thereof, single-cell gel electrophoresis assays were conducted. After treatment with sanguinarine, the colon cancer cells were placed in the gel in a neutral solution and an alkaline solution. Single stranded breaks occur in the alkaline solution and do so typically before double stranded breaks appear in the neutral solution. These "comet" assays allow visualization of a tail that resembles the tail of a comet only when double stranded breaks occur. The double stranded breaks take a longer time to appear than do the single stranded breaks. Because oxidation is under suspicion as the mechanism by which the breaks are being made, cells were treated with anti-oxidative compounds such as N-acetylcysteine before treatment with sanguinarine, and these

compounds were shown to stop the DNA breaks in all three cell lines. One of the most frequent types of oxidation is by that of the nucleoside deoxyguanosine, which is known to bind to the protein avidin. The binding of avidin was coupled with flow cytometry to show increased oxidation in cells treated with sanguinarine as compared to cells not treated, indicating that sanguinarine induces oxidation which causes DNA double stranded breaks (Matkar, et al., 2009).

In addition to intercalation and DNA breaks, sanguinarine also has been reported to improve tight junction integrity, allowing the cell to regain its polarity to be able to control the influx of foreign molecules into the cell, thus lessening the chance of metastasis (Choi, et al., 2009). It has also been shown that sanguinarine has the capability to activate caspases within the cell which help facilitate apoptosis (Jang, et al., 2009).

. 1.4.8 Dihydrosanguinarine

The cytotoxicity of sanguinarine against different cancer cell lines continues to be of interest. This alkaloid possesses different ways of destroying cancer cells. A metabolite of sanguinarine, dihydrosanguinarine is produced in the seeds of *B. frutescens*, and because of its slightly lower toxicity, questions have been raised as to whether this metabolite will kill cancer cells and be less toxic to healthy cells than sanguinarine (Vrba, et al., 2009). Toxicities of both alkaloids were tested against the human leukemia cell line HL-60, which intrinsically does not express p53, by MTT assay, and both were found to be cytotoxic with sanguinarine showing the most toxicity. Flow cytometry was used to determine at what point the cell cycle was disrupted by the alkaloids, and also to show any loss of membrane potential of the mitochondria. For both alkaloids, at certain

concentrations and periods of time, an increased number of sub-G1cells appeared and mitochondrial membrane potential was lowered, both signs of impending apoptosis. Figure 1.9 shows the percentage of cells with low mitochondrial membrane potential in response to increasing doses of sanguinarine at 4 and 24 hours (Vrba, et al., 2009).

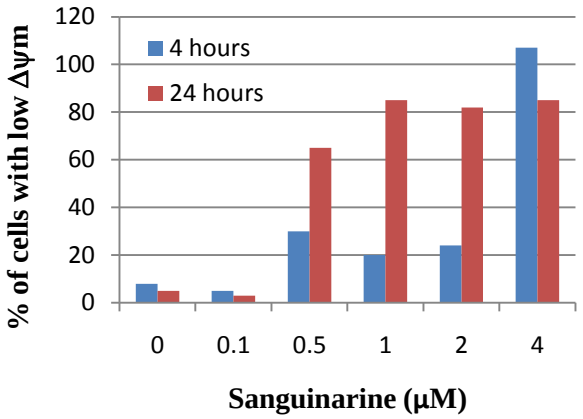

Figure 1.9: The Lowering of Mitochondrial Membrane Potential by Sanguinarine

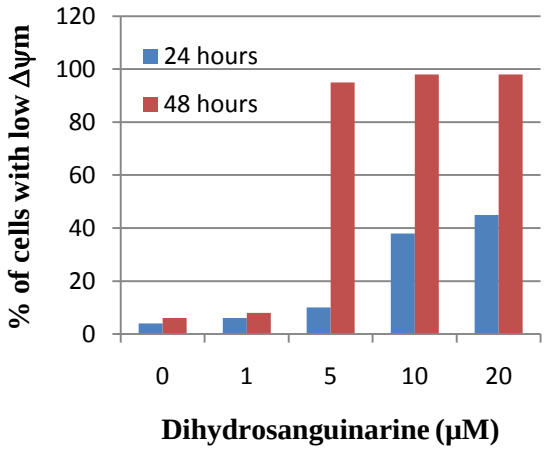

Figure 1.10: The Lowering of Mitochondrial Membrane Potential by Dihydrosanguinarine

Figure 1.10 shows the lowering of mitochondrial membrane potential by dihydrosanguinarine with increasing doses at 24 and 48 hours (Vrba, et al., 2009). Because HL-60 cells do not express p53, these alkaloids provide another way of cancer cell treatment, apparently through disruption of the mitochondrial membrane potential. Dihydrosanguinarine was determined to be less cytotoxic than sanguinarine, but still showed an impressive increase in cells that express low mitochondrial membrane potentials, although this result required higher doses and longer treatment times. Because plants break down sanguinarine into dihydrosanguinarine so that these alkaloids will not be toxic to the plant, this secondary alkaloid may not be toxic to healthy human cells.

1.4.9 Chelerythrine

Chelerythrine is another benzophenanthridine alkaloid, and, because of its planar aromatic structure, is thought to intercalate DNA just as the other isoquinoline alkaloids.

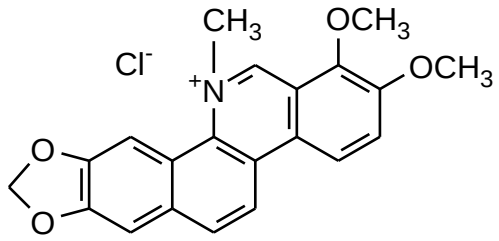

Figure 1.11: Chelerythrine

Figure 1.11 shows the structure of chelerythrine in its chloride form. This iminium form of the molecule was studied to examine the type of binding occurring upon interaction with DNA by absorption spectra, fluorescence measurements and temperature dependence (Su, et al., 2006). The absorption spectra of chelerythrine alone were observed at three peaks in the 300 nm to 500 nm range, and upon addition of calf thymus DNA, isobestic points were taken at 327 nm and 351 nm. These absorption spectra are concurrent with previous intercalation studies done with the isobestic points in this case

representing equilibrium between free and bound molecules. To further confirm the theory of intercalative binding between chelerythrine and DNA, fluorescence emission spectra were observed to shift up to 10 nm upon saturation of chelerythrine with calf thymus DNA. This increased fluorescence is characteristic of intercalative binding. A thermodynamic study was also done and the binding constant found, which allows for the enthalpy and entropy to be calculated from the Gibbs free energy equation. The enthalpy of the system has a much larger negative value at -33.7 kJ/mol (or -8.05 kcal/mol) than does the entropy at -2.9 kJ/mol (or -.693 kcal/mol) (Su, et al., 2006). This type of enthalpy-driven system is also characteristic of intercalative binding. The specific area of DNA to where chelerythrine binds is also an important aspect to understanding its intercalative binding. The DNA used in this particular binding study was poly(dG-dC)poly(dG-dC) and poly(dA-dT) poly(dA-dT) and other specifically designed DNA fragments (Bai, et al., 2006). To determine if chelerythrine possesses sequence specificity, the DNA was titrated into the alkaloid with increasing concentrations. A change in the fluorescence emission of chelerythrine was observed upon contact with the DNA, and the binding constant could then be determined as well as the enthalpy and entropy of the chelerythrine/DNA system. In every case, the chelerythrine showed definite specificity for non-alternating GC pairs.

1.4.10 Ellipticine

Ellipticine is an alkaloid in the 6*H*-pyridocarbazole family found in *Apocyanacea* species of plants and is very structurally similar to the previously-discussed alkaloids in that it has a planar aromatic structure (Saturnino, et al., 2003).

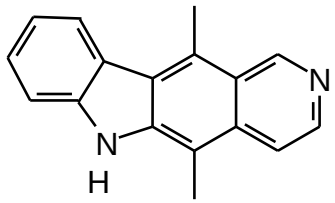

Figure 1.12: Ellipticine

Figure 1.12 shows the structure of ellipticine. Ellipticine is currently used as a chemotherapeutic drug against breast cancer and some leukemias. Ellipticine has previously been found to be cytotoxic to certain cancer cell lines by different methods including inhibition of topoisomerase II, DNA intercalation and DNA adduct formation (Poljakova, et al., 2007). Ellipticine is activated by certain cellular enzymes called cytochromes and peroxidases; upon activation, ellipticine forms covalent bonds with DNA, allowing for the buildup of DNA adducts in the cell (Poljakova, et al., 2007). Three cell lines have been shown to express buildup of these DNA adducts including both the HL-60 and the CCRF-CEM leukemia cell lines and the MCF-7 breast cancer cell line by ^{32}P- postlabeling assay.

The reported intercalative properties of ellipticine which leads to its topoisomerase II inhibition is thought to be due to an added dialklyaminoalkylamino side chain added to the first ring of the standard ellipticine molecule which forms an ellipticine analogue (Ferlin, et al., 2009). A crystallographic study was conducted to investigate the intercalative binding of ellipticine into a six base pair piece of double stranded DNA (Canals, et al., 2005).

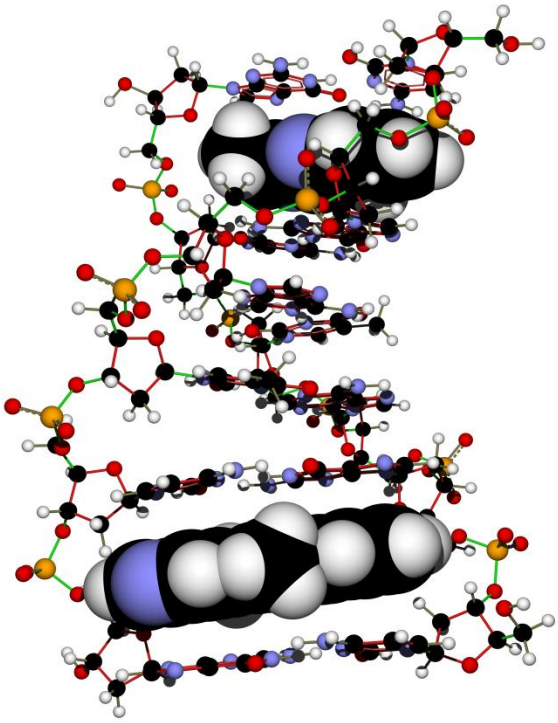

Figure 1.13: Ellipticine Intercalates into DNA

Figure 1.13 illustrates two ellipticine molecules intercalating into DNA. It was found that the ellipticine intercalates into the DNA between the G-C sites, as no ellipticine molecules were found in the A-T sites (Canals, et al., 2005). The nitrogen on the hexagonal ring of ellipticine appears to be facing outward toward the major groove of the DNA. The ellipticine does not appear to be hydrogen bonded to the DNA at all, but rather is held in place solely by π–π stacking interactions. This particular article makes note that the hydrogen bonding taking place between the G and C bases provide a nice fit for the planar structure of ellipticine.

1.4.11 Xanthines

Another family of alkaloids, the xanthines, is a more controversial group in regards to effects on the cell. Two of the alkaloids in this group, caffeine and theophylline, are considered stimulants and have been reported to have both positive and

negative effects on the body. Theophylline is actually a marketed drug used for the treatment of respiratory diseases as it is a bronchodilator. Caffeine is found in fruits and leaves and is ingested by millions of people on a daily basis in tea, coffee, cocoa and various other foods. Because of their wide-spread usage, both caffeine and theophylline have been the focus of many studies for their effects on the body. Caffeine has been shown to be toxic to some plants, and actually serves as a natural pesticide. It has also been linked to heart problems and addiction (Sabisz, et al., 2008). Conversely, caffeine acts as a vasodilator, and hence alleviates pain associated with migraines, and is also a known anti-oxidant as it protects DNA from damage by free radicals. The actual interaction between these xanthines and DNA is a controversial subject; it is not fully understood, but a common belief is that it intercalates with DNA much like the isoquinoline alkaloids.

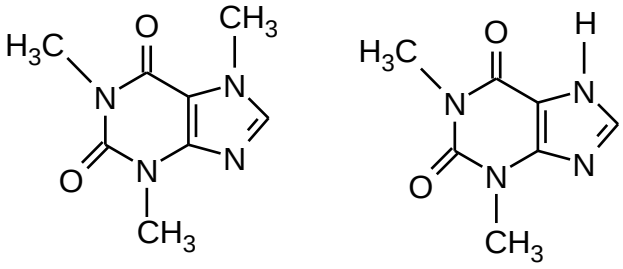

Figure 1.14: The Structures of Caffeine (left) and Theophylline (right)

Effects on the body by xanthine alkaloids, especially caffeine, remains a source for debate. Overuse of caffeine is associated with heart problems, addiction due to its stimulant qualities and reproductive problems. However, moderate use of caffeine is linked to prevention of some autoimmune diseases, diabetes, and it can act as an anti-oxidant (Sabisz, et al., 2008). The use of these alkaloids can be either positive or negative and depends on the situation and the health of the individual ingesting it.

1.5 π–π Molecular Interactions

Noncovalent interactions such as London dispersion forces, hydrogen bonding and π–π interactions between molecules are essential to the organization of systems, for the building of polymers, and for base stacking in genetic materials (Wheeler, et al., 2010). These π–π molecular interactions are perhaps the most misunderstood of the noncovalent interactions. π bonds are formed when two *p* orbitals of neighboring electron orbitals overlap each other. When two of these π bonds from separate molecules come into contact, the result can be termed as π–π molecular interactions. These interactions are noncovalent in nature and refer mostly to the bonding that occurs between two or more aromatic molecules. These π–π interactions are also referred to as "stacking" when involved in aromatic systems. The simplest example of stacking can be seen with a benzene dimer. The two benzene molecules can be arranged in a few different conformations. In order to determine the most energetically favorable orientation, and thus the most probable, *ab initio* quantum mechanics calculations were applied (Wheeler, et al., 2010).

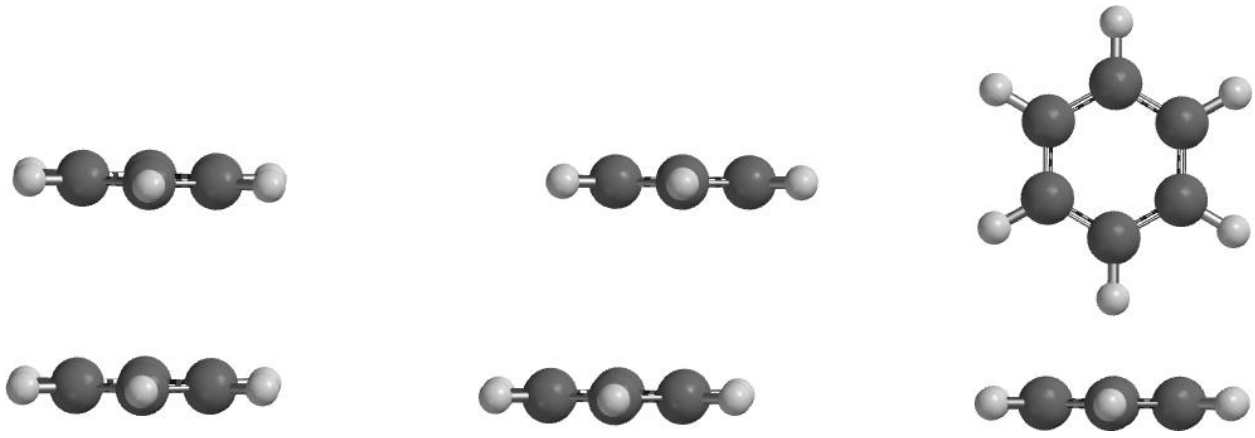

(a) (b) (c)

Figure 1.15: Three Possible States for π–π Interactions: (a) Sandwich, (b) Parallel Displaced and (c) T-shaped

The calculated *ab initio* energies resulted in the sandwich configuration being the least likely conformation with the highest energy of 3.7 kcal/mol, while both the parallel displaced and T-shaped conformations were favored at roughly the same energies of 2.7 kcal/mol (Wheeler, et al., 2010). The energies were calculated on the MP2 level using the aug-cc-pVQZ basis set which is considered to be a large basis set (Sinnokrot, et al., 2006). The benzene molecule is one of the simplest examples of stacking, but gives important insight into what actually happens during a π–π interaction rather than a theoretical proposition.

Noncovalent interactions are crucial to the function and stability of the DNA molecule. Hydrogen bonding occurs between the two bases from opposing strands forming a base pair (Swart, et al., 2007). Base "stacking", or π–π molecular interactions within each strand is essential in the formation of the helical shape of the DNA and for the stabilization of the molecule. As previously mentioned, these π–π molecular

interactions are difficult to fully calculate using *ab initio* and density functional theory methods due to a few reasons, the most imperative being the fact that these interactions depend on the size of the basis sets used, and dispersion forces arising from electrons from the different orbitals of the stacked molecule cannot be correctly predicted and accounted for (Swart, et al., 2007 and Dabkowska, et al., 2005). Careful approaches must be made with large, complicated molecules such as DNA, to accurately determine and assign correct orientations. Considerations must be taken into account as to where to place the compounds to be docked. The docking could depend upon reported DNA base specificities that some compounds possess and correct distances between the two molecules must also be determined.

1.5.1 *Ab initio* methods

Ab initio calculations refer to calculations based on quantum mechanics (QM) that are used to determine the wave function and energy of a structure. There are different types of QM calculations, the most popular being the Hartree-Fock method. Solving the Schrödinger equation for the whole molecule is the goal of these methods, but certain parameters are set and assumptions are made that make it impossible to solve the equation sufficiently for the whole molecule in question. The Hartree-Fock method assumes that all electrons within the same orbital do not have extra energies that are associated with their movement as they approach each other in their orbits. As the electrons move closer to one another, they will naturally repel each other due to their negative charges, a property referred to as correlation. To assume that all electrons have the same energy is false and must be dealt with. Basis sets are functions included in the calculation that in a sense generate the molecular orbitals of the molecule in question.

Every type of orbital present in the molecule must be represented in the basis set (*s*, *p*, *d*, *f*). By increasing the number of basis sets included in the Hartree-Fock calculation, some of the energy that is not taken into consideration can be accounted for. There are many types of basis sets that can be used in addition to the standard required basis set, such as the split-valence basis sets which allows the valence electron orbitals to be split unequally, allowing for adjustment to their current situation and placement. Another type of special basis set is the polarization set which essentially adds a higher level atomic orbital function to each atom. For instance, a *p*-type orbital would be added to hydrogen to supplement its 1*s* orbital, and a *d*-type orbital would be added to *p*-block elements. Another basis set type is the diffuse set, which helps more accurately depict the total energy of the molecule. This type accounts for electron energies in orbitals that are further from the nucleus by adding an *s*-type function to hydrogen atoms and an *sp*-type function to all other atoms.

Providing extra basis sets improves the accuracy of the calculation; however, the more basis sets that are added increases the amount of time that the calculation takes to conclude. In addition to extra basis sets, post-Hartree-Fock methods can be used to try to compensate for this electron correlation and to provide calculations for what is assumed to be closer to the true energy of the molecule. To do this, excited states must be added to the ground state calculation provided by the Hartree-Fock calculation. One of these methods is the Coupled Cluster method which involves the addition of wavefunctions which have multi-electron systems to the calculation. However, the most popular post-Hartree-Fock method is the Møller-Plesset perturbation method. This method involves calculating the electron correlation effects using a mathematical formula, and then adding

this calculation to the Hartree-Fock calculation, thereby "perturbing" it. This post-Hartree-Fock method provides a more accurate description of the total energy of the molecule by allowing for the electron correlation energy. However, the Møller-Plesset perturbation method followed by a post-Hartree-Fock calculation such as the coupled cluster calculation is mostly applicable to the estimation of energies of the π-bonding of molecules with fewer than 20 atoms as a calculation for anything larger than that would be extremely time consuming (Wong, et al., 2008).

1.5.2 Density Functional Theory

Quantum mechanics calculations, specifically the solving of the Schrodinger equation, are essential for finding the wave function of a molecule, which can then be used to find the electron density. Another method can be employed in sort of a backwards fashion, to determine the wave function from the electron density of a molecule. This method is the Density Functional Theory, which uses functionals of electron density to determine the wave function and the energy of the molecule. Determining the construct of the energy functionals is not an exact science and must be estimated using functionals currently developed and several different kinds of basis sets. These basis sets must be able to relate as much as possible, every force that an electron takes place in, such as its repulsive reaction to other nearby electrons and the attractive force that the electron feels from the nucleus. The density functional calculation includes at least three functionals which include potential energy, kinetic energy from non-interacting electrons and kinetic energy from electron correlations. The latter functional must be accounted for using exchange-correlation functionals which account for movement of electrons and their contact with other electrons. There are a few of these

functionals that are used to attempt to account for these electron correlations such as the local density approximation and the generalized gradient approximation. These exchange functionals can be used in combination with the potential energy functional which can be calculated. New exchange and correlation functionals continue to be developed to lessen the complications and failures of simpler ones of the past. Some of the most popular basis sets/exchange functionals are the BLYP, the B3LYP, the M0-5 and the M06-L (Zhao, et al., 2006). Zhao and Truhlar have provided the new M06 functional which is one of the most current functionals and one of the only functionals to be able to correctly assess the energy of a non-covalent π–π molecular interaction between two molecules while more accurately describing its dispersion forces. The M06 functional is a newer form of the M05 functional. It is considered to be a hybrid meta-generalized gradient approximation, meaning it includes both local DFT exchange energy and Hartree-Fock exchange. Because the functional allows for both of those exchanges, it provides a more accurate energy for the bonded molecules. Based on a mean unsigned error calculation which presents the deviation from previously-calculated energies, the M06 functional along with a couple of other hybrid functionals was reported to be one of the best for π–π stacking interactions because of its use of both DFT exchange and Hartree-Fock exchange. Functionals that only employ local DFT approximations have not been reliable for the calculation of π–π stacking interactions (Zhao and Truhlar 2008). In a study conducted by Dkhissi and Blossey, the MPWB1K exchange correlation functional is used to determine the binding energy of stacking and hydrogen bonding in nucleobases (Dkhissi, et al., 2007). In this study, the MPWB1K functional was first used to calculate the energy of two stacked pyrimidines with an anti-parallel displaced structure. Dkhissi

and Blossey cite their reasoning for this choice as this orientation had been studied in previous *ab initio* calculations and provided a rather high energy calculation. Another reason was the simplicity of the stacked molecules.

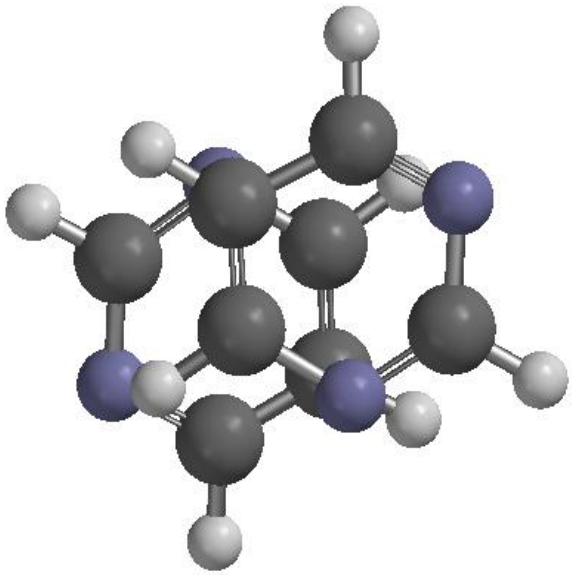

Figure 1.16 Stacked Pyrimidine Molecules

Figure 1.16 shows two pyrimidine molecules in the anti-parallel displaced orientation Previous studies found that calculated *ab initio* values are predicted to be 20% higher than the actual energy value, as calculated by methods such as the second order Møller-Plesset (MP2) perturbation method which was used in a previous study (Dkhissi, et al., 2007 and Hobza, et al., 2002). This method traditionally poses basis set superposition errors which, upon energy minimization, compresses energies from mixed basis sets with unmixed basis sets causing an inequality in the two. This can result in large errors in the energy calculations. The density functional MPWB1K calculation was performed using five different basis sets, and compared to the best estimates from two previous studies with energy values calculated from MP2 methods. As shown in Table 1.1, the vertical separation between the two pyrimidine monomers (Rcc) is varied between 3.39 Å and

3.41 Å, and the stacking energies (De) of the two pyrimidine monomers decreases as the basis sets become larger (Dkhissi, et al., 2007).

Table 1.1: Pyrimidine Dimer Calculated with Different Basis Sets
[Intermolecular distances (A˚) and binding energies (kcal/mol) of pyrimidine dimer calculated with MPWB1K at different basis sets]

	Rcc (Å)	De (kcal/mol)
6-31G**	**3.392**	**3.42**
6-31+G*	**3.401**	**3.02**
6-31+G**	**3.406**	**2.98**
6-31++G**	**3.410**	**3.05**
6-311++G(2d, 2p)	**3.415**	**2.74**
Best estimate[42,43]	**3.39**	**3.40**

(Dkhissi, et al., 2007)

As shown in Table 1.1, the energy from the largest basis set (6-311++G(2d, 2p) employed with the density functional MPWB1K is significantly lower than the best estimates from the energies calculated using an *ab initio* MP2 method in a previous study. This study suggests that using the density functional theory for the calculation of energies due to π–π molecular stacking interactions is superior in accuracy to *ab initio* methods. This serves as a good illustration of density functional theory providing the closest approximation to the total energy of a molecule by providing a way to closely estimate the energy that the interactions of electrons changes about a molecule using different basis sets.

Another study compares the MP2 method to two other methods. Because, as seen in the previous example, MP2 overestimates the dispersion forces in stacked molecules, the energy calculated by MP2 is too high. One, suggested by Grimme and Antony, is an MP2 based method but with adjustments made by separating and scaling the spin components which is an excellent revision for stacked molecules with large dispersion forces (Fiethen, et al., 2008). This revised MP2 method is referred to as SCS-MP2 for

spin component scaled. The other method used was the DFT-SAPT (symmetry-adapted intermolecular perturbation theory) which takes into account all electron densities present in order to more accurately account for the electrostatic, induction and dispersion energies (Fiethen, et al., 2008).

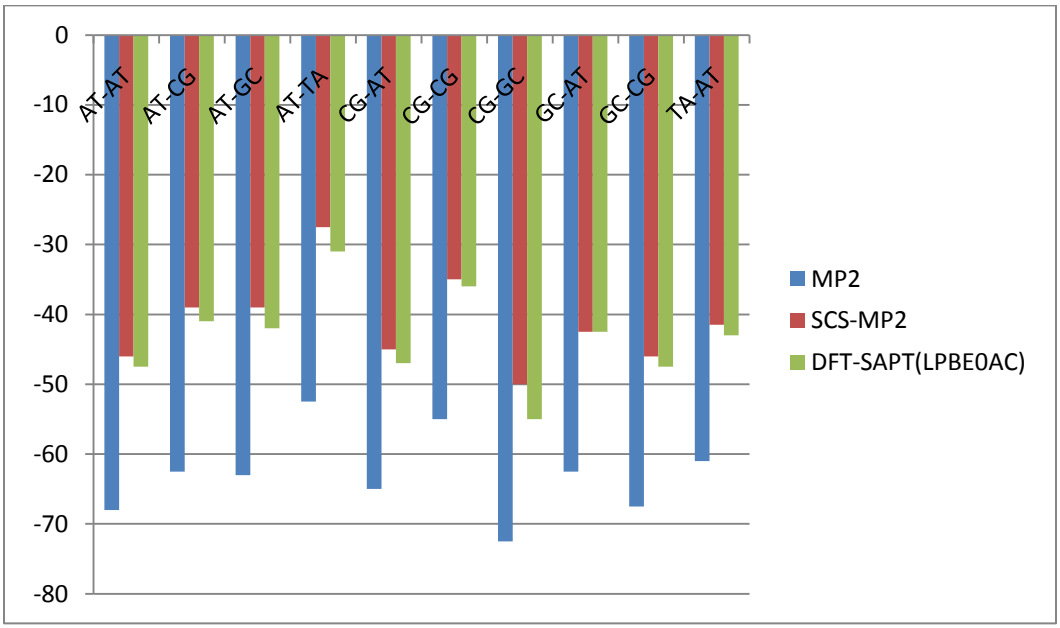

Figure 1.17: Three Methods to Calculate Base Stacking Energies

The MP2 method, the SCS-MP2 method, and the DFT-SAPT method were each employed to calculate the total stacking energy of every combination of nucleobase pairs. Each method was calculated using the same basis set, the aug-cc-pVTZ, which is a triple zeta post-Hartree-Fock set. The results from the study are displayed in Figure 1.17 (Fiethen, et al., 2008). As expected, the MP2 calculated energy is much greater in every case than either of the other two methods due to its overestimation of electron correlation. The SCS-MP2 and the DFT-SAPT calculations stayed very close for every case with the SCS-MP2 being slightly lower (Fiethen, et al., 2008). This study again highlights the improvements made upon total energy calculations for π–π interactions of molecules.

ab initio theory including density functional theory calculations has its place depending upon the information needed and the size of the molecules in question. Computer programs now make calculating stacking energies of two molecules relatively simple. There are several different types of molecular modeling programs that offer calculations with a variety of different basis sets. Most of these programs are relatively easy to use and first require that you construct the molecules to be stacked, then arrange them based on certain molecular characteristics. The modeling process can be set up based on several different π–π molecular interactions including, but not limited to, the direction of opposing dipoles, atomic charges, density potential maps, and orbital configurations.

1.6 Caffeine Interference with Antitumor Agents

As mentioned previously, caffeine is a xanthine alkaloid and has been studied for both its useful and detrimental effects on cells. It is a planar aromatic molecule which leads to the hypothesis that it could very easily form π–π complexes with other planar aromatic molecules such as nucleobases in DNA and several types of cancer drugs known to intercalate DNA based on their planar structure. It has been previously confirmed that caffeine and theophylline can protect DNA by affecting the binding of toxic compounds. However, in cancer patients undergoing chemotherapy, this property is not preferable. Several chemotherapy drugs such as doxorubicin and daunorubicin work by intercalating into DNA, and caffeine and theophylline have been shown to reduce the toxicity of these drugs (Sabisz, et al., 2008). This concept seems to provide a challenge to the previous research that stated that the most probable interaction of caffeine and theophylline on DNA was through hydrogen bonding. However, other

studies have shown that caffeine forms "stacking complexes" with these anti-cancer drugs which affects the binding of the drugs into the DNA and regulates the movement through cell membranes, and also that xanthines actually displace drugs that have already been bound to DNA (Sabisz, et al., 2008). On a positive note, the protective nature of caffeine on DNA and also recent immunological studies point to the theory that it may help reduce some of the negative side effects associated with toxic cancer drugs, especially those that do not fully intercalate with DNA.

One study affirms the issue of caffeine binding to DNA by performing both UV absorption spectroscopy and infrared spectroscopy by Fourier transform (FTIR) (Nafisi, et al., 2008). The FTIR spectra for caffeine revealed that at low caffeine concentrations, the vibrational frequencies changed to what would be correlated with the stabilization of the DNA helix; as caffeine concentrations increased, the vibrational frequency increased reportedly due to the DNA helix destabilizing. The FTIR spectra for theophylline was much the same as that of caffeine at low concentrations, but at higher concentrations the results were inconclusive (Nafisi, et al., 2008). The UV spectra bands indicated that the interactions of both caffeine and theophylline with DNA were suspected to be attributed to hydrogen bonding. This article gives greater insight into the binding of xanthines such as caffeine and theophylline to DNA, and although the exact binding mechanism may not be clear, it serves as definite confirmation that xanthines do definitely bind and change the DNA helix somewhat.

It is then important to explore the mechanism by which caffeine intercalates into DNA and how it binds to planar aromatic drug molecules. One study attempts to explain the most probable framework for these mechanisms by proposing a complex X-Y system

of binding and then calculating equilibrium constants of complexed drug and caffeine, caffeine and DNA, and drug and DNA (Evstigneev, et al., 2008). The mechanism proposed works within a system that consists of two ligands in the presence of DNA. X represents the first ligand, which is the anticancer drug, and Y represents the other binding molecule such as caffeine. The caffeine molecule (Y) can essentially do two things. It can either bind to the anticancer drug, acting as the "interceptor" molecule or it can bind to the DNA, acting as the "protector" molecule as it is "protecting" the DNA molecule from being bound by the anticancer drug (X).

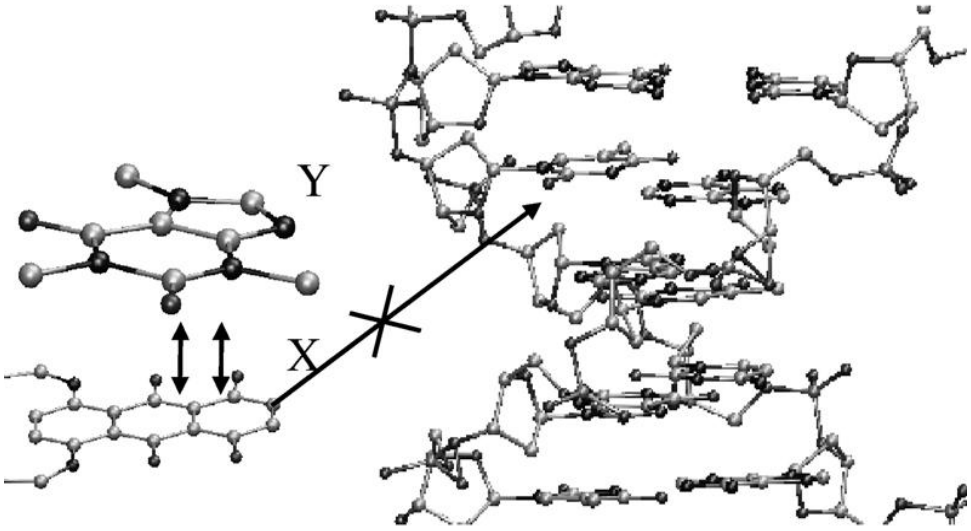

Figure 1.18: The "interceptor" Scheme[1]

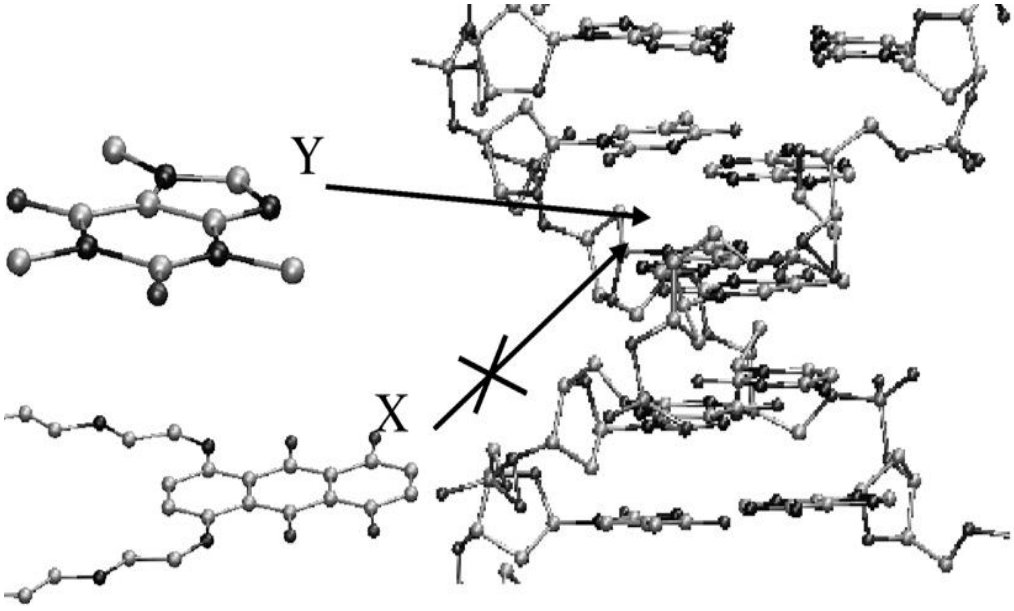

Figure 1.19: The "protector" Scheme[2]

Figure 1.18 shows molecules X (the anticancer drug) and Y (caffeine) forming a $\pi - \pi$ complex with each other, not allowing the drug (X) to intercalate into the DNA. Figure 1.19 illustrates the binding of Y (caffeine) to the DNA molecule, preventing X

[1,2] "Reprinted from Biophysical Chemistry, Vol 132, Evstigneev, M., Lantushenko, A., Evstigneev, V., Mykhina, Y. and Davies, D., Quantitation of the Molecular Mechanisms of Biological Synergism in a Mixture of DNA-acting Aromatic Drugs, Pg. 148-158, 2008, with permission from Elsevier.

(the anticancer drug) from binding the DNA. Because only part of the DNA is available for ligand binding due to part of the DNA being wound around proteins called histones, it is unlikely that both the anticancer drug and the caffeine would intercalate into the DNA simultaneously. With this understanding, the competitive binding of the anticancer drug and caffeine, whether it be the "interceptor" scheme or the "protector" scheme is most likely happening. The next issue is determining which scheme is happening the majority of the time. For this, a specific formula must be followed. The authors developed the formula:

$$R_D = \frac{f^X_{C2(0)} - f^X_{C2(C)}}{f^X_{C2(0)} - f^X_{C2(h)}},$$

where $f^X_{C2(0)}$ corresponds to the mole fraction of drug-DNA (X-DNA) complexes, $f^X_{C2(C)}$ represents the association between caffeine and DNA (Y-DNA) with no complexation between X and Y (the drug and caffeine). $f^X_{C2(h)}$ represents the complexation of X and Y (the drug and caffeine) (Evstigneev, et al., 2008). In a system consisting of the drug caffeine and DNA, this R_D value actually corresponds to the decrease in X (drug) bound with DNA upon the addition of Y (caffeine). When R_D is greater than one, the drug DNA complex is preferred over the complexation of caffeine with the drug, and vice versa. To determine the amount of the drug displaced from DNA by caffeine, the authors developed the formula:

$$A_D = \frac{f^X_{C2(0)} \quad f^X_{C2}}{f^X_{C2(0)}}.$$

The new variable, f^{X}_{C2}, represents the amount of drug bound to DNA when caffeine is present (Evstigneev, et al., 2008). The authors chose concentrations of drugs and of caffeine that had been used in previous related studies, and the concentration of DNA was chosen from calculated A_D values from previous papers. The concentration chosen was .01mM, based on the fact that this A_D value showed a good variation of results when in the presence of different drugs (Evstigneev, et al., 2008).

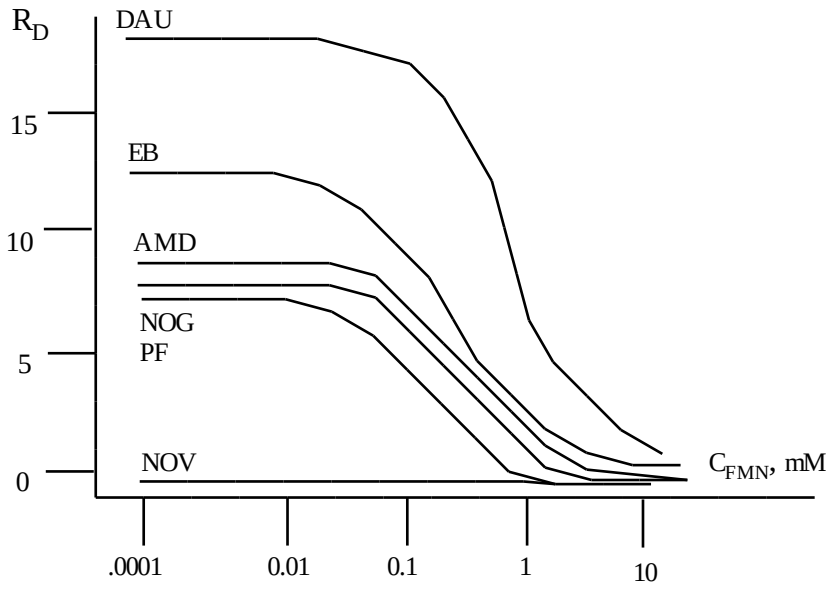

Figure 1.20: System with Drug, Caffeine and DNA

Figure 1.20 illustrates the drug, caffeine and DNA system in which the caffeine concentration begins at 0.001 mM and is increased to 10 mM (Evstigneev, et al., 2008). The DNA concentration of the system is held steady at 0.01 mM, and the R_D values of the drugs (on the *y* axis). μM concentrations of the drugs were used for the calculation of R_D . As the caffeine concentration (on the *x* axis) is increased, the DNA-drug complexes began to decline around the 0.75 mM concentration of caffeine (Evstigneev, et al., 2008). It is at this point that the drug is being displaced from the DNA by the caffeine and/or the caffeine is binding to the drug which prevents the drug from binding the DNA.

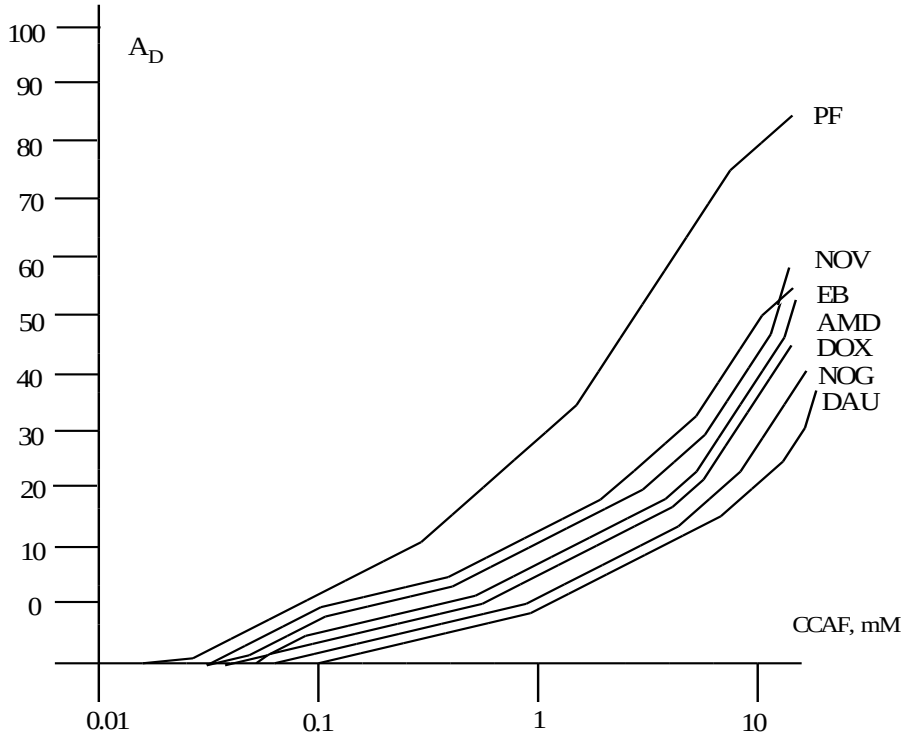

Figure 1.21: Drug Displacement from DNA

Figure 1.21 represents the A_D value, or the amount of drug actually being displaced from the DNA (Evstigneev, 2008). Caffeine is again increased from 0.01 mM to 10 mM, the DNA concentration is held at 0.01 mM, and the drugs are actually represented by their A_D calculations. As the caffeine concentration is increased, the A_D value for each drug goes up signaling increasing displacement of the drug from the DNA by the caffeine.

The drugs in this study are classic DNA intercalators that are currently being used as anticancer drugs. These drugs include: doxorubicin (DOX), daunorubicin (DAU), actinomycin D (AMD), mitoxantrone (NOV), topotecan (TPT) and amsacrine (AMSA). This study is important because it includes actual cancer drugs already on the market and illustrates the effects of caffeine and other xanthines such as theophylline can have on their efficacies in fighting cancer. By using drug concentrations from previous studies to

calculate the R_D and A_D for the drug, caffeine and DNA systems, this study proposes some real scenarios regarding what could actually happen within the body.

Another study from the Kapuscinski lab use different techniques to explore the effect of caffeine on the cytotoxicity of doxorubicin and mitoxantrone, both known DNA intercalators.

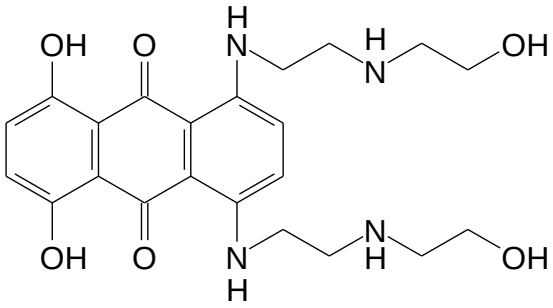

Figure 1.22 Mitoxantrone

Figure 1.22 shows the structure of mitoxantrone. Mitoxantrone is an anthraquinone drug closely related to anthracycline antibiotics in that they are both isolated from natural products and they are both considered anticancer antibiotics and work in much the same way. Just as doxorubicin is an anthracycline and is toxic to DNA by its intercalating action, mitoxantrone also intercalates into DNA and is a topoisomerase II inhibitor (Le Deley, et al., 2007). The purpose of the Le Deley study is to point out that binding due to π-π molecular interactions is indeed what is happening in the drug-caffeine system. By calculating equilibrium constants for the doxorubicin-caffeine complex and the mitoxantrone-caffeine complex, based on data determined previously, the molecular concentrations of each system can be compared.

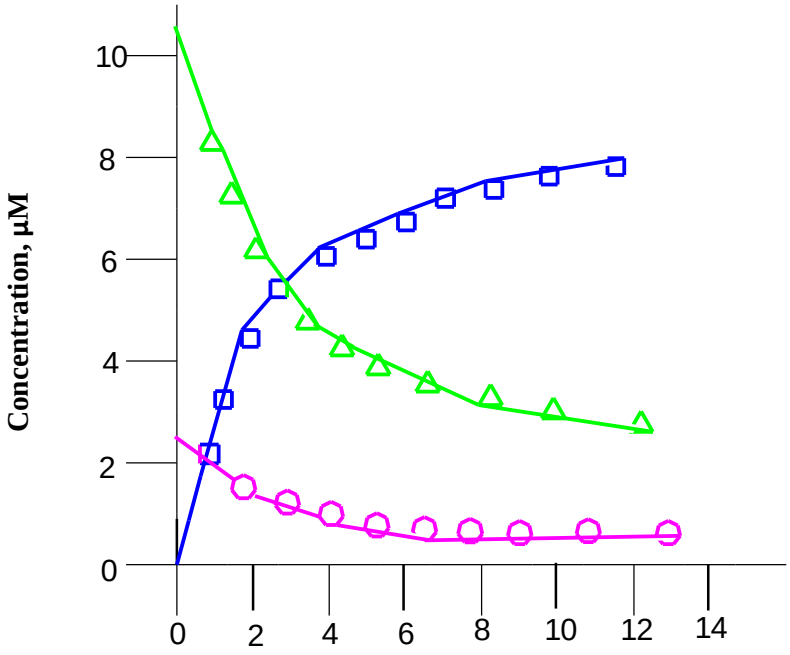

Figure 1.23: The Caffeine and Doxorubicin System

Figure 1.23 illustrates the effect of doxorubicin on a system consisting of caffeine (Piosik, et al., 2002). In Figure 1.23, the squares represent doxorubicin bound to caffeine, the triangles represent free doxorubicin monomer, and the circles represent the dimer of the drug. As the caffeine concentration increases, both the dimeric and monomeric forms of doxorubicin are decreasing (presumably due to binding the caffeine) and the doxorubicin concentration already bound to caffeine is rising (Piosik, et al., 2002).

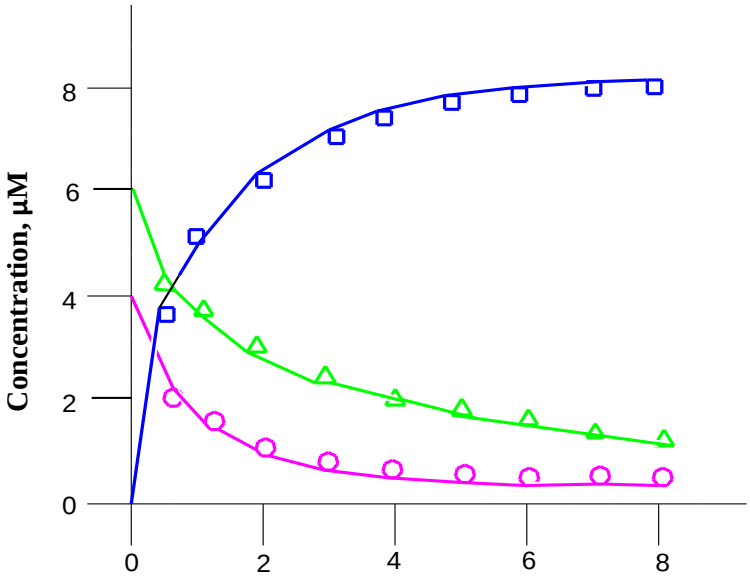

Figure 1.24: The System of Mitoxantrone and Caffeine

Figure 1.24 represents a system consisting of an increasing caffeine concentration and different forms of mitoxantrone (Piosik, et al., 2002). The symbols shown on the graph have the same representations as did the previous graph of caffeine and doxorubicin. The results are also very similar. As caffeine increases, the free dimeric and monomeric forms of the drug are decreasing and are being complexed with caffeine. Also, as the caffeine concentration increases, the mitoxantrone already bound with caffeine is increasing (Piosik, et al., 2002).

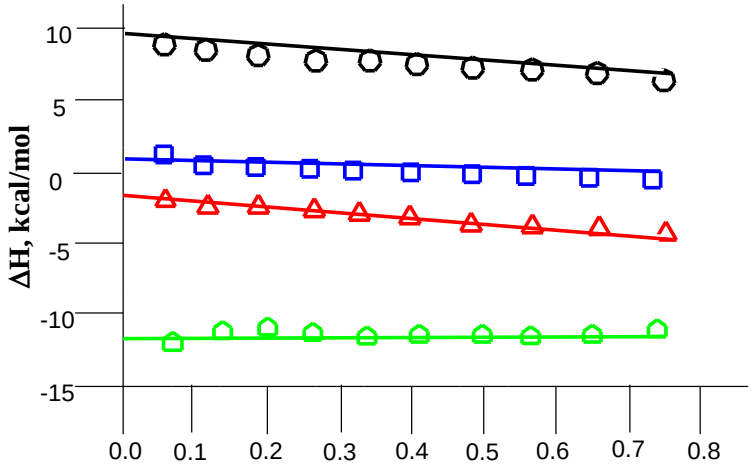

Figure 1.25: Determination of Heat of Formation

of Mitoxantrone-Caffeine Complex

Figure 1.25 represents a microcalorimetry assay used to determine the heat of formation of the mitoxantrone-caffeine complex (Piosik, et al., 2002). A 1.3 mL portion of a caffeine solution was titrated ten times with 10 μL of mitoxantrone to determine the heat of formation for the complex. In the figure, the black circles represent a caffeine titration by a buffer solution, and the blue squares represent a mitoxantrone titration by the same buffer solution to establish a baseline for the calorimetry. The red triangles represent caffeine being titrated by mitoxantrone, and the green modified squares represent ΔH (enthalpy of formation) for the mitoxantrone-caffeine complex by subtracting the two baseline titrations from the caffeine-mitoxantrone titration. The ΔH calculated is -11.3 kcal/mol which is a valid figure and supports the hypothesis of π–π molecular interactions between caffeine and mitoxantrone (Piosik, et al., 2002). To further validate these findings, a molecular mechanics study was performed using HyperChem computer software for both mitoxantrone and doxorubicin in the presence of water molecules. This study employed the use of a semi-empirical PM3 method which is

a simple quantum mechanics program that does not account for electron correlation. However, the energies calculated from this program were found to be exothermic which do agree with the microcalorimetry findings. The water molecules were added to the calculation because both mitoxantrone and doxorubicin are protonated in solution but were removed after the calculation had concluded (Piosik, et al., 2002). The atoms in Figures 1.26 and 1.27 are represented by colors as teal, carbon; gray, hydrogen; dark blue, nitrogen; and red, oxygen. The water molecules shown in Figures 1.26 and 1.27 remain because they are involved in hydrogen bonding (Piosik, et al., 2002).

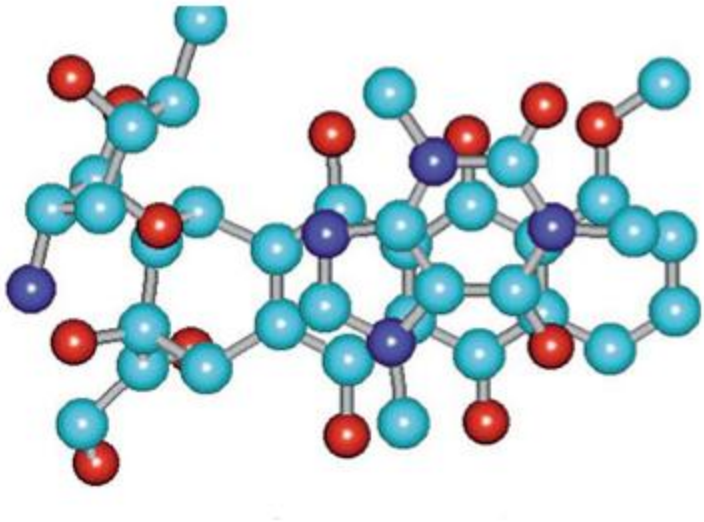

Figure 1.26: Caffeine and Doxorubicin[3]

Figure 1.26 shows caffeine bound to doxorubicin. The caffeine molecule is resting on top of the doxorubicin molecule. The ΔE (energy of formation) for this complex was calculated by the HyperChem program as -7.4 kcal/mol, which is a valid energy for π-π molecular interactions (Piosik, et al., 2002).

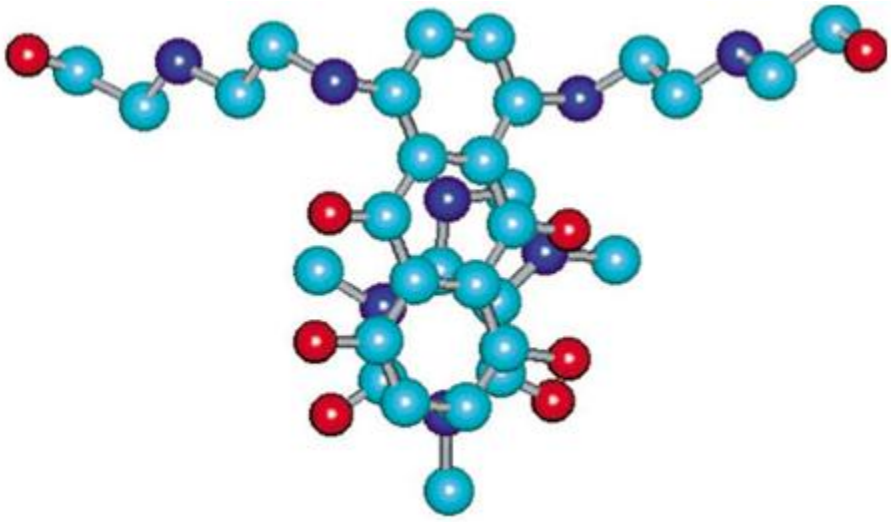

Figure 1.27: Caffeine and Mitoxantrone[4]

[3,4] "Reprinted from Biochemical Pharmacology, Vol 63, Piosik, J., Zdunek, M. and Kapuscinski, J. The Modulation by Xanthines of the DNA-Damaging Effect of Polycyclic Aromatic Agents. Part II. The Stacking Complexes of Caffeine with Doxorubicin and Mitoxantrone., Pg. 635-646, 2002, with permission from Elsevier.

Figure 1.27 illustrates the bound complex of caffeine and mitoxantrone. The ΔE for this complex is -8.7 kcal/mol, again a good energy of formation for stacking molecules (Piosik, et al., 2002).

The purpose of this three-fold study serves to confirm the π–π interaction occurring between the xanthine caffeine and cancer drugs that are known to bind DNA by the mechanism of intercalation. The combination of calculating the equilibrium constants and molecular concentrations of caffeine and two known intercalators, mixing the drugs and caffeine to determine the concentrations needed for binding, by microcalorimetry, and by molecular mechanics studies give a well-rounded view into the mechanism of the binding taking place and point to the aromatic rings of the caffeine and the drugs forming stacking complexes.

1.7 Research Plan and Hypothesis

Based on background information and previous studies performed, the isoquinoline alkaloids show an intercalative binding scheme with DNA, similar in mechanism to several cancer drugs on the market. Because the alkaloids possess a planar aromatic structure, they are able to form π–π molecular complexes with DNA and other aromatic structures such as the xanthine alkaloids. Caffeine, a xanthine alkaloid, also has the ability to intercalate into DNA and form π–π molecular complexes with other planar alkaloids and cancer drugs. It is then logical to assume that the presence of caffeine could interfere with the intercalating alkaloid/cancer drug thereby lowering the toxicity to the cancer cells. Therefore, I hypothesize that caffeine intercalates into double-stranded DNA of cancer cells as well as forms π–π molecular bonds with the alkaloid/drug,

thereby blocking planar aromatic alkaloids/drugs from intercalating into the DNA and causing the effect of the drug to be lessened.

By testing the cytotoxicity of the several isoquinoline alkaloids and two known cancer drugs on MCF-7 breast cancer cells, the IC_{50} values of these compounds can be determined. To determine if caffeine is responsible for attenuation in the cytotoxic activity of these alkaloids/drugs, caffeine solutions at varying concentrations can be plated with the MCF-7 cells to determine an appropriate concentration of caffeine to use in the presence of the alkaloids/drugs. Once an appropriate caffeine concentration that is not toxic to the cell line itself has been determined, it can then be used in conjunction with the alkaloids/drugs to determine whether or not there is attenuation in the cytotoxicity of the alkaloids/drugs due to the presence of caffeine.

Computational molecular modeling studies involving the alkaloids chelerythrine, camptothecin, ellipticine, doxorubicin, berberine and sanguinarine with caffeine were also performed using the density functional theory (DFT) and the recently developed M06 functional (Zhao, et al., 2008). For each drug, the two molecules (drug and caffeine) were docked in many different orientations to discover the most probable configuration of the two interacting molecules.

CHAPTER TWO

EXPERIMENTAL

2.1 Cytotoxicity Screening

Human MCF-7 adenocarcinoma cells (ATCC No. HTB-22) were grown in a 5.0% CO_2 environment at 37˚C in RPMI 1640 medium with L-glutamine and 7.5% $NaHCO_3$, 100,000 units of Penicillin and 10.0 mg Streptomycin per liter, 15 mM Hepes at a pH of 7.35, and supplemented with 10% fetal bovine serum. MCF-7 cells were cultured by the author.

2.1.1. Cytotoxicity Assays

MCF-7 cells were plated in 96-well cell culture plates at a concentration of 1.0×10^5 cells per well for a final volume of 100 µL. The cells in the media totaled 100 µL in each well. Plates were allowed to incubate for 48 hours in a 5% CO_2 environment at 37˚C. After 48 hours, the media was removed by suction from each well, and 100 µL of fresh media containing the test compounds (at a final concentration of 0.01% in DMSO) were added to each well for a final concentration of 100 µg/mL of each compound. All tests were done in eight replicates. Medium and DMSO control wells were also included, as well as Tingenone for a positive control. Concentrations of individual compounds were then adjusted for additional assays to obtain an IC_{50} (half maximal inhibitory concentration) for each compound. After the compounds in media were added to each well, the plate was again incubated for 48 hours. After 48 hours, the media and compound mixture was removed by suction and 100 µL of a 0.83 mg/mL MTT solution in media was added to each well and allowed to incubate for 4 hours. The

MTT solution was made by adding 2 mL of 0.05 g thiazolyl blue in 10 mL of 10 mM phosphate buffered saline, pH 7.36, to 10 mL of media. Live cells metabolize this solution to form insoluble formazan crystals. After 4 hours, the MTT mixture and media were removed by suction, and 100 µL of DMSO was added to each well to dissolve the crystals. The plates were then incubated for fifteen minutes at 37ºC. After fifteen minutes, the absorbance in each well was determined with a microplate reader (Molecular Devices SpectraMax Plus384) at 570 nm. The data output provides the results of average absorbances, standard deviations and percent kill ratios (Setzer, 2005). All cytotoxicity assays were carried out by the author.

2.1.2. Determination of Caffeine Concentration for use in Media

Anhydrous caffeine (Sigma) was treated as a compound in a cytotoxicity assay to determine the highest concentration possible at which the cells were still viable. The assay was carried out as described in the above procedure. The caffeine concentrations were varied from 25 µg/mL to 200 µg/mL.

2.1.3. Preparation of Caffeine Media

Anhydrous caffeine (Sigma) was added to the afore-described RPMI 1640 stock media supplemented with 10% fetal bovine serum to give a concentration of 200 µg/mL caffeine, a concentration determined by cytotoxicity assay to provide a large percentage of viable cells (see Table 3.2). This caffeine media was then used in the cytotoxicity assays of each test compound to determine the effect of the compounds on the cells in the presence of caffeine.

2.1.4. Preparation of Intercalating Compounds

The intercalating compounds used in the assays were berberine, doxorubicin, camptothecin, ellipticine, sanguinarine and chelerythrine (Sigma). The compounds in media were plated in 100 µL in each well of a 96-well plate at a concentration of 100 µg/mL per well. This was the starting concentration for each of the compounds. From the results of the initial assay, the concentrations were then altered to vary the percent kill both higher and lower than 50% so as to obtain an IC_{50} value. IC_{50} values were determined by the Reed-Muench method (Reed, et al., 1938).

2.1.5 Preparation of Drugs in the Caffeine Media

The intercalating compounds used in the assays in the caffeine media were berberine, doxorubicin, camptothecin, ellipticine, sanguinarine and chelerythrine. The compounds were added to the media containing caffeine as described above and were plated in each well of a 96-well plate to give the concentration of 100 µg/mL per well. This was the starting concentration for each of the compounds. From the results of the beginning assay, the concentrations were then altered to vary the percent kill both higher and lower than 50% so as to obtain an IC_{50} value.

2.2 Molecular Modeling

Molecular modeling calculations were carried out using SPARTAN '08 for Windows software (Spartan, 2008) using the M06 hybrid functional and the 6-31G* basis set. The molecules to be docked were placed at a distance of 3.3 Å apart before the calculation was started.

2.2.1 Caffeine

The caffeine molecule was built using SPARTAN '08 software and a geometry optimization calculation was run using the M06 functional with the 6-31G* basis set. The surfaces included in the optimization were an electrostatic potential map and the HOMO (highest occupied molecular orbital).

2.2.2 The Intercalating Compounds

The intercalating compounds berberine, doxorubicin, camptothecin, ellipticine, sanguinarine and chelerythrine molecules were built using SPARTAN '08 software and a geometry optimization calculation was run using the M06 functional with the 6-31G* basis set. The surfaces included in the optimization consisted of the electrostatic potential map and the LUMO (lowest unoccupied molecular orbital).

2.2.3 π–π Complexes Between Caffeine and Intercalating Compounds

Caffeine and each intercalating compound were docked at a distance of 3.3 Å at several different orientations determined by several factors that included, but were not limited to, highest occupied molecular orbital and lowest unoccupied molecular orbital (HOMO-LUMO) interactions, dipole-dipole interactions and electrostatic interactions. The docking was performed after a complete geometry optimization calculation was run using the M06 functional with the 6-31G* basis set for each compound and for caffeine separately. The compound and caffeine were oriented on the computer screen using the SPARTAN '08 program considering one of the molecular interactions listed previously, then the caffeine was carefully overlayed onto the compound in the orientation selected, and a complete geometry optimization calculation was then run on the docked molecules. When considering the dipole-dipole interactions, the dipole of the compound and the

dipole of caffeine were directed so as to oppose each other, then the caffeine was carefully overlayed onto the compound, and a complete geometry calculation was run (see Section 4.4 and Figures 4.40 and 4.41). When the electrostatic interactions were considered for orienting the compound and the caffeine, the electrostatic maps of each molecule were observed for areas of high electron density and areas of low electron density which are represented by opposing colors. The areas of electron density of the compound that differed with the areas of electron density of the caffeine were then oriented with respect to each other before the caffeine was overlayed onto the compound and a complete geometry optimization was run (see Section 4.4 and Figures 4.42 and 4.43). When considering the frontier molecular orbital interactions, the highest occupied molecular orbital (HOMO) of caffeine and the lowest unoccupied molecular orbital (LUMO) of the compound, represented by nodes in the SPARTAN '08 program, were aligned so as to overlap each other as completely as possible before a complete geometry optimization was run on the docked molecules (see Section 4.4 and Figure 4.39). To achieve other orientations, the compound and caffeine can be situated in various ways while still considering the molecular factors listed previously, but varying them slightly.

CHAPTER THREE

RESULTS

3.1 Cytotoxicity Results

The cytotoxicity assays were carried out as previously described for six compounds: berberine, camptothecin, chelerythrine, doxorubicin, ellipticine and sanguinarine. The assays were completed using the RPMI 1640 media supplemented with 10% fetal bovine serum to determine the IC_{50} of the six compounds. In a separate assay, an appropriate concentration of caffeine based on the % kill of the cells in the presence of caffeine to be supplemented into the media was determined to be 200 μg/mL, as caffeine appeared to have little effect on the cells. Separate assays were then conducted to determine the IC_{50} of the compounds in the RPMI 1640 media supplemented with 10% fetal bovine serum also supplemented with 200 μg/mL caffeine. The effects of caffeine on the cytotoxic activity of the intercalating antitumor agents are shown in Table 3.1.

Table 3.1: Cytotoxicity attenuation of intercalating antitumor agents by caffeine.

Compound	IC_{50} (μM)[a]	
	no caffeine	with caffeine[b]
Berberine	**50.0(4.3)**	**511(59)**
Camptothecin	**9.21(1.41)**	**335(31)**
Chelerythrine	**32.1(0.5)**	**37.4(0.8)**
Doxorubicin	**11.4(2.2)**	**31.7(3.9)**
Ellipticine	**12.8(0.5)**	**333(7)**
Sanguinarine	**5.78(0.22)**	**6.66(0.16)**

[a] Standard deviations in parentheses.
[b] Caffeine concentration = 1030 μM

The cytotoxicity data for the determination of the amount of caffeine that could be tolerated on the cells is shown in Table 3.2. As is shown, high concentrations of caffeine have little effect on the cells.

Table 3.2: Cytotoxicity Determination of Caffeine on MCF-7 Cells.

Compound	Conc (µg/mL)	% Kill	Standard Deviation
Caffeine	**200**	**11.17**	**9.54**
	175	**12.40**	**7.19**
	150	**12.86**	**7.02**
	125	**1.40**	**8.86**
	100	**10.23**	**6.85**
	75	**11.03**	**14.28**
	50	**5.30**	**8.94**
	25	**2.68**	**7.15**

The standard deviations for the IC_{50} determination of the compounds with and without caffeine were determined by standard t-test and are represented in Table 3.3. t was determined by the formula: $t = \frac{X1-X2}{\sqrt{\frac{2s^2p}{n}}}$, where *n* is the number of measurements, X1 is the first group of measurements, X2 is the second group of measurement, s is the standard deviation and ν represents the degrees of freedom which is $(n_1 + n_2) - 2$, and *P* is the probability value that the observed statistics are significant or not (Zar, 1996).

Table 3.3 : t-test for Reliability of Cytotoxicity Assays.

Compound	No caffeine mean	Standard Deviation	With Caffeine mean	Standard Deviation	t	ν	*P*
Berberine	50	4.3	511	59	22.04162	14	<0.001
Camptothecin	9.21	1.41	335	31	29.69424	14	<0.001
Chelerythrine	32.1	0.5	37.4	0.8	15.89007	14	<0.001
Doxorubicin	11.4	2.2	31.7	3.9	12.82283	14	<0.001
Ellipticine	12.8	0.5	333	7	129.0515	14	<0.001
Sanguinarine	5.78	0.22	6.66	0.16	9.149804	14	<0.001

Table 3.3 shows the values for the t-test conducted for all the compounds tested in the absence of caffeine and in the presence of caffeine. Based on this t-test, all of the comparisons in values for the compounds with and without caffeine are considered statistically significant with the *P* value for each compound <0.001.

3.2 Molecular Interaction Data

As described above, each intercalating compound was constructed and a geometry optimization run on SPARTAN '08 using the M06 functional with the 6-31G* basis set. The π–π interaction energies of the six intercalating compounds and caffeine are summarized in Table 3.4.

Table 3.4: π-π Interaction energies of intercalating antitumor agents and caffeine.

Compounds	E_{vac} (kcal/mol)[a]	E_{aq} (kcal/mol)[b]
Caffeine + Berberine	-19.34	-12.60
Caffeine + Camptothecin	-18.04	-13.05
Caffeine + Chelerythrine	-20.33	-16.51
Caffeine + Doxorubicin	-19.16	-15.86
Caffeine + Ellipticine	-16.83	-11.02
Caffeine + Sanguinarine	-21.60	-16.47

[a]Calculated interaction energies in the gas phase.
[b]Calculated interaction energies using the SM5.4 aqueous solvation model (Chambers, et al., 1996).

CHAPTER FOUR

DISCUSSION

4.1 The Effects of Caffeine on the Cytotoxic Activities of the Intercalating Drugs

As expected, caffeine resulted in attenuation on the cytotoxic activities of all the intercalating drugs in the present study. Some of the intercalating drugs were more effected than others as shown in their IC_{50} calculation in Table 3.1. A significant attenuation was seen for berberine, camptothecin, doxorubicin and ellipticine, while chelerythrine and sanguinarine were only marginally attenuated. Because the IC_{50} is raised, the assumption can be intelligently made that caffeine is either first intercalating into the DNA before the compound can intercalate into the DNA, or that the caffeine has first formed a π–π interaction with the compound. Both of these scenarios have been previously mentioned as possibilities and given the terms the "interceptor scheme" which refers to caffeine forming a π–π interaction with the intercalator and the "protector scheme" which refers to caffeine intercalating into the DNA thereby blocking the intercalative drug from binding the DNA (Evstigneev, et al., 2008). The molecular modeling study discussed in a subsequent section will help differentiate between the two proposed schemes.

4.1.1 Berberine

The IC_{50} calculated for berberine using the data from the cytotoxicity assays performed is 50 µM with a standard deviation of 4.3 µM. This number was calculated using the % kill values represented in the results of the cytotoxicity assays performed on

the MCF-7 human breast adenocarcinoma cell line. This 50 µM value translates to 16.8 µg/mL, which is higher than the <1 µg/mL value presented by the cytotoxicity assays performed in another study (Letasiova, et al., 2006). A different cell line, the Ehrlich ascites carcinoma cells, were used in the Letasiova study, perhaps accounting for the difference in the IC_{50} calculated for that study and for the present study. An earlier study conducted employed both HeLa cells, an immortal cervical cancer cell line, and L1210 cells, a leukemia cell line found in mice (Jantova, et al., 2003). The IC_{50} for these cell lines were also found to be lower than what is reported in our present study. When the cytotoxicity assays were performed in the presence of caffeine at 1030 µM, the IC_{50} of berberine was raised to 511 µM with a 59 µM standard deviation. This IC_{50} value supports the hypothesis that caffeine interferes with the intercalation process of berberine into DNA. Table 4.1 shows the concentrations attempted for determining the IC_{50} of berberine in the absence and presence of caffeine.

Table 4.1: Cytotoxicity Data for Berberine in the Absence and Presence of Caffeine.

Compound	**Conc (µg/mL)**	**% Kill**	**Standard Deviation**	**IC_{50} (µg/mL)**	**IC_{50} (µM)**
Berberine	100	61.61	6.56		
	20	51.14	6.64		
	10	13.16	3.99	18.61 (1.58)	50.04 (4.26)
Berberine with Caffeine	500	100	---	estimated	
	100	12.77	8.43	189.95 (22.00)	510.87 (59.17)

4.1.2 Chelerythrine

The IC_{50} calculated for chelerythrine using the data from the cytotoxicity assays performed is 32.1 μM with a standard deviation of 0.5 μM. This IC_{50} is slightly higher than one previously reported as being 12.3 μM for the MCF-7 cell line (Matkar, et al., 2008). When the cytotoxicity assays were performed in the presence of caffeine at 1030 μM, the IC_{50} of chelerythrine was raised to 37.4 μM with a 0.8 μM standard deviation. As expected, the IC_{50} was raised for chelerythrine in the presence of caffeine, though with not as large a magnitude as the values observed for berberine. Table 4.2 shows the concentrations attempted for determining the IC_{50} of chelerythrine in the absence and presence of caffeine.

Table 4.2: Cytotoxicity Data for Chelerythrine in the Absence and Presence of Caffeine.

Compound	Conc (µg/mL)	% Kill	Standard Deviation	IC_{50} (µg/mL)	IC_{50} (µM)
Chelerythrine	100	100.00	---		
	50	100.00	---		
	10	100.00	---		
	13	70.15	7.77		
	12	45.62	8.13	12.30 (0.19)	32.05 (0.49)
	5	0.00	---		
Chelerythrine with Caffeine	20	100	---		
	18	92.15	6.11		
	16	81.68	6.42		
	14	46.08	7.75	14.37 (0.31)	37.43 (0.80)
	12	0.00	---		

4.1.3 Ellipticine

The IC_{50} calculated for ellipticine using the data from the cytotoxicity assays performed is 12.8 µM with a standard deviation of 0.5 µM. Previous studies have reported IC_{50} values for ellipticine with several different types of cells, two of which are the HL-60 leukemia cell line and the MCF-7 breast cancer cell line. The reported value

for HL-60 cells is 0.64 μM (Poljakova, et al., 2007) and the value for MCF-7 cells is 0.94 μM (Ferlin, et al., 2009). This IC_{50} value for the MCF-7 cell line differs from the results that are represented in this thesis. This could be due to slightly differing technique in cytotoxicity assay procedure, perhaps with how long the cells were exposed to the intercalative drug. When the cytotoxicity assays were performed in the presence of caffeine at 1030 μM, the IC_{50} of ellipticine was raised to 333 μM with a 7 μM standard deviation. Again, in the presence of caffeine, the IC_{50} was raised a significant amount indicating binding of either DNA or ellipticine by caffeine. Table 4.3 shows the concentrations attempted for determining the IC_{50} of ellipticine in the absence and presence of caffeine.

Table 4.3: Cytotoxicity Data for Ellipticine in the Absence and Presence of Caffeine.

Compound	Conc (µg/mL)	% Kill	Standard Deviation	IC_{50} (µg/mL)	IC_{50} (µM)
Ellipticine	100	100.00	---		
	20	71.76	5.04		
	4	98.74	1.84		
	3	37.26	9.89	3.14 (0.11)	12.76 (0.46)
	2.5	23.63	17.55		
Ellipticine with Caffeine	100	71.74	2.90		
	90	79.33	4.75		
	80	44.42	11.14	82.19 (1.84)	333.68 (7.45)
	50	7.74	8.77		

4.1.4 Sanguinarine

The IC_{50} calculated for sanguinarine using the data from the cytotoxicity assays performed is 5.78 µM with a standard deviation of 0.22 µM. This IC_{50} is similar to the one previously reported as being 4.4 µM for the MCF-7 cell line (Matkar, et al., 2008). When the cytotoxicity assays were performed with in the presence of caffeine at 1030 µM, the IC_{50} of sanguinarine was raised to 6.66 µM with a 0.16 µM standard deviation. This concurs with the all of the previous data of caffeine/DNA intercalation

and/or caffeine and drug π–π interactions. Table 4.4 shows the concentrations attempted for determining the IC_{50} of sanguinarine in the absence and presence of caffeine.

Table 4.4: Cytotoxicity Data for Sanguinarine in the Absence and Presence of Caffeine.

Compound	Conc (µg/mL)	% Kill	Standard Deviation	IC_{50} (µg/mL)	IC_{50} (µM)
Sanguinarine	100	100.00	---		
	20	100.00	---		
	5	100.00	---		
	4	100.00	---		
	3	99.97	1.39		
	2.5	99.08	4.84		
	2	26.48	13.63	2.13 (0.08)	5.78 (0.22)
	1	0.00	---		
Sanguinarine with Caffeine	100	100.00	---		
	10	100.00	---		
	5	100.00	---		
	3	100.00	0.17		
	2	0.00	7.77	2.45 (0.06)	6.66 (0.16)
	1	0.00	---		

4.1.5 Camptothecin

The IC_{50} calculated for camptothecin using the data from the cytotoxicity assays performed is 9.21 µM with a standard deviation of 1.41 µM. When the cytotoxicity assays were performed with in the presence of caffeine at 1030 µM, the IC_{50} of camptothecin was raised to 335 µM with a 31 µM standard deviation. Table 4.5 shows the concentrations attempted for determining the IC_{50} of camptothecin in the absence and presence of caffeine.

Table 4.5: Cytotoxicity Data for Camptothecin in the Absence and Presence of Caffeine.

Compound	Conc (µg/mL)	% Kill	Standard Deviation	IC_{50} (µg/mL)	IC_{50} (µM)
Camptothecin	100	100.00	---		
	20	97.21	3.04		
	10	61.20	2.49		
	4	61.11	3.73		
	1	3.57	9.16	3.21 (0.49)	9.21 (1.41)
Camptothecin with Caffeine	500	100	---	estimated	
	100	42.15	4.75	116.72 (10.77)	335.05 (30.92)

4.1.6 Doxorubicin

The IC_{50} calculated for doxorubicin using the data from the cytotoxicity assays performed is 11.4 µM with a standard deviation of 2.2 µM. When the cytotoxicity assays

were performed with in the presence of caffeine at 1030 µM, the IC_{50} of doxorubicin was raised to 31.7 µM with a 3.9 µM standard deviation. Table 4.6 shows the concentrations attempted for determining the IC_{50} of doxorubicin in the absence and presence of caffeine.

Table 4.6: Cytotoxicity Data for Doxorubicin in the Absence and Presence of Caffeine.

Compound	Conc (µg/mL)	% Kill	Standard Deviation	IC_{50} (µg/mL)	IC_{50} (µM)
Doxorubicin	100	100.00	---		
	20	90.26	5.01		
	10	50.31	7.36		
	4	47.97	7.32	6.60 (1.28)	11.38 (2.21)
Doxorubicin with Caffeine	100	100	---		
	50	78.73	2.30		
	10	33.47	4.94	18.36 (2.27)	31.65 (3.91)
	1	0.00	---		

4.2 Comparison of Structures of the Intercalating Drugs

Though all of the intercalating drugs are considered planar, some show more similarity in structure to others. Even though their IC_{50} values differed slightly, the two benzophenanthridines sanguinarine (IC_{50} 5.78 µM) and chelerythrine (IC_{50} 32.1 µM) had only slight jumps in their IC_{50} values when in the presence of caffeine. This indicates that the cytotoxic efficacies of these two intercalators were not impeded very

much by the presence of caffeine, with the IC_{50} for sanguinarine moving from 5.78 µM to 6.66 µM and the IC_{50} for chelerythrine moving from 32.1 µM to 37.4 µM. These comparable changes in values could be related to the similar structures of sanguinarine and chelerythrine shown in Figure 4.1.

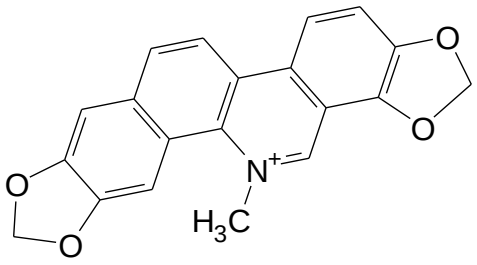

Sanguinarine

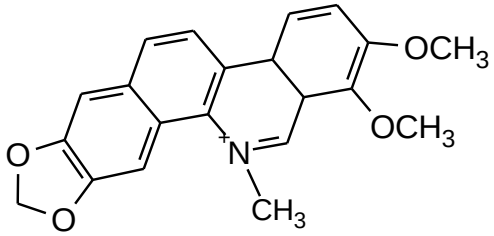

Chelerythrine

Figure 4.1 Sanguinarine and Chelerythrine

The slight attenuation in the IC_{50} values of sanguinarine and chelerythrine from the system with no caffeine to the system with caffeine could indicate another method of action in addition to intercalation. It has been reported that sanguinarine also induces oxidation within the cell which causes double-stranded DNA break as suggested by the gel electrophoresis assays discussed previously (Matkar, et al., 2009). Also, within certain cell lines, sanguinarine was found to induce caspase activation, which helps to facilitate apoptosis (Jang, et al., 2009). It has also been suggested that both sanguinarine and chelerythrine initiate the production of H_2O_2 which causes oxidation, and thus apoptosis, within the cell (Matkar, et al., 2008).

Although not structurally similar to sanguinarine or chelerythrine, doxorubicin also only showed a small change in IC_{50} when in the presence of caffeine with a jump from 11.4 µM to 31.7 µM. The structure of doxorubicin is shown in Figure 4.2.

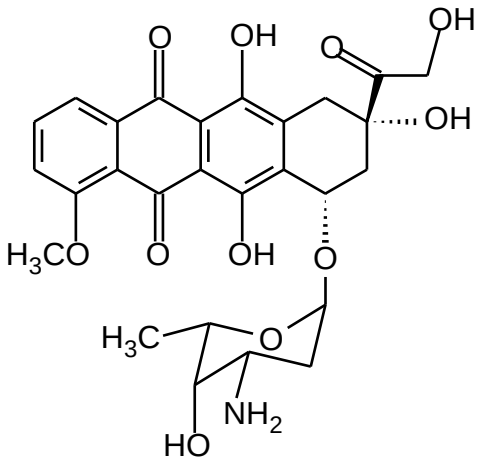

Figure 4.2 Doxorubicin

Berberine, camptothecin and ellipticine all exhibited very large increases in IC_{50} values in the presence of caffeine. The IC_{50} for camptothecin rose from 9.21 µM to 335 µM and the IC_{50} for berberine rose from 50.0 µM to 511 µM. Camptothecin and berberine are structurally similar, as indicated by their line structures in Figure 4.3.

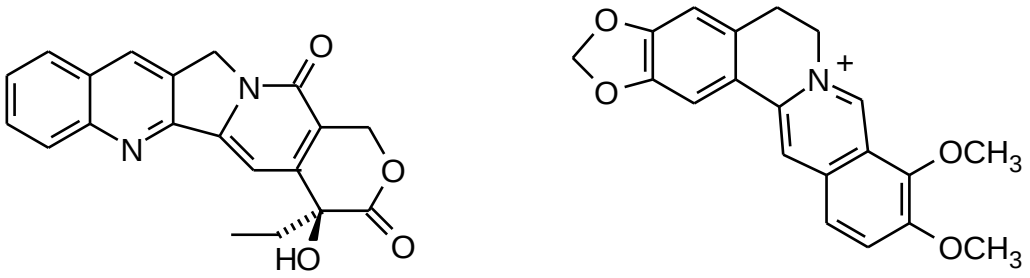

Camptothecin Berberine

Figure 4.3: Camptothecin (left) and Berberine (right)

Figure 4.4 shows the slightly buckled structures of camptothecin (a) and berberine (b). The molecules are rotated horizontally for better viewing.

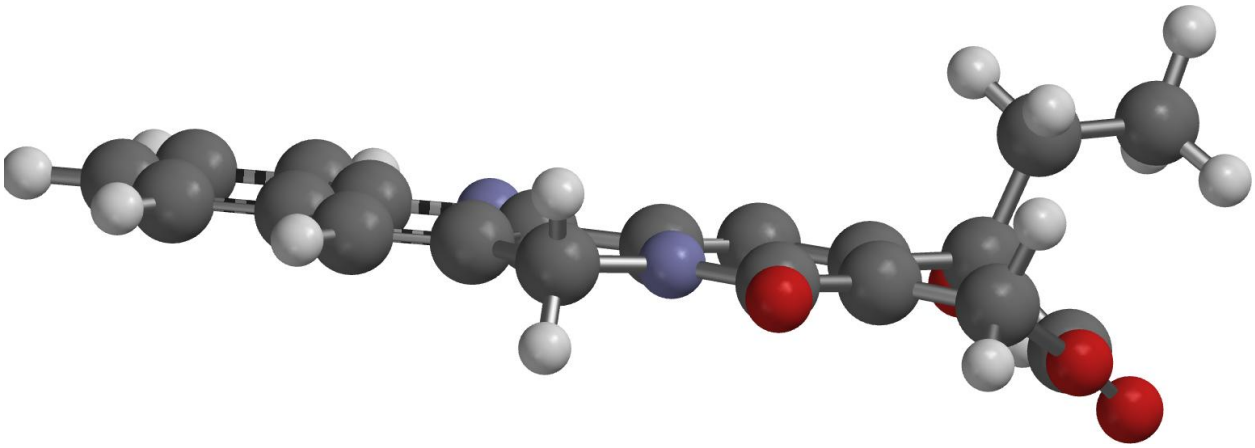

(a)

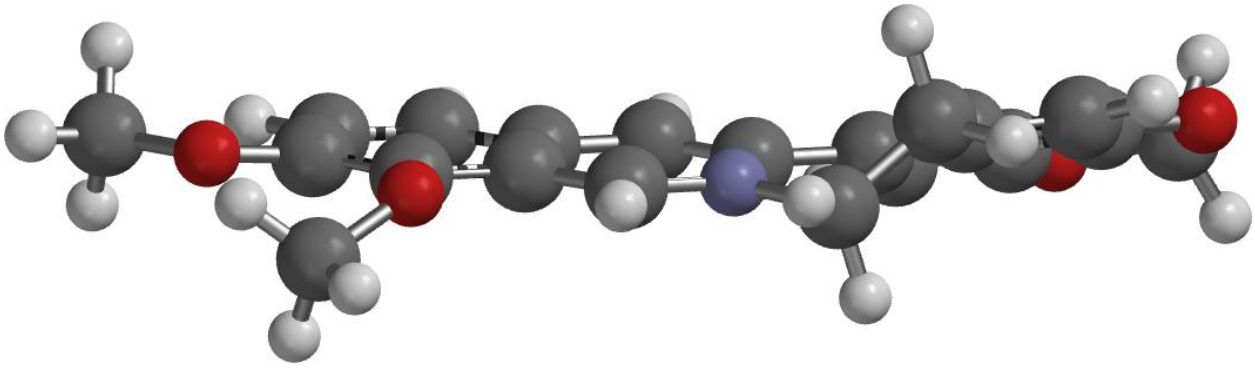

(b)

Figure 4.4: Buckled Structures of (a) camptothecin and (b) berberine

Ellipticine, whose line structure (a) and horizontal molecular structure (b) are shown in Figure 4.5 is a tetracyclic alkaloid as opposed to the other intercalators which have five or more rings. The IC_{50} for ellipticine rose from 12.8 µM to 333 µM. Unlike camptothecin and berberine, ellipticine has a completely planar structure as shown in Figure 4.5 (b), which may allow for more complete intercalation.

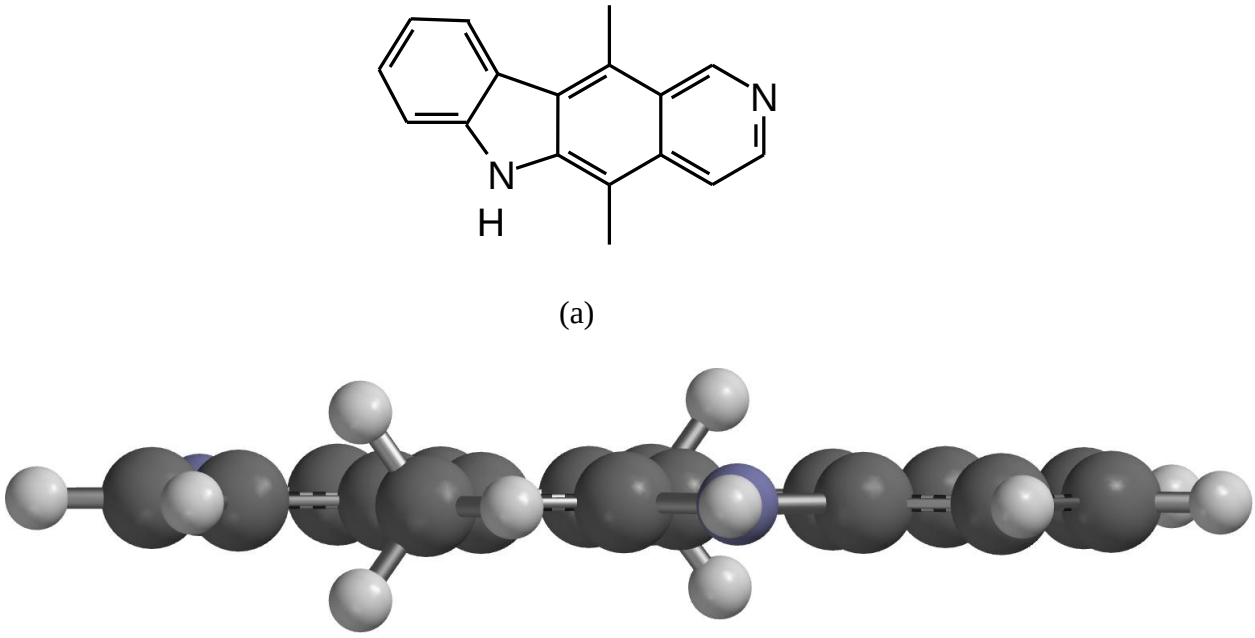

(a)

(b)

Figure 4.5: Ellipticine Shown as (a) Line Drawing and (b) Ball and Spoke Model

4.3 π-π Interaction Energies of Intercalating Antitumor Agents and Caffeine

The molecular modeling studies carried out on SPARTAN '08 give further insight as to what is happening when the intercalating compounds are in the presence of caffeine, by docking each molecule with caffeine and instructing the computer program to calculate the interaction energies for each compound/caffeine pair. Each pair of intercalating compound/caffeine was oriented in different positions by arranging the intercalator and caffeine in ways that will give the most likely π–π interaction energy to indicate what is actually happening experimentally. The orientation with the lowest interaction energy is considered the most probable. The individual energies calculated for the compounds and for caffeine, as well as the interaction energies and the energy differences from the sum of energies of each compound and caffeine are listed in Tables 4.7 through 4.12.

4.3.1 Berberine

The calculated interaction energy of the most probable orientation of berberine and caffeine was found to be -19.34 kcal/mol in the gas phase and -12.60 kcal/mol in aqueous solution. These values were found by adding the individual energies found separately for caffeine and for berberine, then subtracting that value from energies derived from different orientations of the caffeine/berberine pair. Out of the four caffeine/berberine orientations, the orientation that showed the most probability for what is actually happening between the two molecules in aqueous solution exhibited good overlap of molecular orbitals (HOMO and LUMO), good electrostatic interactions and outstanding dipole-dipole interactions. The total energies of the berberine molecules and caffeine and their energy differences (interaction energies) are listed in Table 4.7.

Table 4.7: Interaction energies of berberine and caffeine in different orientations.

	E_{vac} (kcal/mol)	E_{aq} (kcal/mol)
Caffeine	-426682.26	-426689.01
Berberine	-707608.27	-707644.25
Sum of energies	-1134290.53	-1134333.26
Orientation 1 (lowest)	-1134309.87	-1134345.86
Interaction energy	-19.34	-12.60
Orientation 2	-1134308.20	-1134344.86
Interaction energy	-17.67	-11.60
Orientation 3	-1134307.03	-1134344.20
Interaction energy	-16.50	-10.94
Orientation 4	-1134309.7	-1134344.99
Interaction energy	-19.17	-11.73

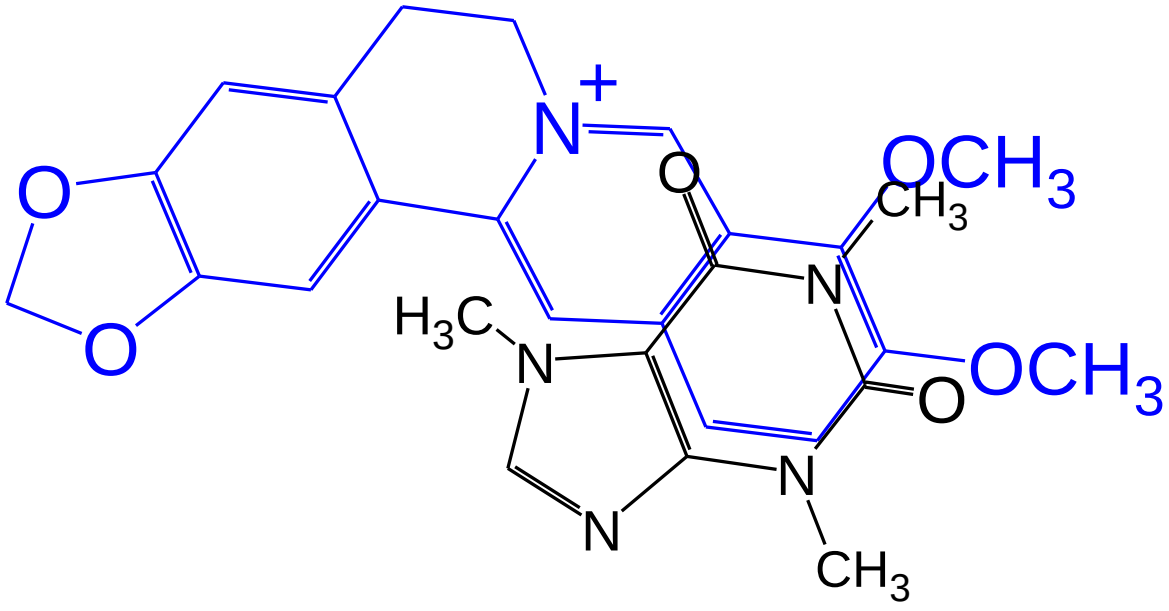

Figure 4.6: Most Probable Orientation of Berberine and Caffeine

Figure 4.6 shows the most probable orientation (orientation one) of berberine and caffeine represented as a line drawing with caffeine in black and berberine in blue to give a better view of how the two molecules are overlaid onto each other. This orientation was chosen as the most probable because its three factors that agreed with another (the interactions listed above) gave it the best interaction energy in comparison with the other orientations attempted. Figures 4.7-4.10 illustrate the four orientations of berberine and caffeine attempted.

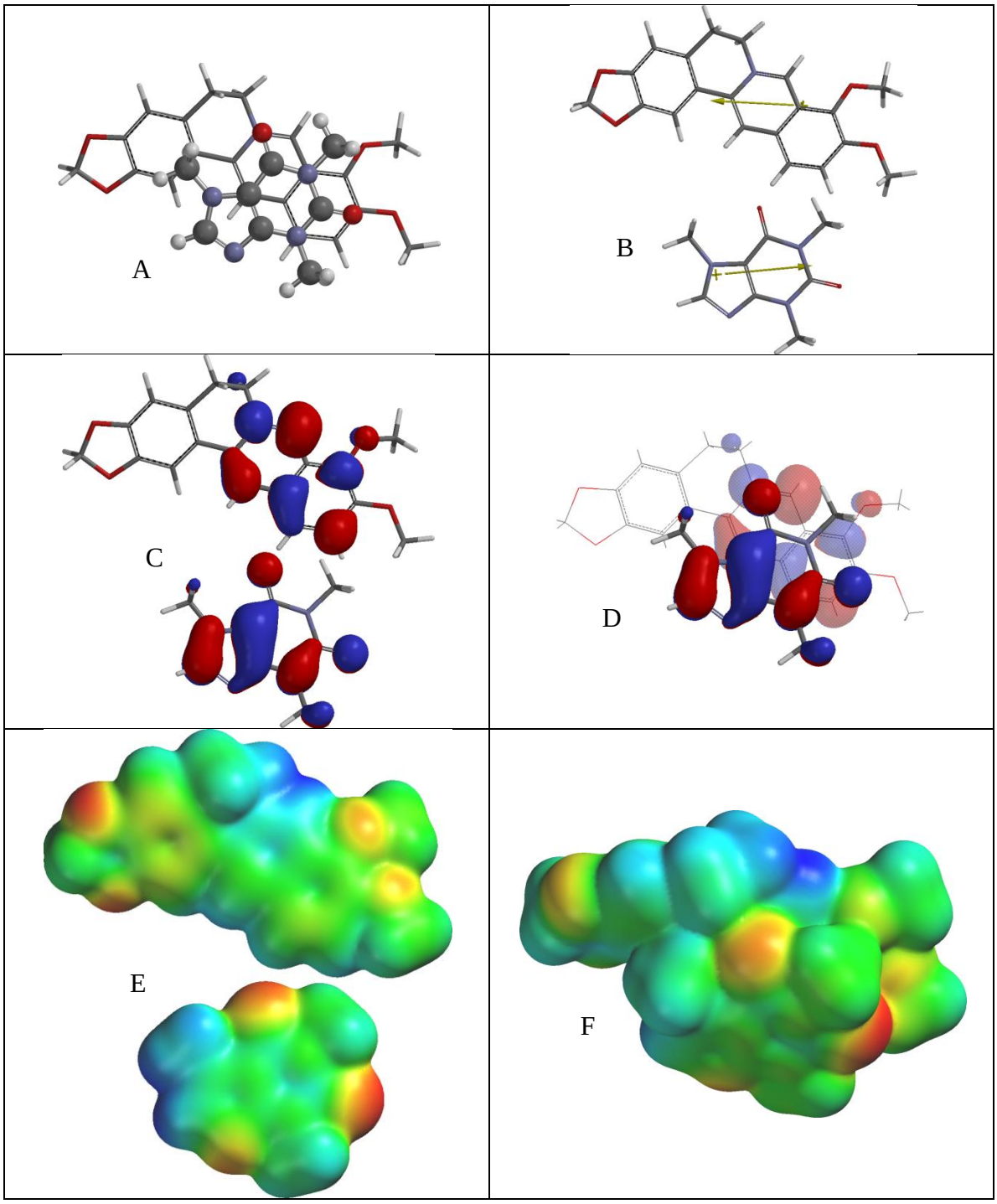

Figure 4.7. Lowest-Energy Orientation of the π – π Complex between Berberine and Caffeine. [(A) Face-to face orientation of caffeine (ball and spoke model) in its lowest-energy orientation with berberine (tube model). (B) Molecular dipoles of berberine (top) and caffeine (bottom). (C) LUMO of berberine (top) and HOMO of caffeine (bottom). (D) Frontier molecular orbital overlap of caffeine with berberine in the lowest-energy orientation. (E) Electrostatic potential maps of berberine (top) and caffeine (bottom). (F) Electrostatic potential map of the lowest-energy π – π complex between berberine and caffeine.]

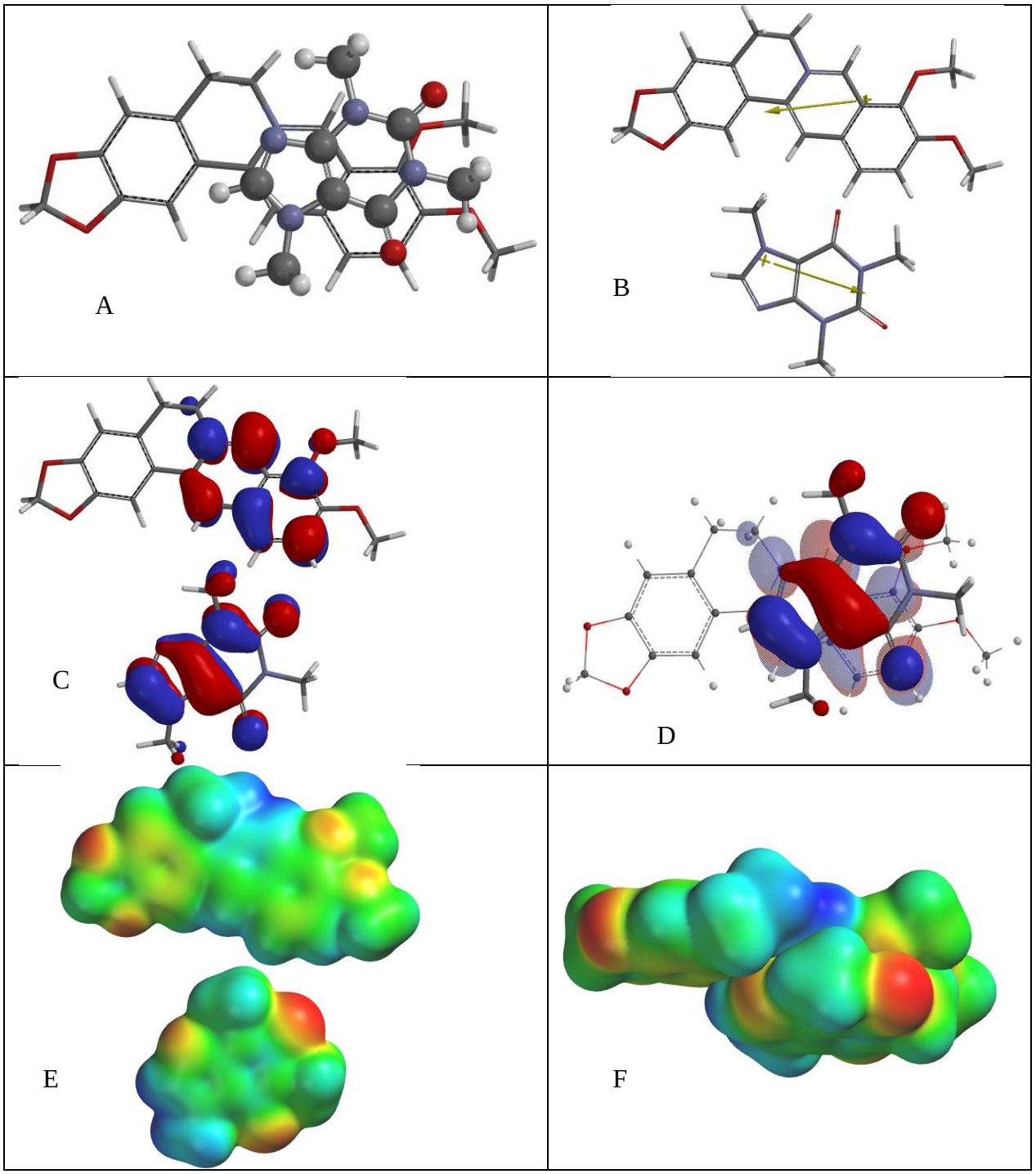

Figure 4.8. Second Orientation of the π – π Complex between Berberine and Caffeine. [(A) Face-to face orientation of caffeine (ball and spoke model) with berberine (tube model). (B) Molecular dipoles of berberine (top) and caffeine (bottom). (C) LUMO of berberine (top) and HOMO of caffeine (bottom). (D) Frontier molecular orbital overlap of caffeine with berberine. (E) Electrostatic potential maps of berberine (top) and caffeine (bottom). (F) Electrostatic potential map of the π – π complex between berberine and caffeine.]

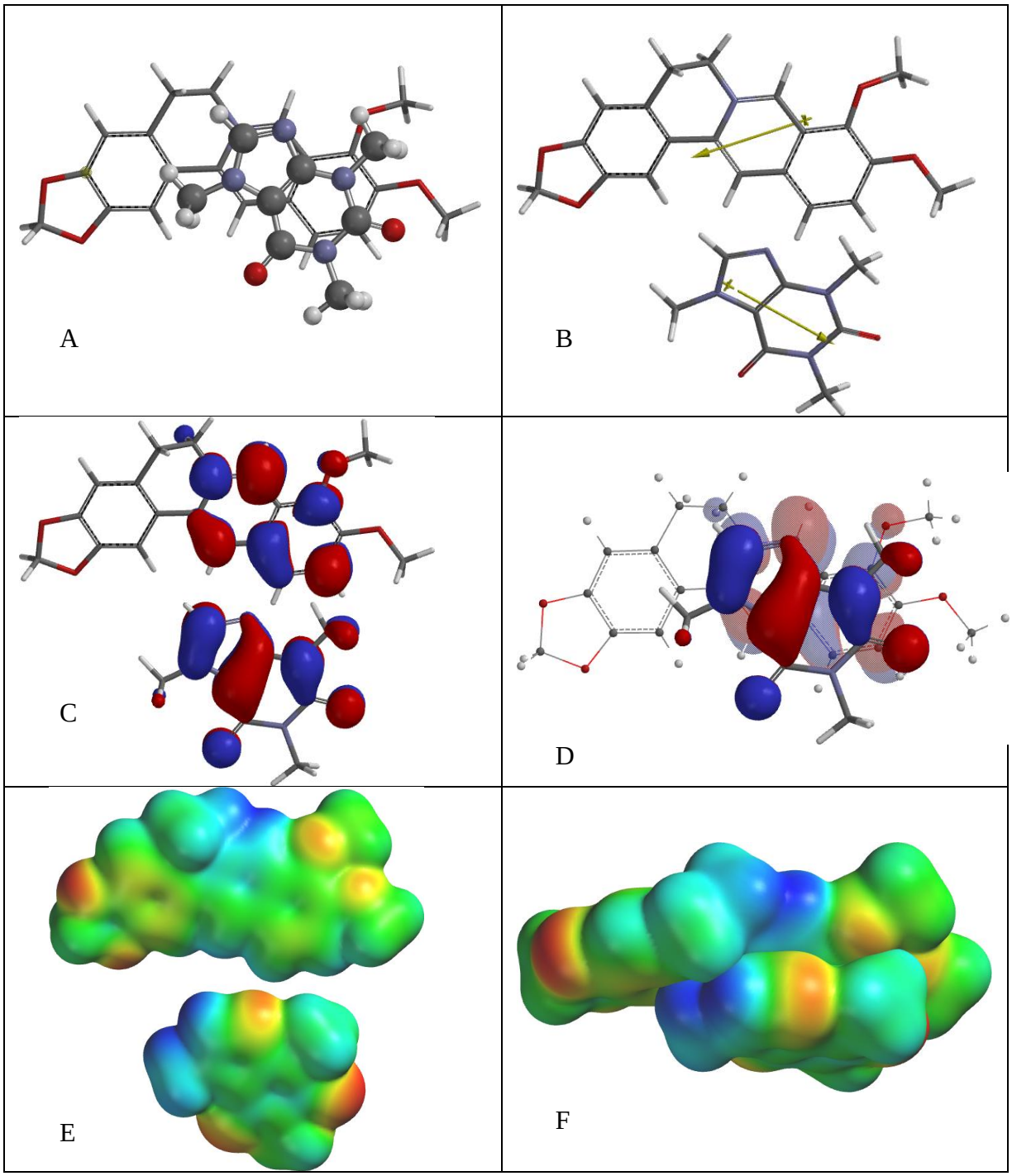

Figure 4.9. Third Orientation of the π – π Complex between Berberine and Caffeine. [(A) Face-to face orientation of caffeine (ball and spoke model) with berberine (tube model). (B) Molecular dipoles of berberine (top) and caffeine (bottom). (C) LUMO of berberine (top) and HOMO of caffeine (bottom). (D) Frontier molecular orbital overlap of caffeine with berberine. (E) Electrostatic potential maps of berberine (top) and caffeine (bottom). (F) Electrostatic potential map of the π – π complex between berberine and caffeine.]

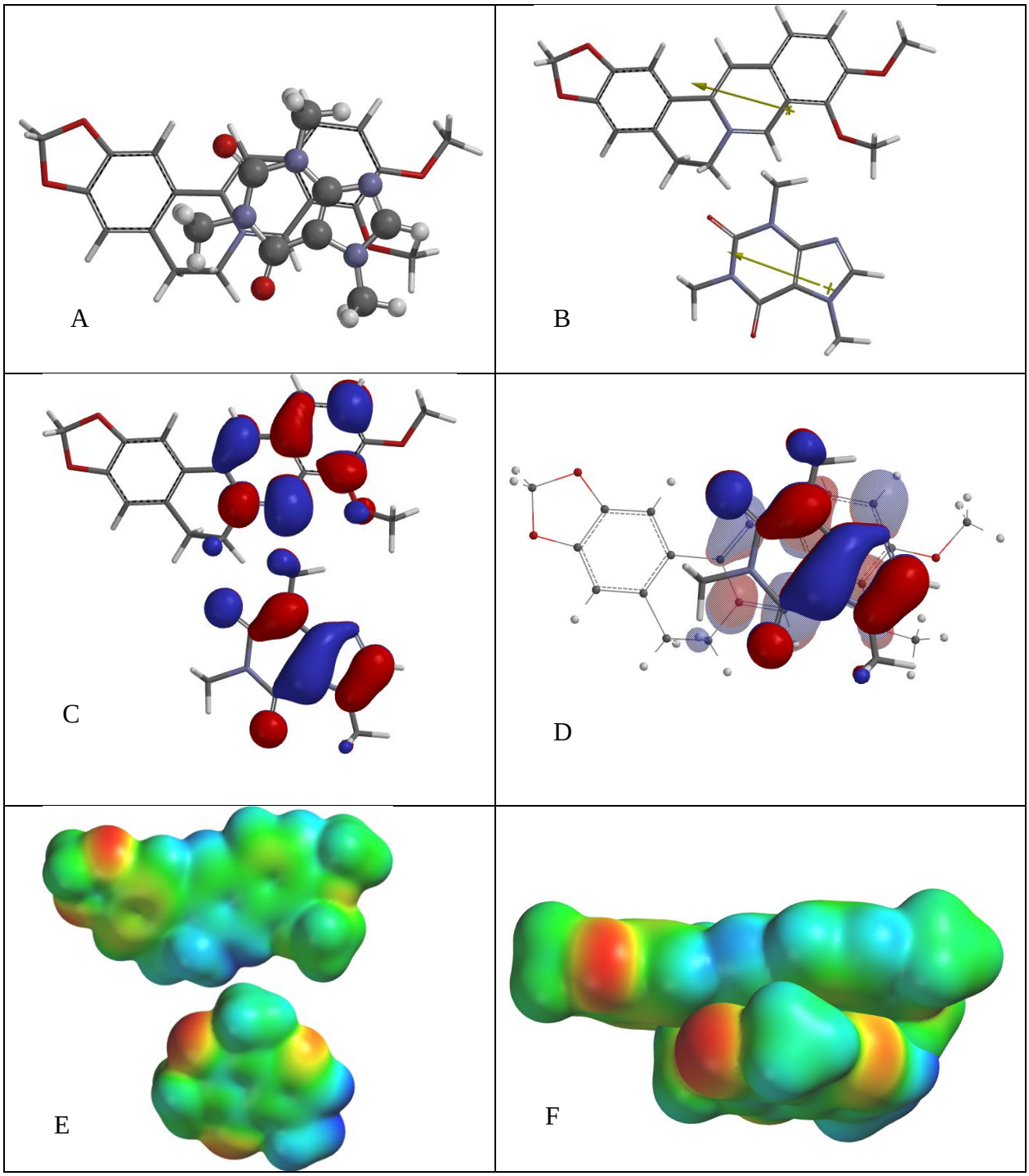

Figure 4.10. Fourth Orientation of the π – π Complex between Berberine and Caffeine. [(A) Face-to face orientation of caffeine (ball and spoke model) with berberine (tube model). (B) Molecular dipoles of berberine (top) and caffeine (bottom). (C) LUMO of berberine (top) and HOMO of caffeine (bottom). (D) Frontier molecular orbital overlap of caffeine with berberine. (E) Electrostatic potential maps of berberine (top) and caffeine (bottom). (F) Electrostatic potential map of the π – π complex between berberine and caffeine.]

For the most probable orientation shown in Figure 4.7, berberine and caffeine exhibit excellent dipole-dipole interaction as the dipoles are opposing each other, and also exhibit good frontier molecular orbital alignment and good electrostatic potential. For the orientation shown in Figure 4.8, berberine and caffeine exhibit excellent dipole-dipole interaction as the dipoles are opposing each other, good electrostatic potential, but poor frontier molecular orbital alignment. For the orientation shown in Figure 4.9, berberine and caffeine exhibit excellent dipole-dipole interaction as the dipoles are opposing each other, good electrostatic potential, but poor frontier molecular orbital alignment. For the orientation shown in Figure 4.10, berberine and caffeine exhibit poor dipole-dipole interaction as the dipoles align with each other, poor electrostatic potential, but fair frontier molecular orbital alignment.

4.3.2 Chelerythrine

The interaction energy of the most probable orientation of chelerythrine and caffeine (the sixth orientation) was found to be -20.33 kcal/mol in the gas phase and -16.51 kcal/mol in aqueous solution. These values were found by adding the individual energies found separately for caffeine and for chelerythrine, then subtracting that value from energies derived from different orientations of the caffeine/chelerythrine pair. The total energies of the chelerythrine and caffeine molecules and their energy differences (interaction energies) are listed in Table 4.8.

Table 4.8: Interaction energies of chelerythrine and caffeine in different orientations.

	E_{vac} (kcal/mol)	E_{aq} (kcal/mol)
Caffeine	-426682.1	-426688.59
Chelerythrine	-731498.99	-731534.32
Sum of energies	-1158181.09	-1158222.91
Orientation 1	-1158198.71	-1158234.49
Interaction energy	-17.62	-11.58
Orientation 2	-1158199.48	-1158235.5
Interaction energy	-18.39	-12.59
Orientation 3	-1158199.58	-1158234.8
Interaction energy	-18.49	-11.89
Orientation 4	-1158200.04	-1158235.4
Interaction energy	-18.95	-12.49
Orientation 5	-1158201.63	-1158237.03
Interaction energy	-20.54	-14.12
Orientation 6 (lowest)	-1158201.42	-1158239.42
Interaction energy	-20.33	-16.51

Out of six caffeine/chelerythrine orientations, the sixth orientation showed the most probability for what is actually happening between the two molecules in aqueous solution, exhibiting good overlap of molecular orbitals (HOMO and LUMO) and good electrostatic interactions. In this alignment, the docked molecules also showed opposing dipoles which made this orientation more agreeable.

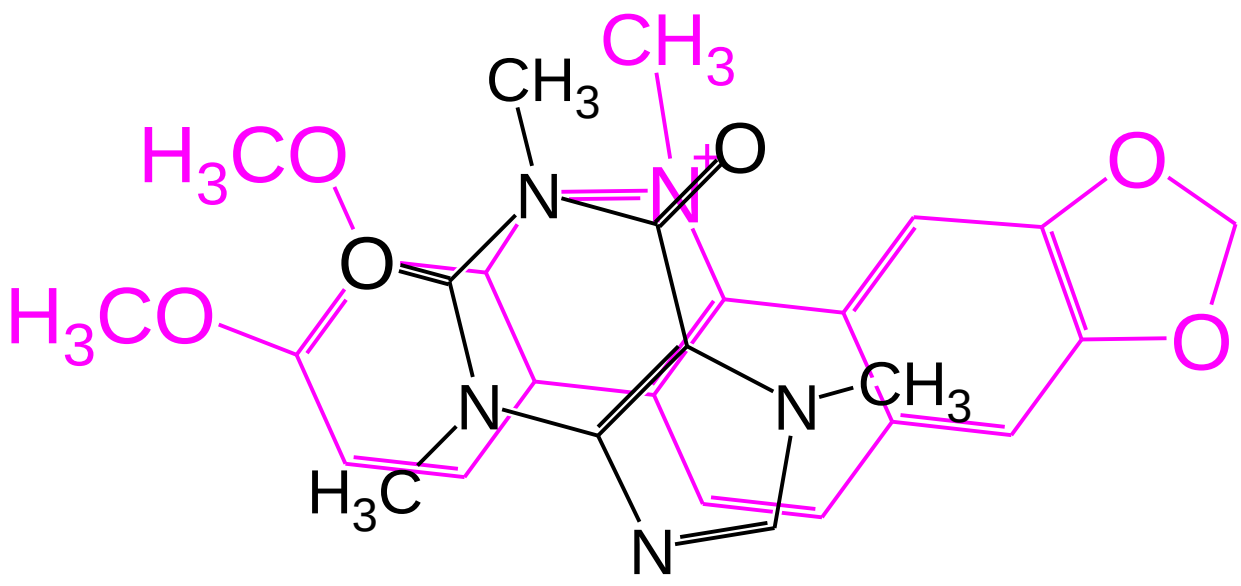

Figure 4.11: Most Probable Orientation of Chelerythrine and Caffeine

Figure 4.11 shows the most probable orientation of chelerythrine and caffeine represented as a line drawing with caffeine in black and chelerythrine in pink to give a better view of how the two molecules are overlaid onto each other. This orientation was chosen as the most probable because its three factors that agreed with another (the interactions listed above) gave it the best interaction energy in comparison with the other orientations attempted. Figures 4.12-4.17 illustrate the six orientations of chelerythrine and caffeine attempted.

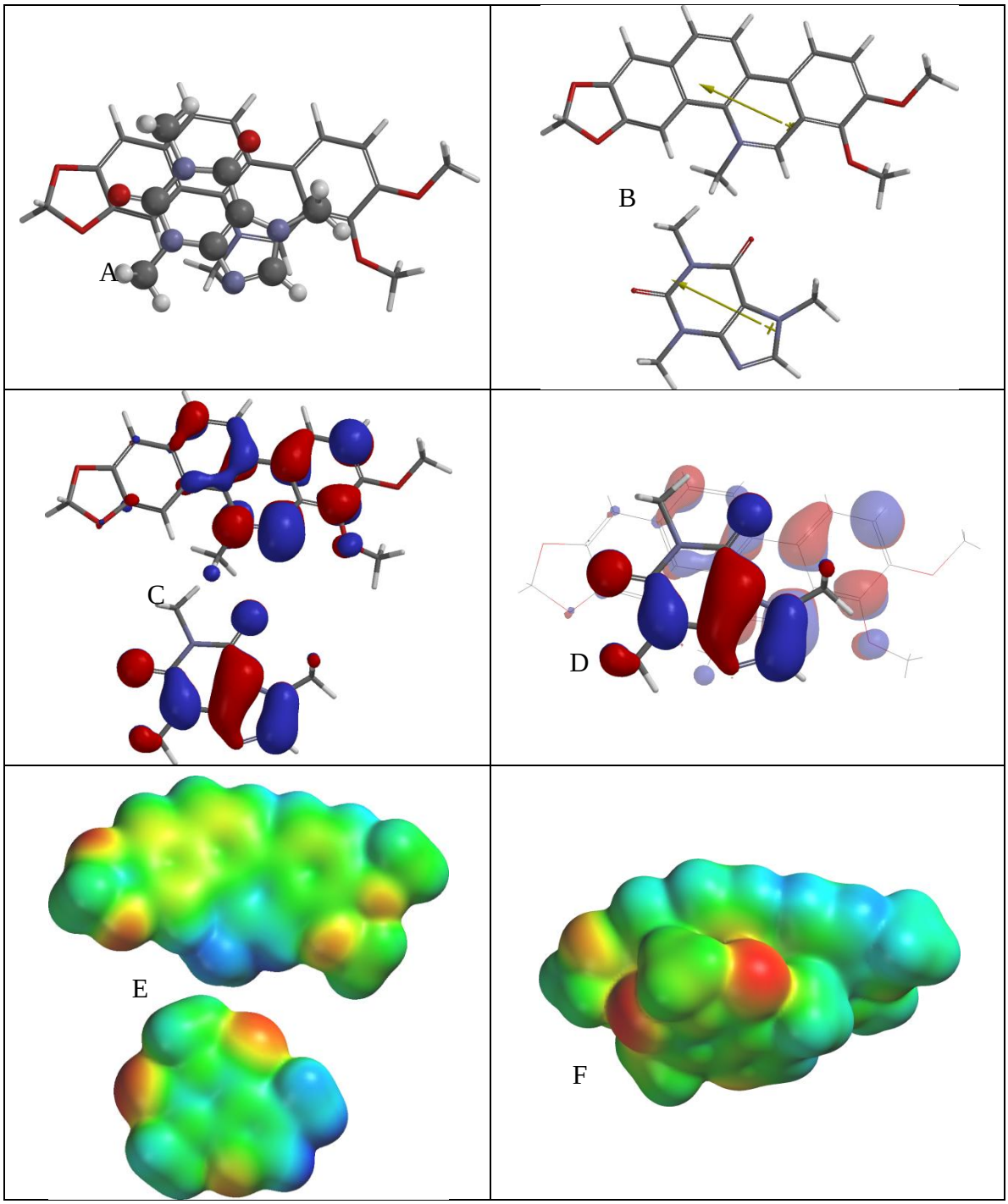

Figure 4.12. First Orientation of the π – π Complex between Chelerythrine and Caffeine. [(A) Face-to face orientation of caffeine (ball and spoke model) with chelerythrine (tube model). (B) Molecular dipoles of chelerythrine (top) and caffeine (bottom). (C) LUMO of chelerythrine (top) and HOMO of caffeine (bottom). (D) Frontier molecular orbital overlap of caffeine with chelerythrine. (E) Electrostatic potential maps of chelerythrine (top) and caffeine (bottom). (F) Electrostatic potential map of the π – π complex between chelerythrine and caffeine.]

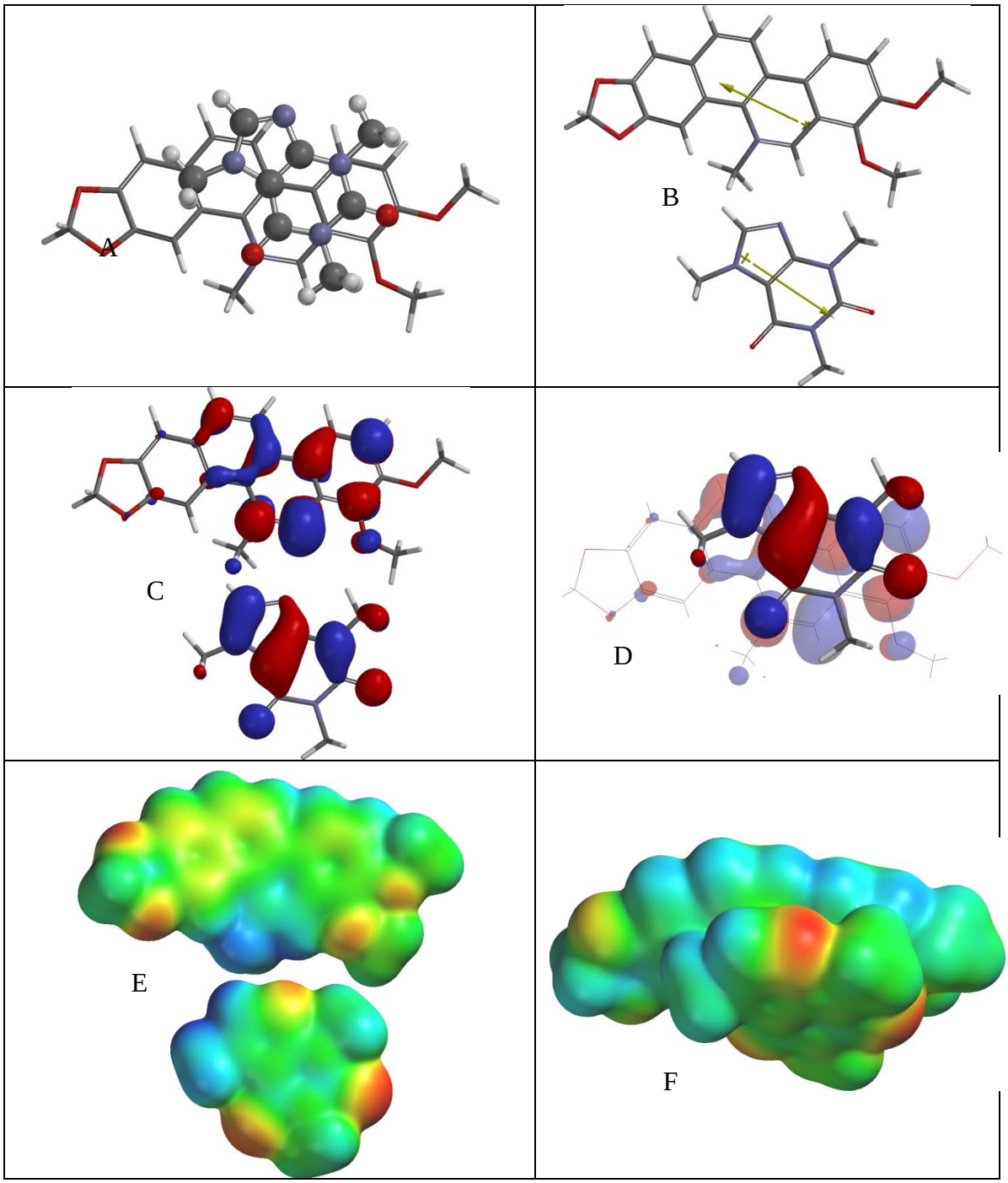

Figure 4.13. Second Orientation of the π – π Complex between Chelerythrine and Caffeine. [(A) Face-to face orientation of caffeine (ball and spoke model) with chelerythrine (tube model). (B) Molecular dipoles of chelerythrine (top) and caffeine (bottom). (C) LUMO of chelerythrine (top) and HOMO of caffeine (bottom). (D) Frontier molecular orbital overlap of caffeine with chelerythrine. (E) Electrostatic potential maps of chelerythrine (top) and caffeine (bottom). (F) Electrostatic potential map of the π – π complex between chelerythrine and caffeine.]

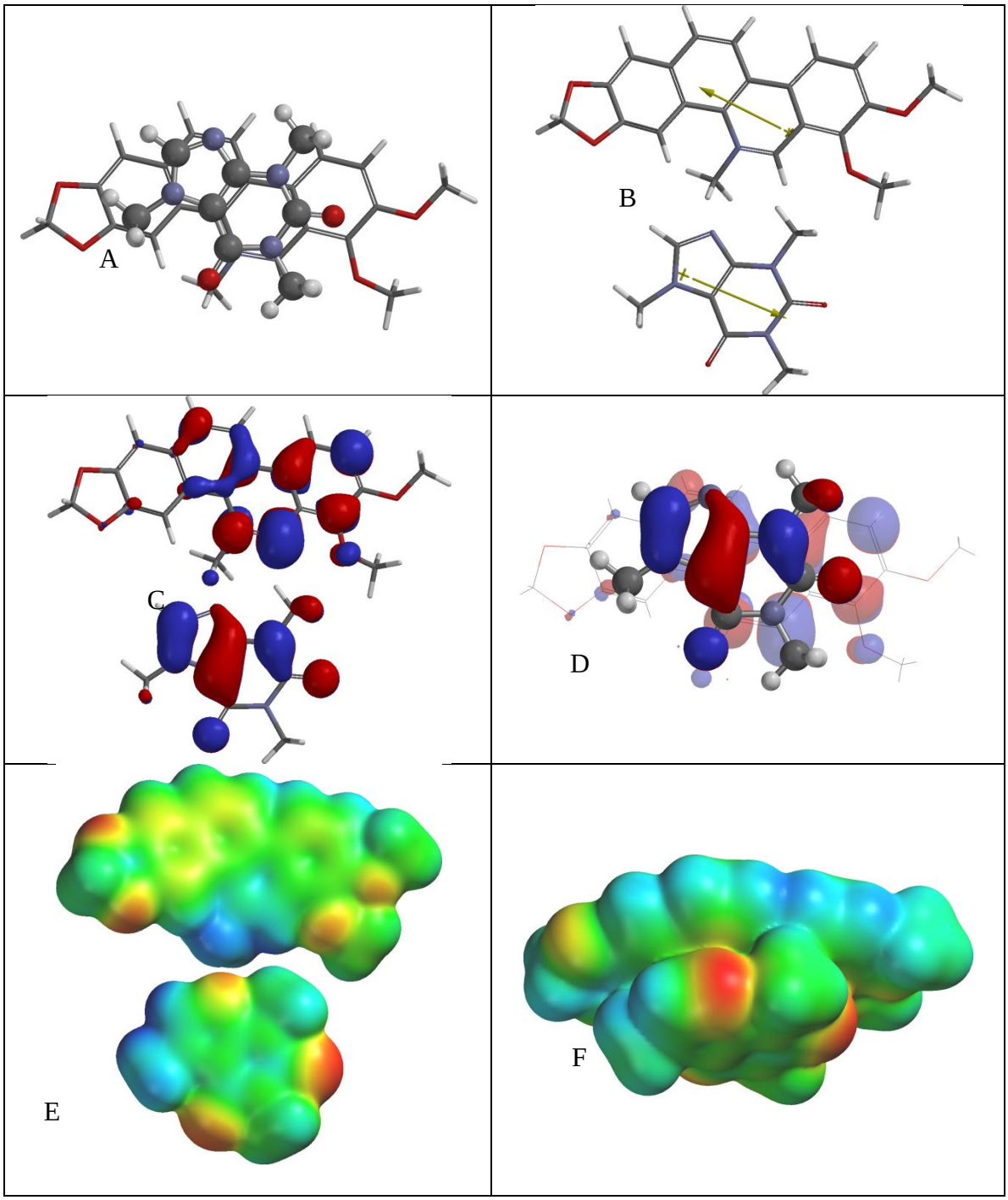

Figure 4.14. Third Orientation of the π – π Complex between Chelerythrine and Caffeine. [(A) Face-to face orientation of caffeine (ball and spoke model) with chelerythrine (tube model). (B) Molecular dipoles of chelerythrine (top) and caffeine (bottom). (C) LUMO of chelerythrine (top) and HOMO of caffeine (bottom). (D) Frontier molecular orbital overlap of caffeine with chelerythrine. (E) Electrostatic potential maps of chelerythrine (top) and caffeine (bottom). (F) Electrostatic potential map of the π – π complex between chelerythrine and caffeine.]

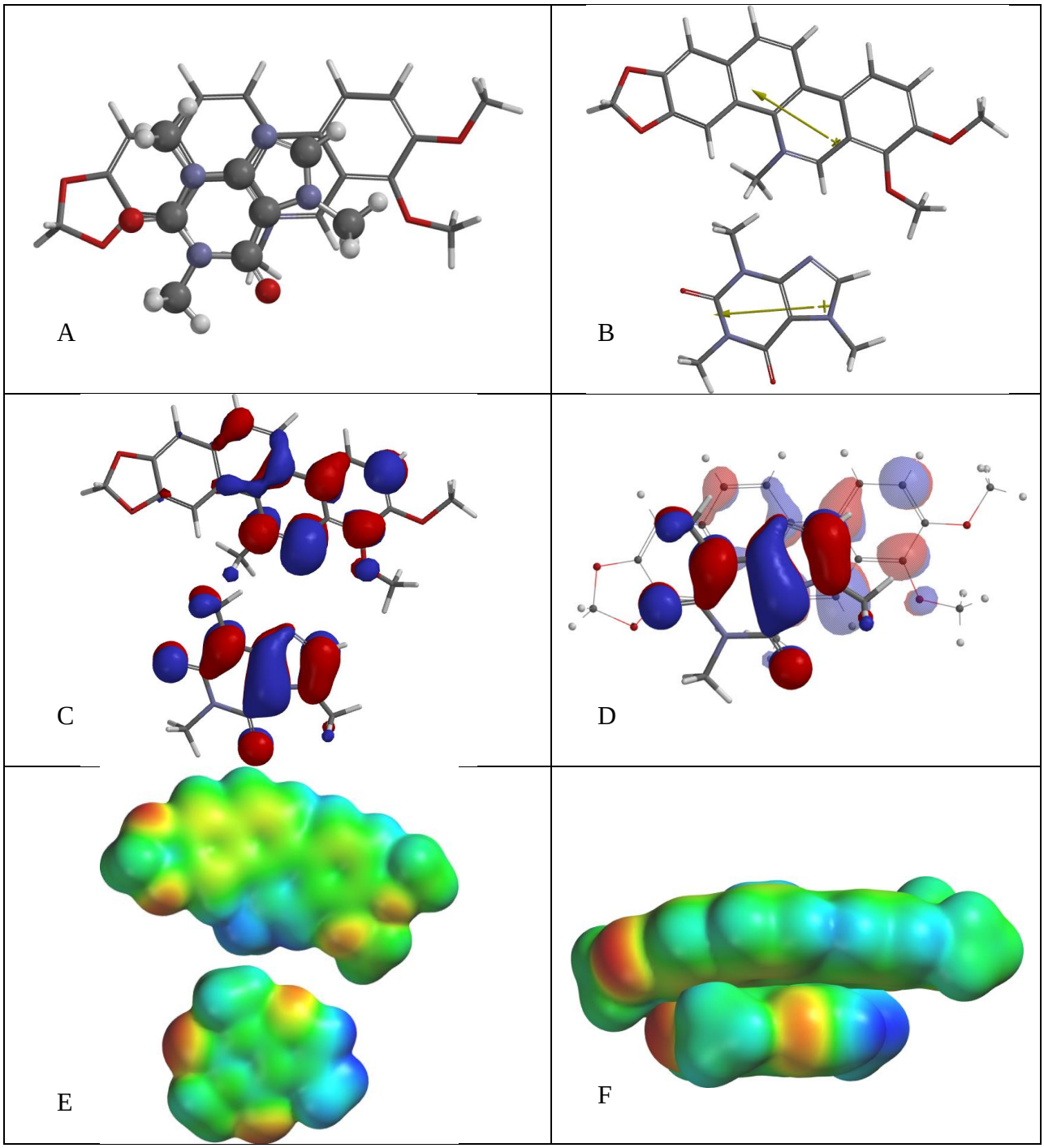

Figure 4.15. Fourth Orientation of the π – π Complex between Chelerythrine and Caffeine. [(A) Face-to face orientation of caffeine (ball and spoke model) with chelerythrine (tube model). (B) Molecular dipoles of chelerythrine (top) and caffeine (bottom). (C) LUMO of chelerythrine (top) and HOMO of caffeine (bottom). (D) Frontier molecular orbital overlap of caffeine with chelerythrine. (E) Electrostatic potential maps of chelerythrine (top) and caffeine (bottom). (F) Electrostatic potential map of the π – π complex between chelerythrine and caffeine.]

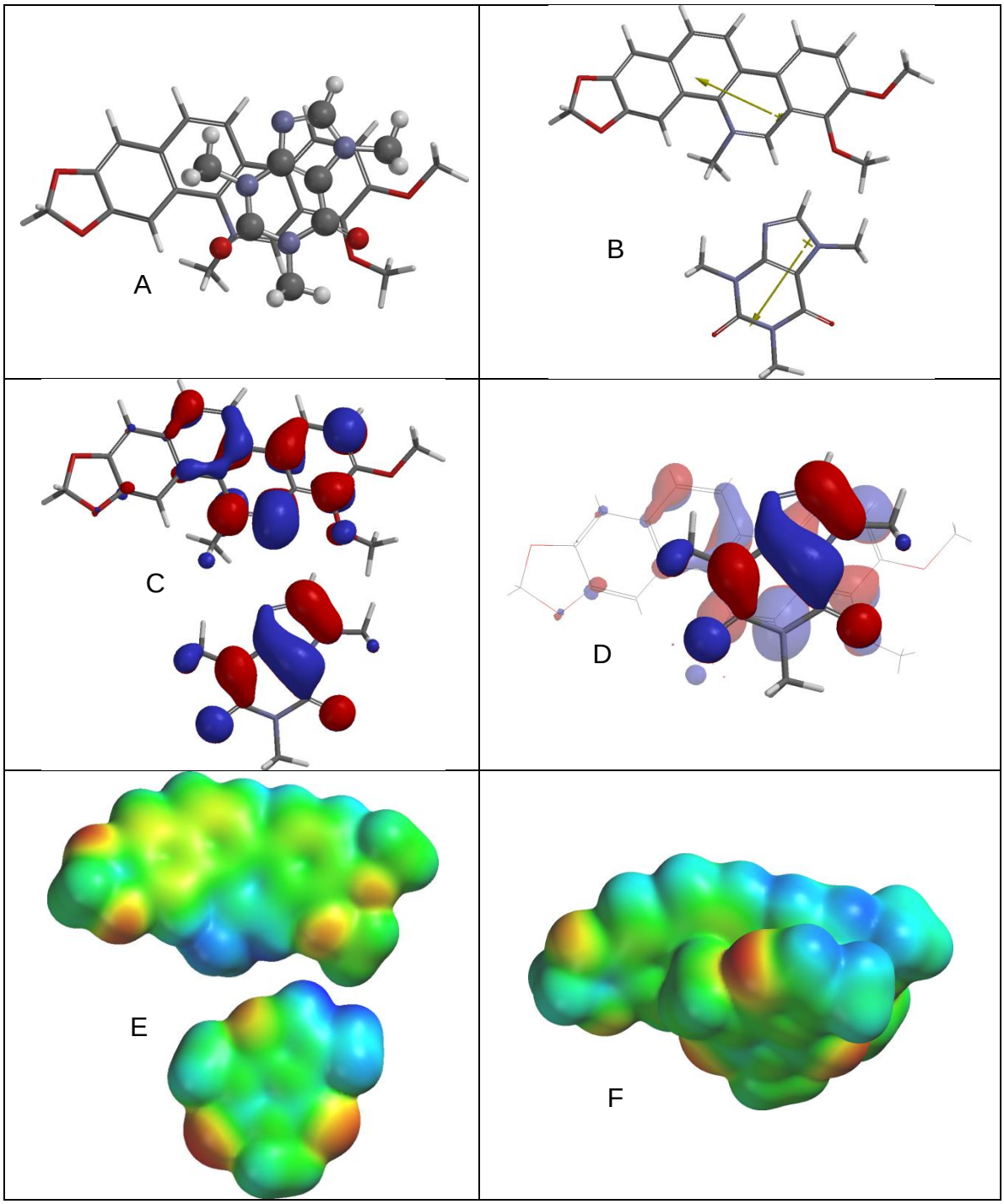

Figure 4.16. Fifth Orientation of the π – π Complex between Chelerythrine and Caffeine. [(A) Face-to face orientation of caffeine (ball and spoke model) with chelerythrine (tube model). (B) Molecular dipoles of chelerythrine (top) and caffeine (bottom). (C) LUMO of chelerythrine (top) and HOMO of caffeine (bottom). (D) Frontier molecular orbital overlap of caffeine with chelerythrine. (E) Electrostatic potential maps of chelerythrine (top) and caffeine (bottom). (F) Electrostatic potential map of the π – π complex between chelerythrine and caffeine.]

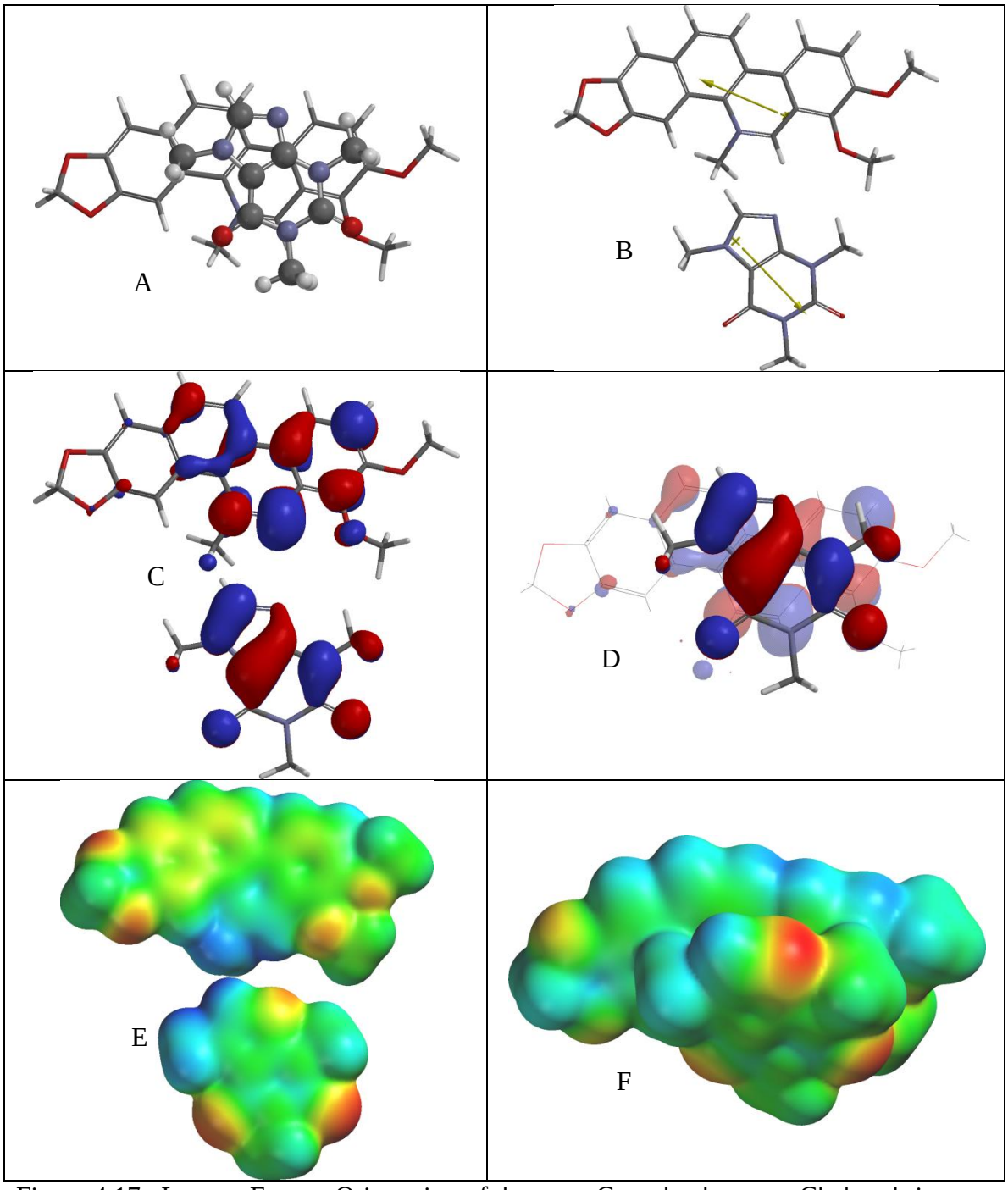

Figure 4.17. Lowest-Energy Orientation of the π – π Complex between Chelerythrine and Caffeine. [(A) Face-to face orientation of caffeine (ball and spoke model) in its lowest-energy orientation with chelerythrine (tube model). (B) Molecular dipoles of chelerythrine (top) and caffeine (bottom). (C) LUMO of chelerythrine (top) and HOMO of caffeine (bottom). (D) Frontier molecular orbital overlap of caffeine with chelerythrine in the lowest-energy orientation. (E) Electrostatic potential maps of chelerythrine (top) and caffeine (bottom). (F) Electrostatic potential map of the lowest-energy π – π complex between chelerythrine and caffeine.]

For the orientation shown in Figure 4.12, chelerythrine and caffeine exhibit poor dipole-dipole interaction as the dipoles align with each other, good electrostatic potential, and good frontier molecular orbital alignment. For the orientation shown in Figure 4.13, chelerythrine and caffeine exhibit excellent dipole-dipole interaction as the dipoles are opposing each other, good electrostatic potential, and good frontier molecular orbital alignment. For the orientation shown in Figure 4.14, chelerythrine and caffeine exhibit excellent dipole-dipole interaction as the dipoles are opposing each other, good electrostatic potential, and good frontier molecular orbital alignment. For the orientation shown in Figure 4.16, chelerythrine and caffeine exhibit good dipole-dipole interaction as the dipoles are 90º to each other, good electrostatic potential, and good frontier molecular orbital alignment. For the orientation shown in Figure 4.17, the lowest energy orientation, chelerythrine and caffeine exhibit good dipole-dipole interaction as the dipoles are opposing each other, good electrostatic potential, but poor frontier molecular orbital alignment.

4.3.3 Ellipticine

The interaction energy of ellipticine and caffeine was found to be -16.83 kcal/mol in the gas phase and -11.02 kcal/mol in aqueous solution. These values were found by adding the individual energies found separately for caffeine and for ellipticine, then subtracting that value from energies derived from different orientations of the caffeine/ellipticine pair. Out of four caffeine/ellipticine orientations, the orientation (orientation 3) that showed the most probability for what is actually happening between the two molecules in aqueous solution exhibited good overlap of molecular orbitals (HOMO and LUMO) and good electrostatic and charge interactions. The dipole-dipole

interactions, however, were not opposed, and thus did not agree. The total energies of the ellipticine and caffeine molecules and their energy differences (interaction energies) are listed in Table 4.9.

Table 4.9: Interaction energies of ellipticine and caffeine in different orientations.

	E_{vac} (kcal/mol)	E_{aq} (kcal/mol)
Caffeine	-426682.26	-426689.01
Ellipticine	-480176.77	-480183.84
Sum of energies	-906859.03	-906872.85
Orientation 1	-906873.16	-906882.75
Interaction energy	-14.13	-9.90
Orientation 2	-906872.95	-906881.96
Interaction energy	-13.92	-9.11
Orientation 3 (lowest)	-906875.86	-906883.87
Interaction energy	-16.83	-11.02
Orientation 4	-906872.54	-906882.56
Interaction energy	-13.51	-9.71

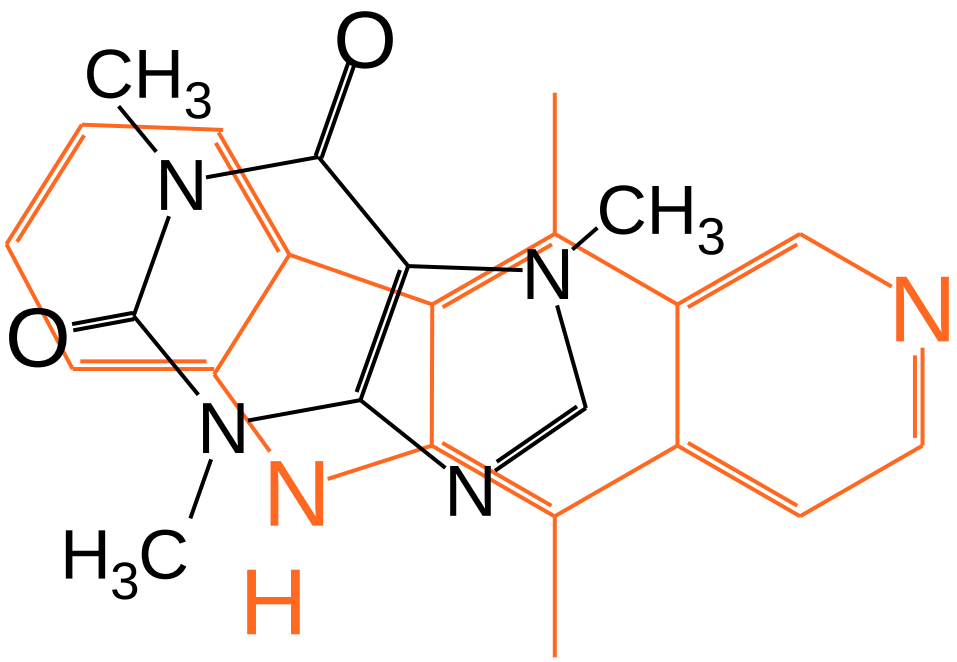

Figure 4.18: Most Probable Orientation of Ellipticine and Caffeine

Figure 4.18 shows the most probable orientation of ellipticine and caffeine represented as a line drawing with caffeine in black and ellipticine in orange to give a better view of how the two molecules are overlaid onto each other. This orientation (orientation three) was chosen as the most probable because its two factors that agreed with another (the interactions listed above) gave it the best interaction energy in comparison with the other orientations attempted. Figures 4.19-4.24 illustrate the six orientations of ellipticine and caffeine attempted.

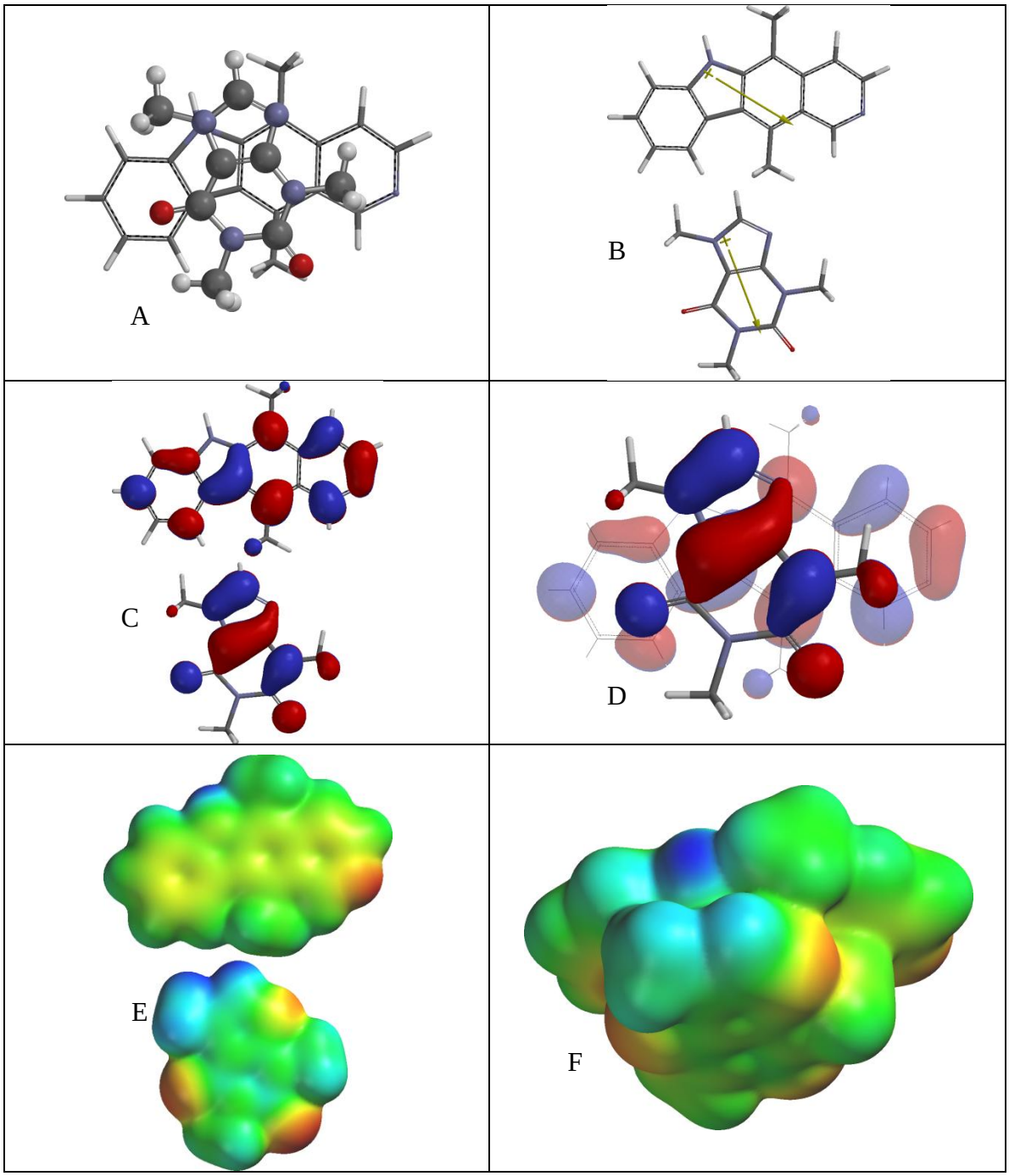

Figure 4.19. First Orientation of the π – π Complex between Ellipticine and Caffeine. [(A) Face-to face orientation of caffeine (ball and spoke model) with ellipticine (tube model). (B) Molecular dipoles of ellipticine (top) and caffeine (bottom). (C) LUMO of ellipticine (top) and HOMO of caffeine (bottom). (D) Frontier molecular orbital overlap of caffeine with ellipticine. (E) Electrostatic potential maps of ellipticine (top) and caffeine (bottom). (F) Electrostatic potential map of the π – π complex between ellipticine and caffeine.]

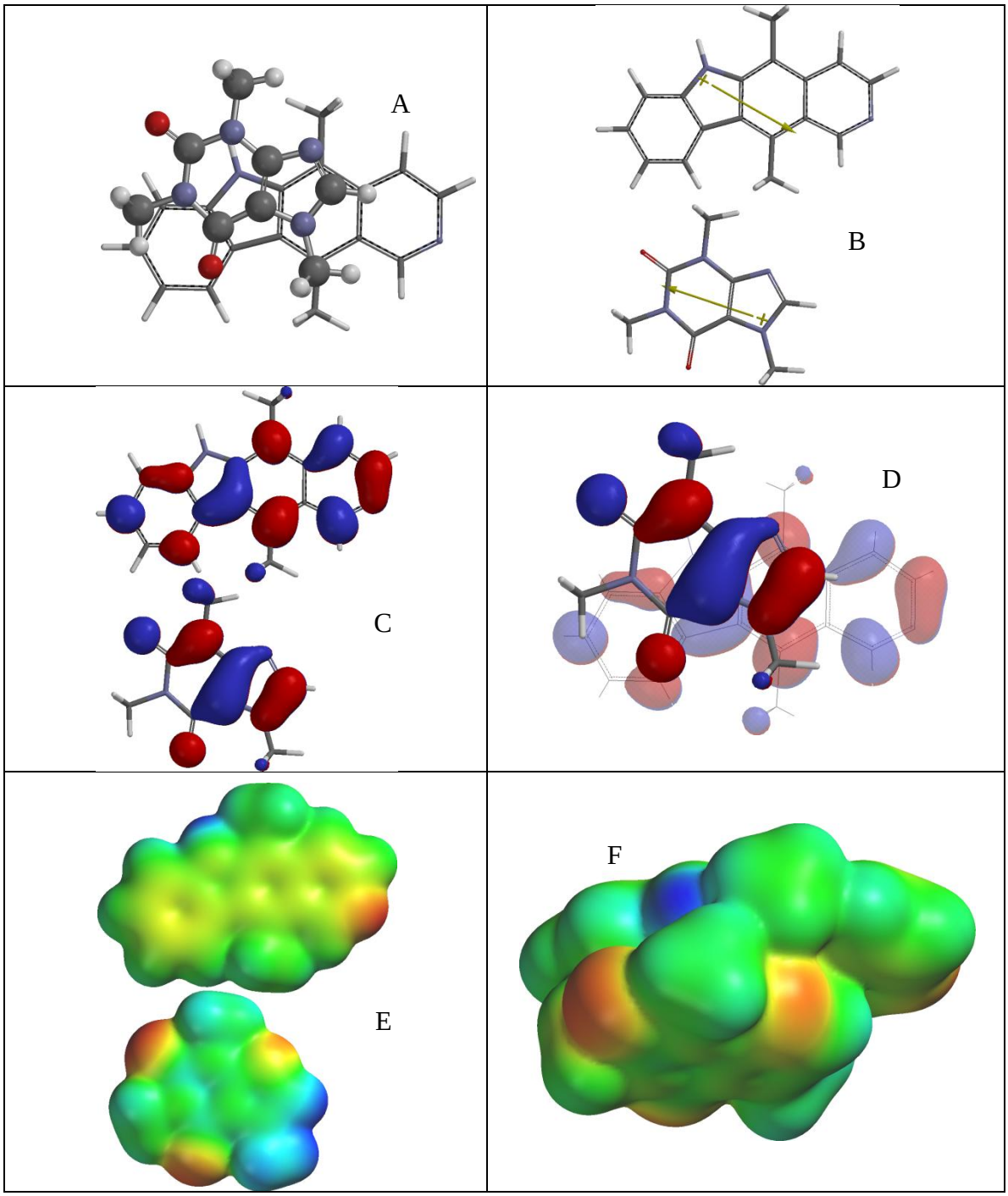

Figure 4.20. Second Orientation of the π – π Complex between Ellipticine and Caffeine. [(A) Face-to face orientation of caffeine (ball and spoke model) with ellipticine (tube model). (B) Molecular dipoles of ellipticine (top) and caffeine (bottom). (C) LUMO of ellipticine (top) and HOMO of caffeine (bottom). (D) Frontier molecular orbital overlap of caffeine with ellipticine. (E) Electrostatic potential maps of ellipticine (top) and caffeine (bottom). (F) Electrostatic potential map of the π – π complex between ellipticine and caffeine.]

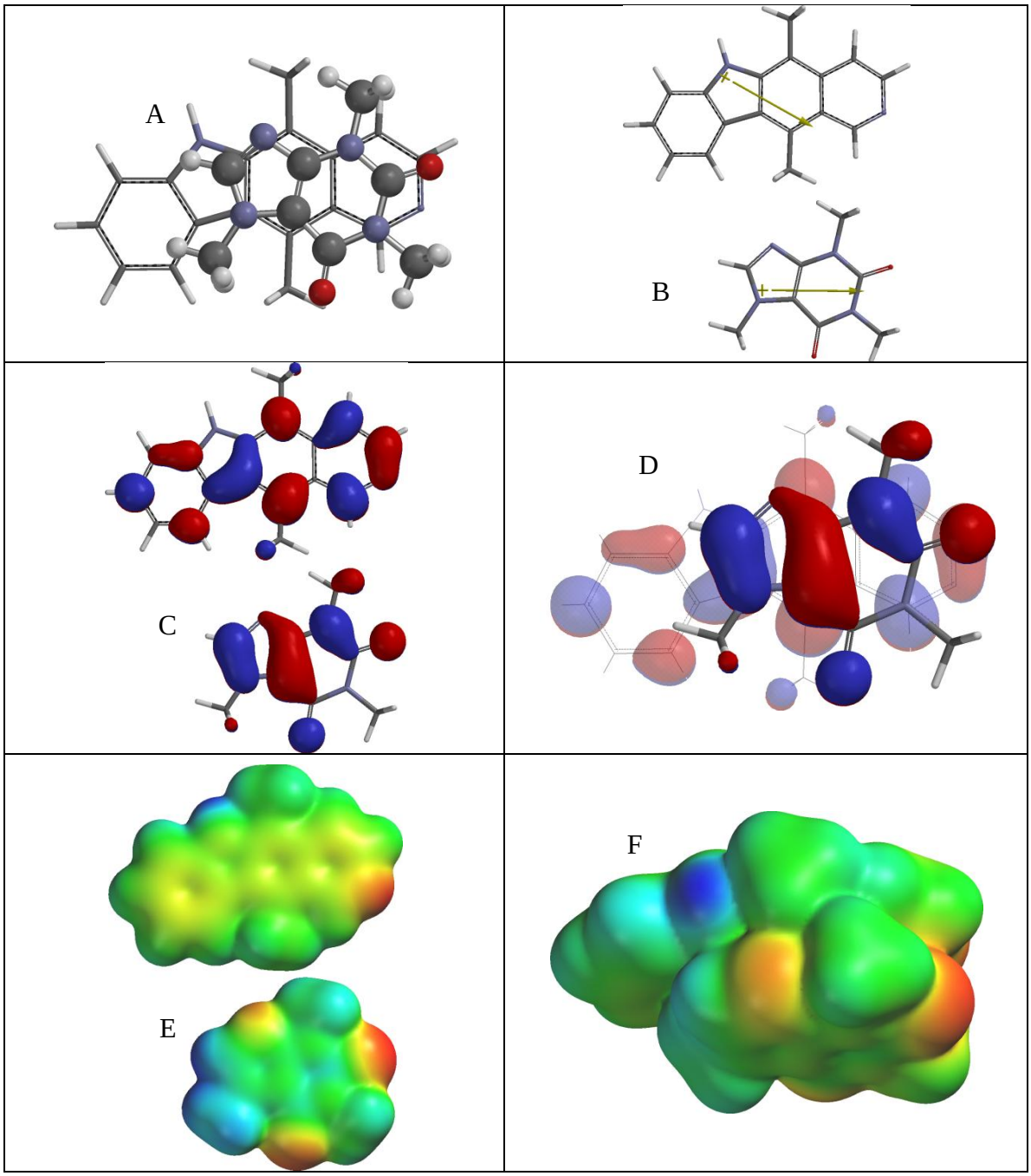

Figure 4.21. Lowest-Energy Orientation of the π – π Complex between Ellipticine and Caffeine. [(A) Face-to face orientation of caffeine (ball and spoke model) in its lowest-energy orientation with ellipticine (tube model). (B) Molecular dipoles of ellipticine (top) and caffeine (bottom). (C) LUMO of ellipticine (top) and HOMO of caffeine (bottom). (D) Frontier molecular orbital overlap of caffeine with ellipticine in the lowest-energy orientation. (E) Electrostatic potential maps of ellipticine (top) and caffeine (bottom). (F) Electrostatic potential map of the lowest-energy π – π complex between ellipticine and caffeine.]

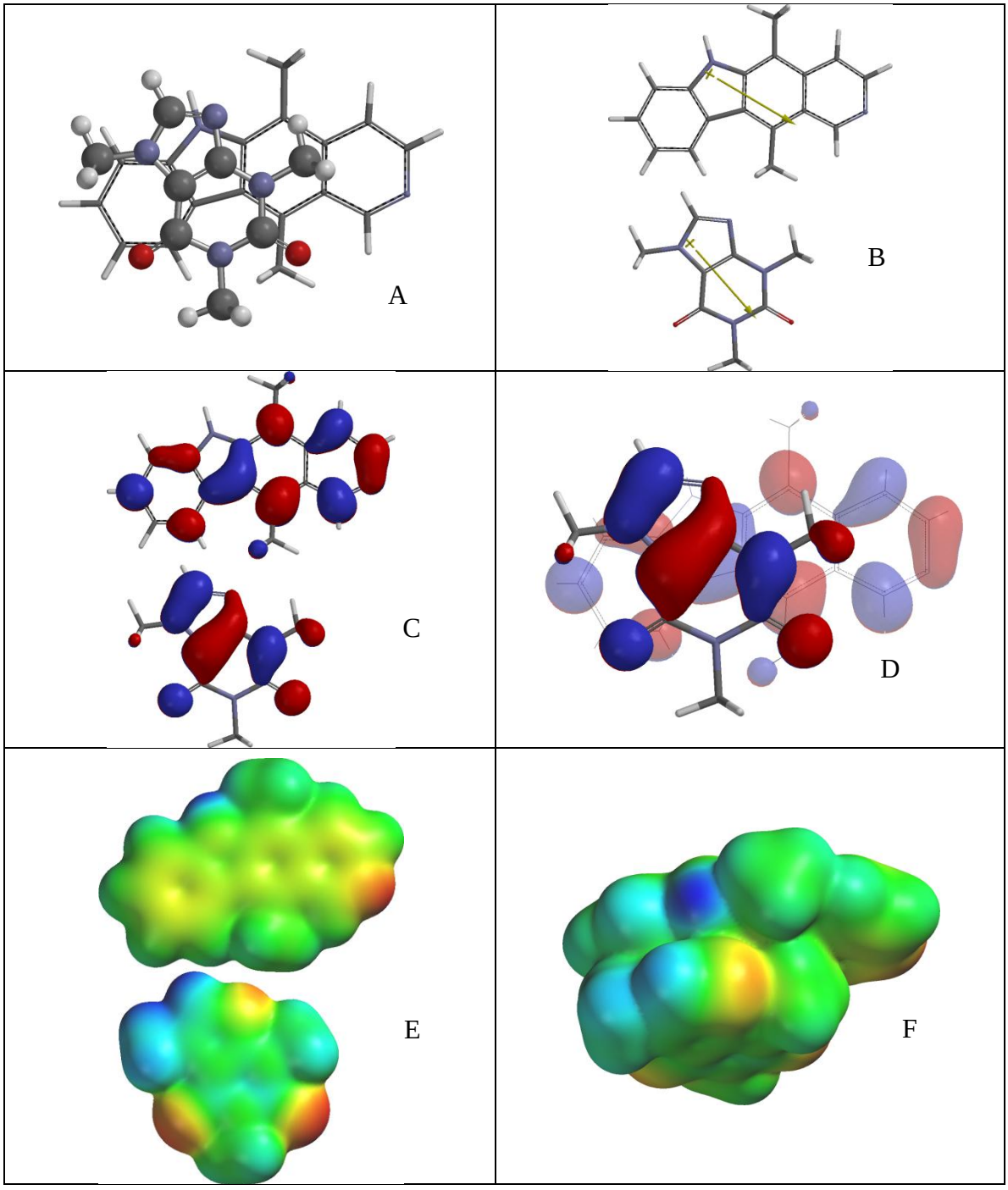

Figure 4.22. Fourth Orientation of the π – π Complex between Ellipticine and Caffeine. [(A) Face-to face orientation of caffeine (ball and spoke model) with ellipticine (tube model). (B) Molecular dipoles of ellipticine (top) and caffeine (bottom). (C) LUMO of ellipticine (top) and HOMO of caffeine (bottom). (D) Frontier molecular orbital overlap of caffeine with ellipticine. (E) Electrostatic potential maps of ellipticine (top) and caffeine (bottom). (F) Electrostatic potential map of the π – π complex between ellipticine and caffeine.]

For the orientation shown in Figure 4.19, ellipticine and caffeine exhibit good electrostatic potential and good frontier molecular orbital alignment, but poor dipole-dipole interaction as the dipoles align with each other. For the orientation shown in Figure 4.20, ellipticine and caffeine exhibit good electrostatic potential, good frontier molecular orbital alignment, and excellent dipole-dipole interaction as the dipoles oppose each other. For the orientation shown in Figure 4.21, ellipticine and caffeine exhibit good electrostatic potential and good frontier molecular orbital alignment, but poor dipole-dipole interaction as the dipoles align with each other. This figure represents the lowest energy orientation between caffeine and ellipticine. For the orientation shown in Figure 4.22, ellipticine and caffeine exhibit good electrostatic potential and good frontier molecular orbital alignment, but poor dipole-dipole interaction as the dipoles align with each other.

4.3.4 Sanguinarine

The interaction energy of sanguinarine and caffeine was found to be -21.60 kcal/mol in the gas phase and -16.47 kcal/mol in aqueous solution. These values were found by adding the individual energies found separately for caffeine and for sanguinarine, then subtracting that value from energies derived from different orientations of the caffeine/sanguinarine pair. Out of five caffeine/sanguinarine orientations, several of the orientations had aspects about them that made them acceptable orientations. For example, one orientation had good dipole opposition but the frontier molecular orbitals did not line up correctly. The orientation (orientation four) that showed the most probability for what is actually happening between the two molecules in aqueous solution exhibited good overlap of molecular orbitals (HOMO

and LUMO), good electrostatic interaction, and great dipole-dipole opposition. The total energies of the sanguinarine and caffeine molecules and their energy differences (interaction energies) are listed in Table 4.10.

Table 4.10: Interaction energies of sanguinarine and caffeine in different orientations.

	E_{vac} (kcal/mol)	E_{aq} (kcal/mol)
Caffeine	-426682.26	-426689.01
Sanguinarine	-706098.84	-706137.93
Sum of energies	-1132781.10	-1132826.94
Orientation 1	-1132797.68	-1132836.47
Interaction energy	-16.58	-9.53
Orientation 2	-1132797.92	-1132836.95
Interaction energy	-16.82	-10.01
Orientation 3	-1132801.86	-1132840.26
Interaction energy	-20.76	-13.32
Orientation 4 (lowest)	-1132802.18	-1132840.86
Interaction energy	-21.08	-13.92
Orientation 5	-1132802.70	-1132843.41
Interaction energy	-21.60	-16.47

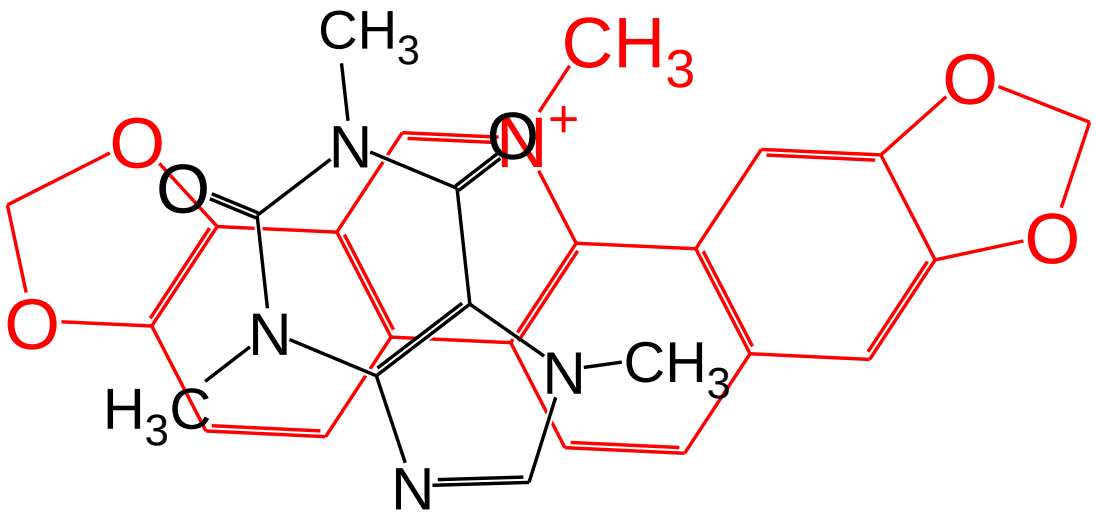

Figure 4.23: Most Probable Orientation of Sanguinarine and Caffeine

Figure 4.23 shows caffeine docked with sanguinarine in red and caffeine in black in its most favorable orientation based on the calculated energies. Because this orientation (orientation four) had three factors that agreed with another (the interactions listed previously) which gave it the best interaction energy in comparison with the other orientations attempted. Figures 4.24-4.28 illustrate the five orientations of sanguinarine and caffeine attempted.

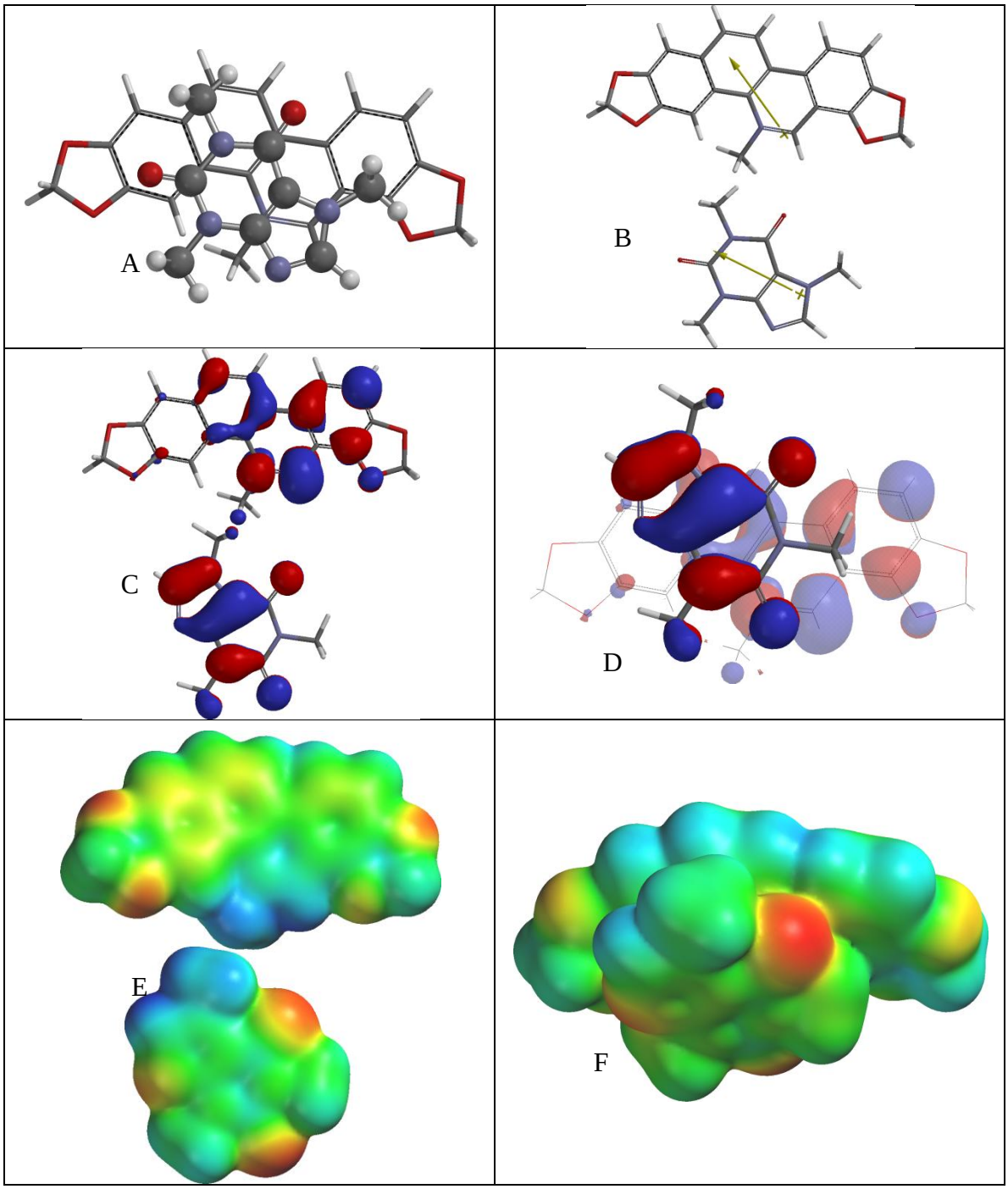

Figure 4.24. First Orientation of the π – π Complex between Sanguinarine and Caffeine. [(A) Face-to face orientation of caffeine (ball and spoke model) with sanguinarine (tube model). (B) Molecular dipoles of sanguinarine (top) and caffeine (bottom). (C) LUMO of sanguinarine (top) and HOMO of caffeine (bottom). (D) Frontier molecular orbital overlap of caffeine with sanguinarine. (E) Electrostatic potential maps of sanguinarine (top) and caffeine (bottom). (F) Electrostatic potential map of the π – π complex between sanguinarine and caffeine.]

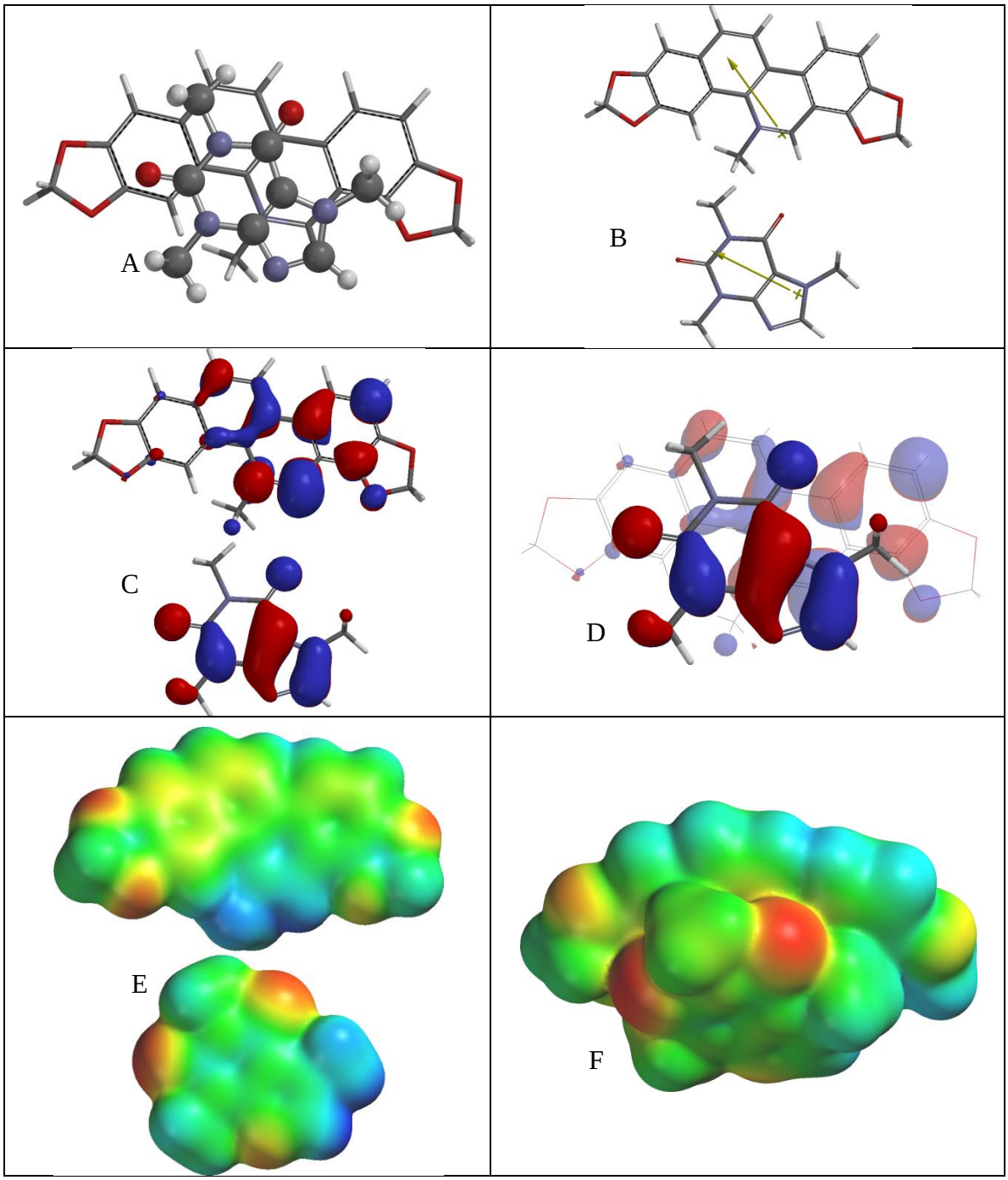

Figure 4.25. Second Orientation of the π – π Complex between Sanguinarine and Caffeine. [(A) Face-to face orientation of caffeine (ball and spoke model) with sanguinarine (tube model). (B) Molecular dipoles of sanguinarine (top) and caffeine (bottom). (C) LUMO of sanguinarine (top) and HOMO of caffeine (bottom). (D) Frontier molecular orbital overlap of caffeine with sanguinarine. (E) Electrostatic potential maps of sanguinarine (top) and caffeine (bottom). (F) Electrostatic potential map of the π – π complex between sanguinarine and caffeine.]

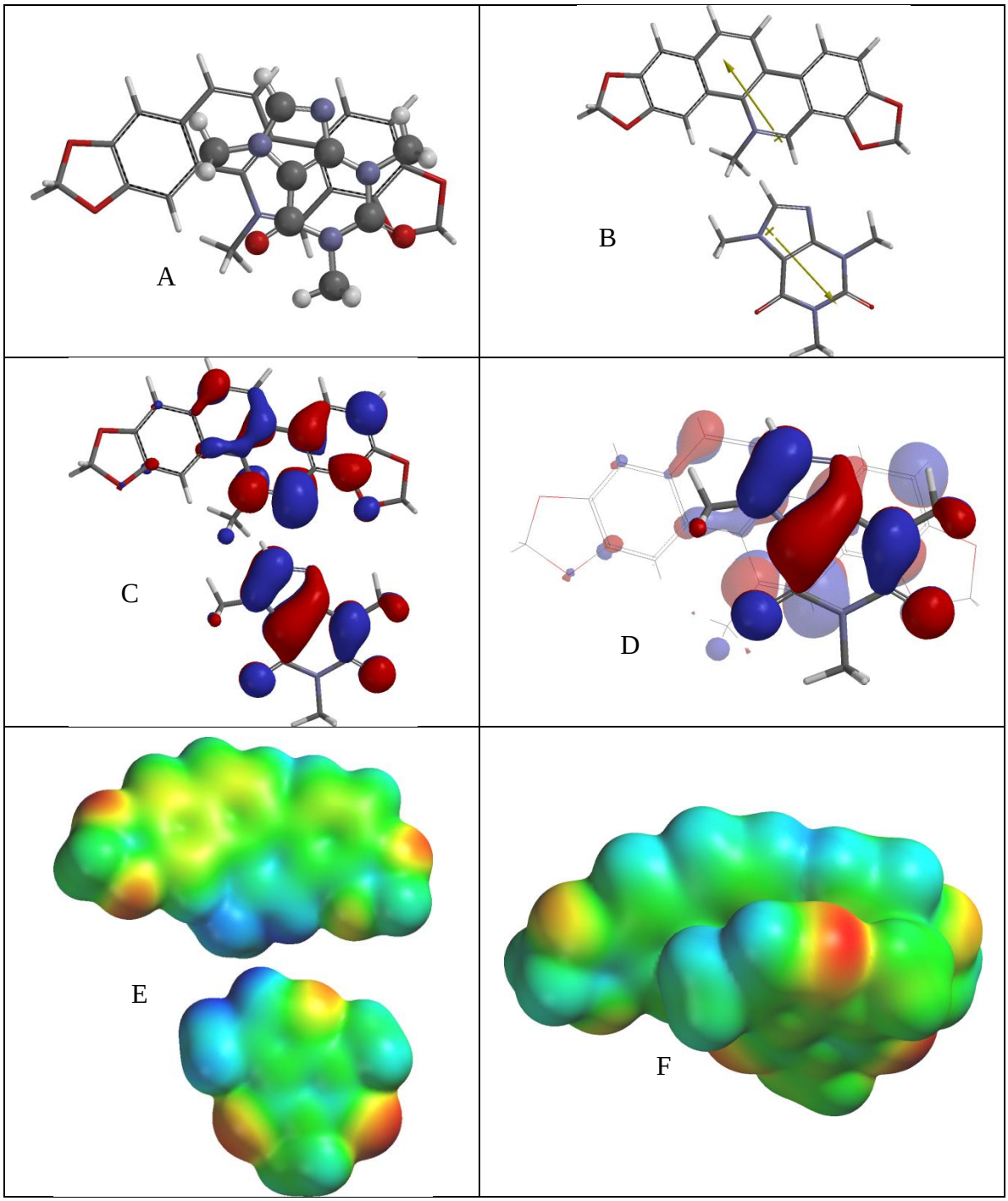

Figure 4.26. Third Orientation of the π – π Complex between Sanguinarine and Caffeine. [(A) Face-to face orientation of caffeine (ball and spoke model) with sanguinarine (tube model). (B) Molecular dipoles of sanguinarine (top) and caffeine (bottom). (C) LUMO of sanguinarine (top) and HOMO of caffeine (bottom). (D) Frontier molecular orbital overlap of caffeine with sanguinarine. (E) Electrostatic potential maps of sanguinarine (top) and caffeine (bottom). (F) Electrostatic potential map of the π – π complex between sanguinarine and caffeine.]

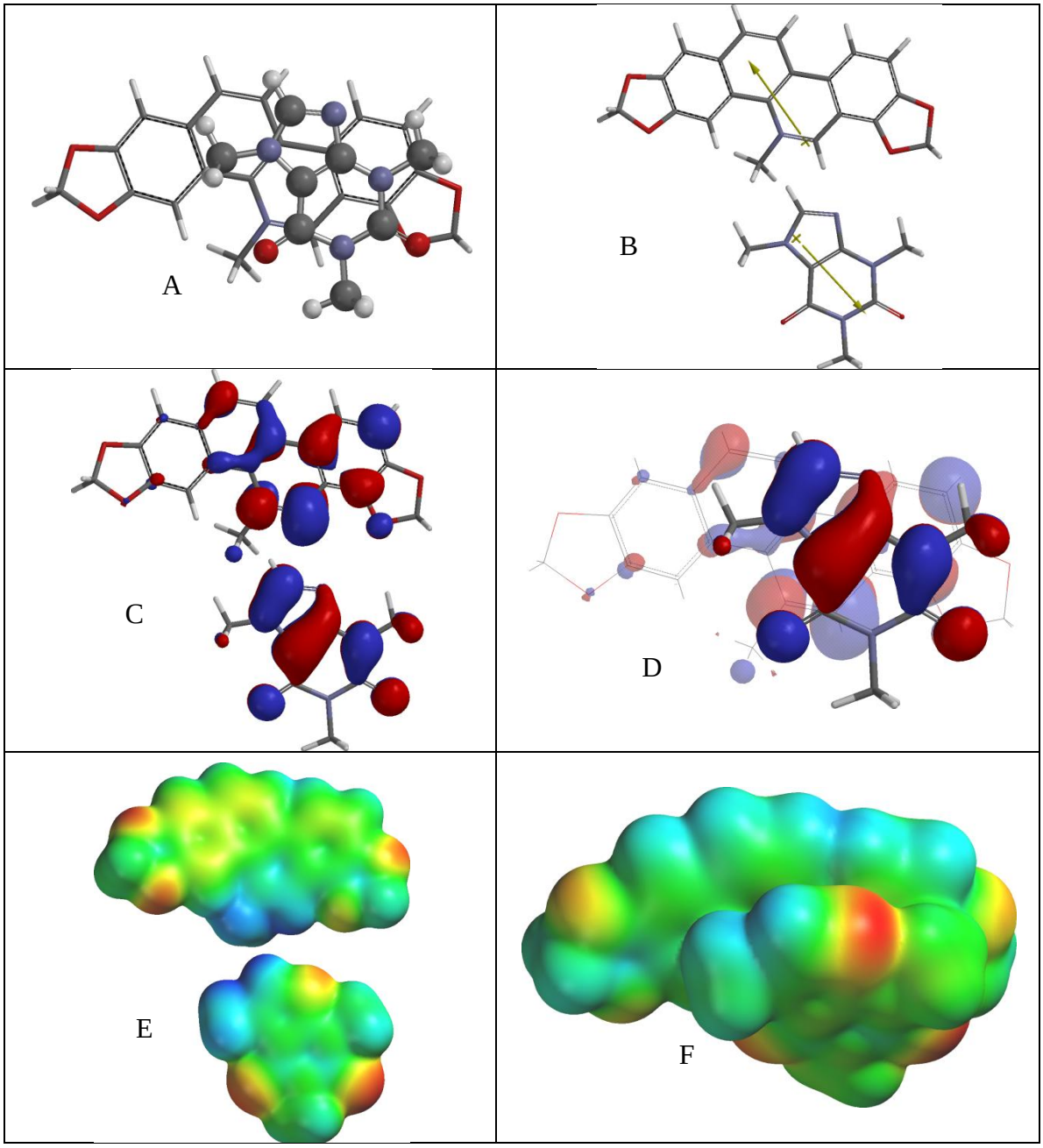

Figure 4.27. Lowest-Energy Orientation of the π – π Complex between Sanguinarine and Caffeine. [(A) Face-to face orientation of caffeine (ball and spoke model) in its lowest-energy orientation with sanguinarine (tube model). (B) Molecular dipoles of sanguinarine (top) and caffeine (bottom). (C) LUMO of sanguinarine (top) and HOMO of caffeine (bottom). (D) Frontier molecular orbital overlap of caffeine with sanguinarine in the lowest-energy orientation. (E) Electrostatic potential maps of sanguinarine (top) and caffeine (bottom). (F) Electrostatic potential map of the lowest energy π – π complex between sanguinarine and caffeine.]

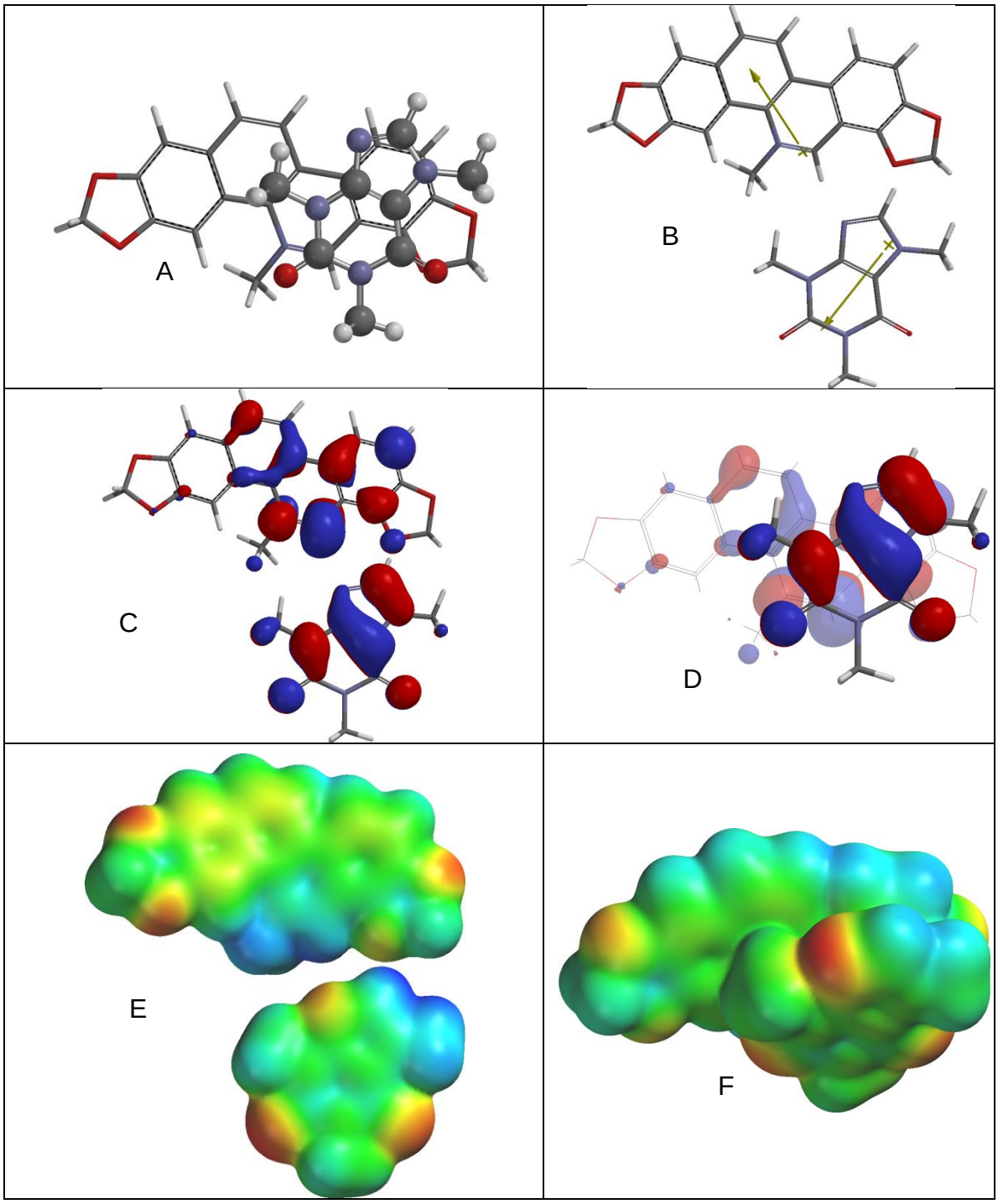

Figure 4.28. Fifth Orientation of the π – π Complex between Sanguinarine and Caffeine. [(A) Face-to face orientation of caffeine (ball and spoke model) with sanguinarine (tube model). (B) Molecular dipoles of sanguinarine (top) and caffeine (bottom). (C) LUMO of sanguinarine (top) and HOMO of caffeine (bottom). (D) Frontier molecular orbital overlap of caffeine with sanguinarine. (E) Electrostatic potential maps of sanguinarine (top) and caffeine (bottom). (F) Electrostatic potential map of the π – π complex between sanguinarine and caffeine.]

For the orientation shown in Figure 4.24, sanguinarine and caffeine exhibit good electrostatic potential, but poor frontier molecular orbital alignment and poor dipole-dipole interaction as the dipoles align with each other. For the orientation shown in Figure 4.25, sanguinarine and caffeine exhibit good electrostatic potential and good frontier molecular orbital alignment, but poor dipole-dipole interaction as the dipoles align with each other. For the orientation shown in Figure 4.26, sanguinarine and caffeine exhibit good electrostatic potential, good frontier molecular orbital alignment, and excellent dipole-dipole interaction as the dipoles oppose each other. For the orientation shown in Figure 4.27, sanguinarine and caffeine exhibit good electrostatic potential, good frontier molecular orbital alignment, and excellent dipole-dipole interaction as the dipoles oppose each other. This figure represents the lowest energy orientation between caffeine and sanguinarine. For the orientation shown in Figure 4.28, sanguinarine and caffeine exhibit good electrostatic potential, good frontier molecular orbital alignment, and good dipole-dipole interaction as the dipoles are 90º to each other.

4.3.5 Camptothecin

The interaction energy of camptothecin and caffeine was found to be -18.04 kcal/mol in the gas phase and -13.05 kcal/mol in aqueous solution. These values were found by adding the individual energies found separately for caffeine and for camptothecin, then subtracting that value from energies derived from different orientations of the caffeine/camptothecin pair. Out of four caffeine/camptothecin orientations, the most probable orientation (orientation three) exhibited good HOMO/LUMO interaction but poor electrostatic interactions and poor dipole-dipole interaction as the two dipoles were aligned with each other. The total energies of the

camptothecin and caffeine molecules and their energy differences (interaction energies) are listed in Table 4.11.

Table 4.11: Interaction energies of camptothecin and caffeine in different orientations

	E_{vac} (kcal/mol)	E_{aq} (kcal/mol)
Caffeine	-426682.26	-426689.01
Camptothecin	-741370.18	-741377.00
Sum of energies	-1168052.44	-1168066.01
Orientation 1	-1168070.02	-1168078.71
Interaction energy	-17.58	-12.70
Orientation 2	-1168069.62	-1168078.46
Interaction energy	-17.18	-12.45
Orientation 3 (lowest)	-1168070.48	-1168079.06
Interaction energy	-18.04	-13.05
Orientation 4	-1168069.88	-1168078.34
Interaction energy	-17.44	-12.33

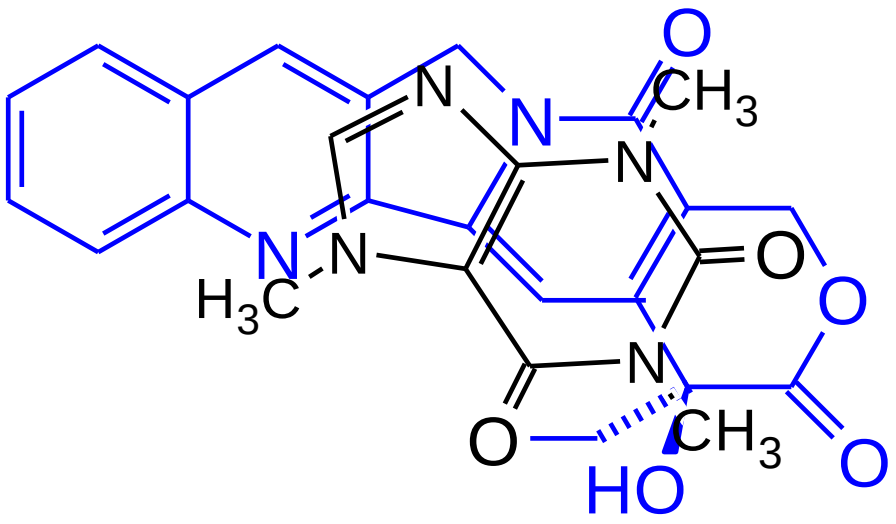

Figure 4.29: Most Probable Orientation of Camptothecin and Caffeine

Figure 4.29 shows the most probable orientation of camptothecin and caffeine represented as a line drawing with caffeine in black and camptothecin in blue to give a better view of how the two molecules are overlaid onto each other. This orientation (orientation three) was chosen as the most probable because of its agreeing HOMO/LUMO interactions which gave it the best interaction energy in comparison with the other orientations attempted. Figures 4.30-4.33 illustrate the four orientations of camptothecin and caffeine attempted.

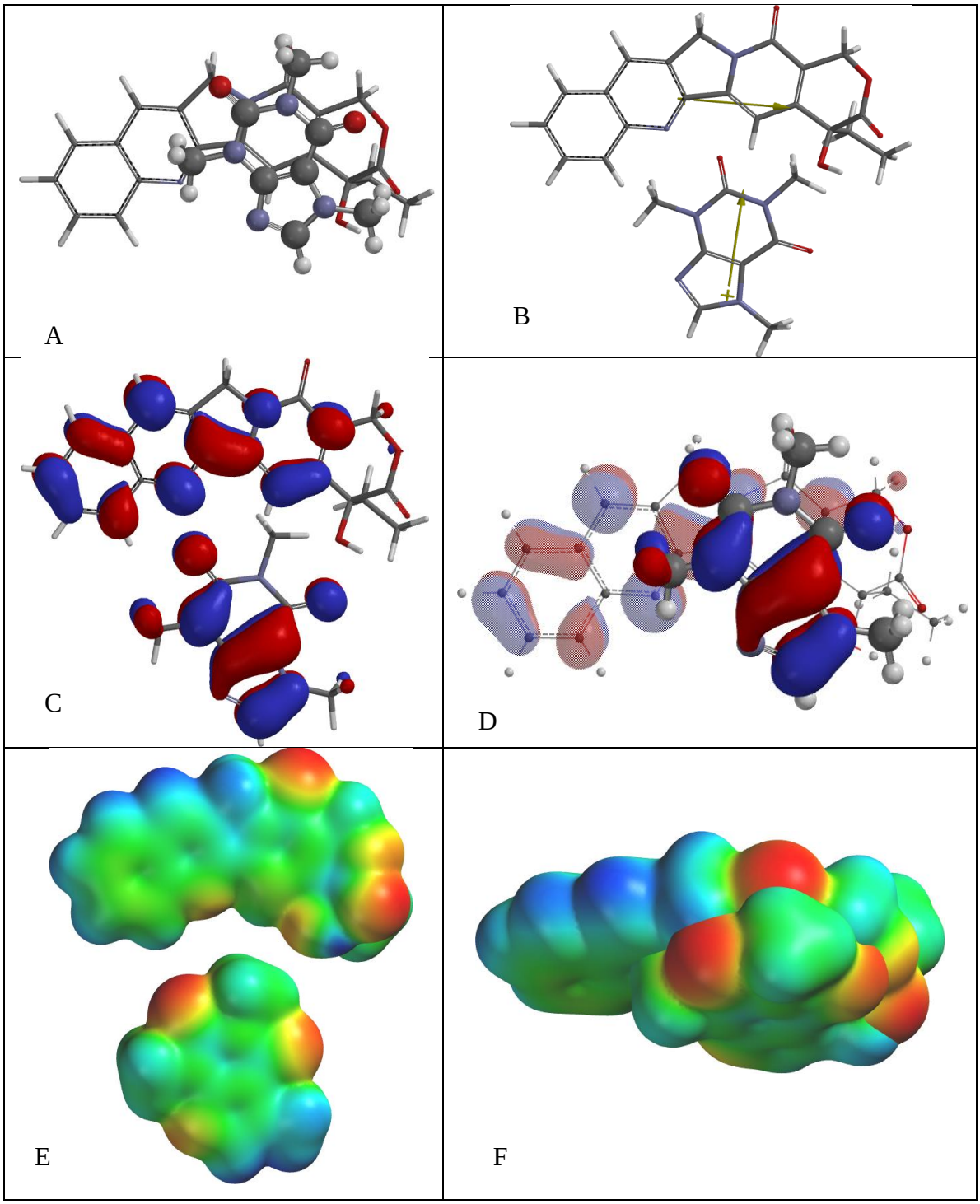

Figure 4.30. First Orientation of the π – π Complex between Camptothecin and Caffeine. [(A) Face-to face orientation of caffeine (ball and spoke model) with camptothecin (tube model). (B) Molecular dipoles of camptothecin (top) and caffeine (bottom). (C) LUMO of camptothecin (top) and HOMO of caffeine (bottom). (D) Frontier molecular orbital overlap of caffeine with camptothecin. (E) Electrostatic potential maps of camptothecin (top) and caffeine (bottom). (F) Electrostatic potential map of the π – π complex between camptothecin and caffeine.]

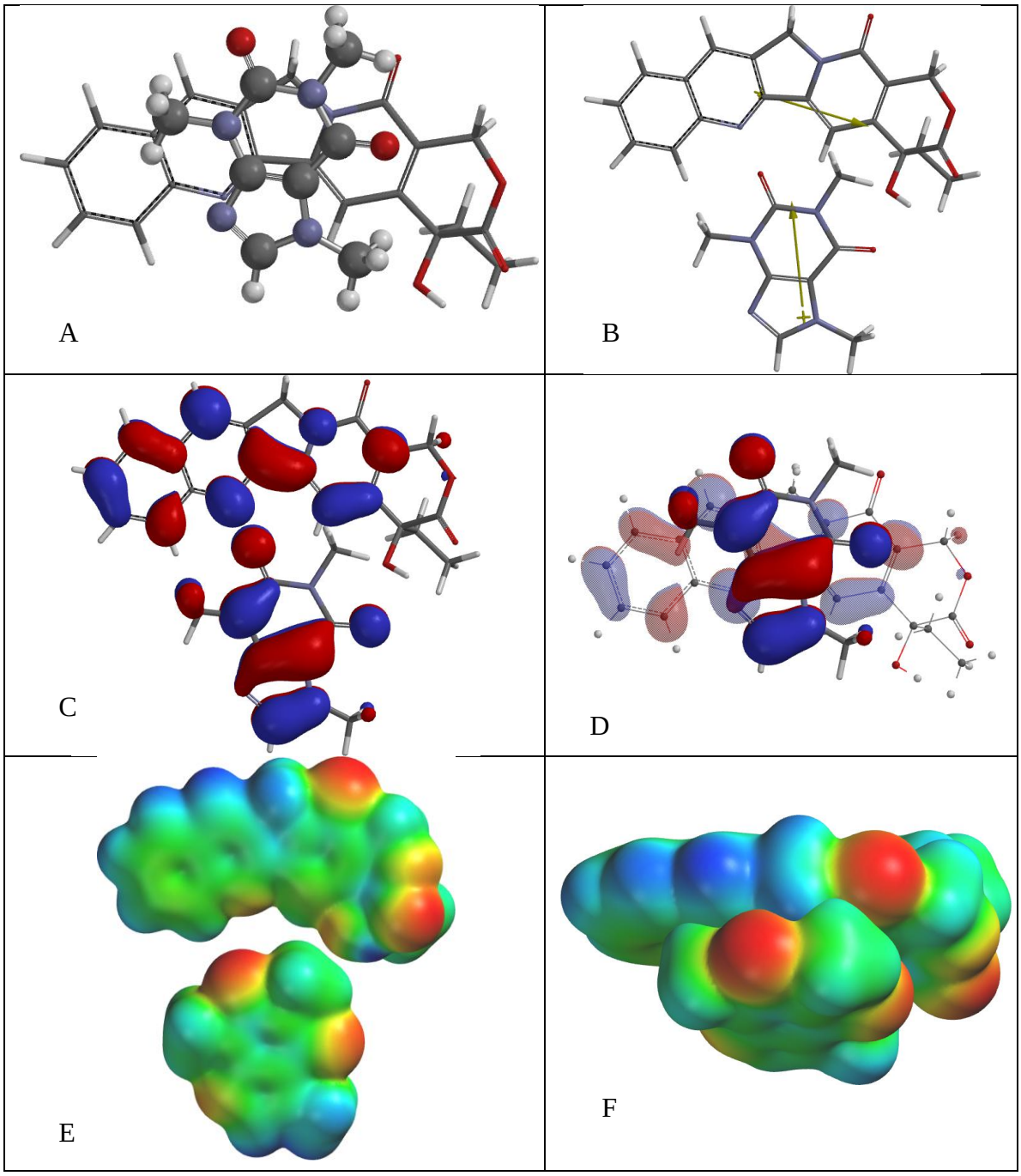

Figure 4.31. Second Orientation of the π – π Complex between Camptothecin and Caffeine. [(A) Face-to face orientation of caffeine (ball and spoke model) with camptothecin (tube model). (B) Molecular dipoles of camptothecin (top) and caffeine (bottom). (C) LUMO of camptothecin (top) and HOMO of caffeine (bottom). (D) Frontier molecular orbital overlap of caffeine with camptothecin. (E) Electrostatic potential maps of camptothecin (top) and caffeine (bottom). (F) Electrostatic potential map of the π – π complex between camptothecin and caffeine.]

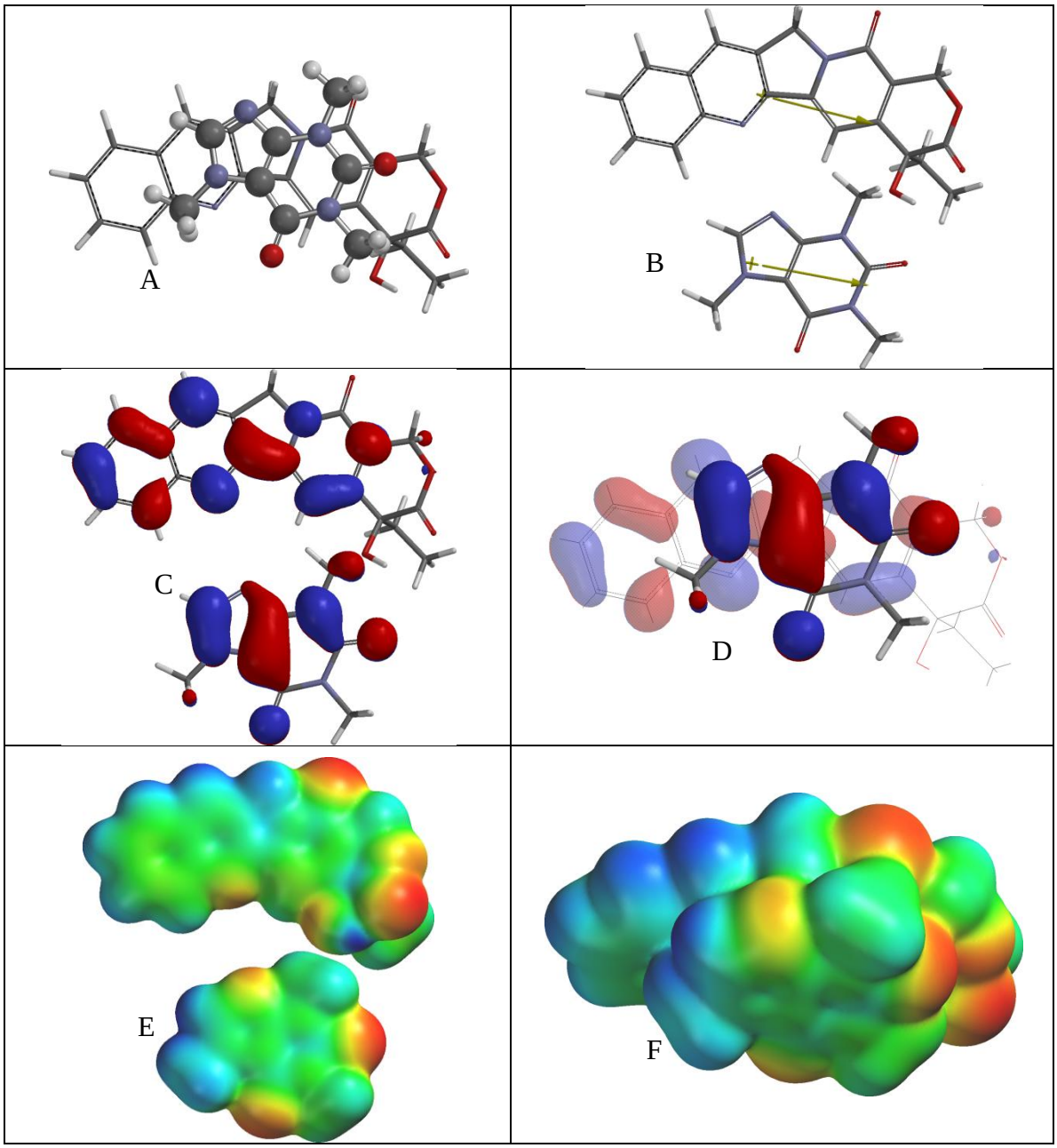

Figure 4.32. Lowest-Energy Orientation of the π – π Complex between Camptothecin and Caffeine. [(A) Face-to face orientation of caffeine (ball and spoke model) in its lowest-energy orientation with camptothecin (tube model). (B) Molecular dipoles of camptothecin (top) and caffeine (bottom). (C) LUMO of camptothecin (top) and HOMO of caffeine (bottom). (D) Frontier molecular orbital overlap of caffeine with camptothecin in the lowest-energy orientation. (E) Electrostatic potential maps of camptothecin (top) and caffeine (bottom). (F) Electrostatic potential map of the lowest-energy π – π complex between camptothecin and caffeine.]

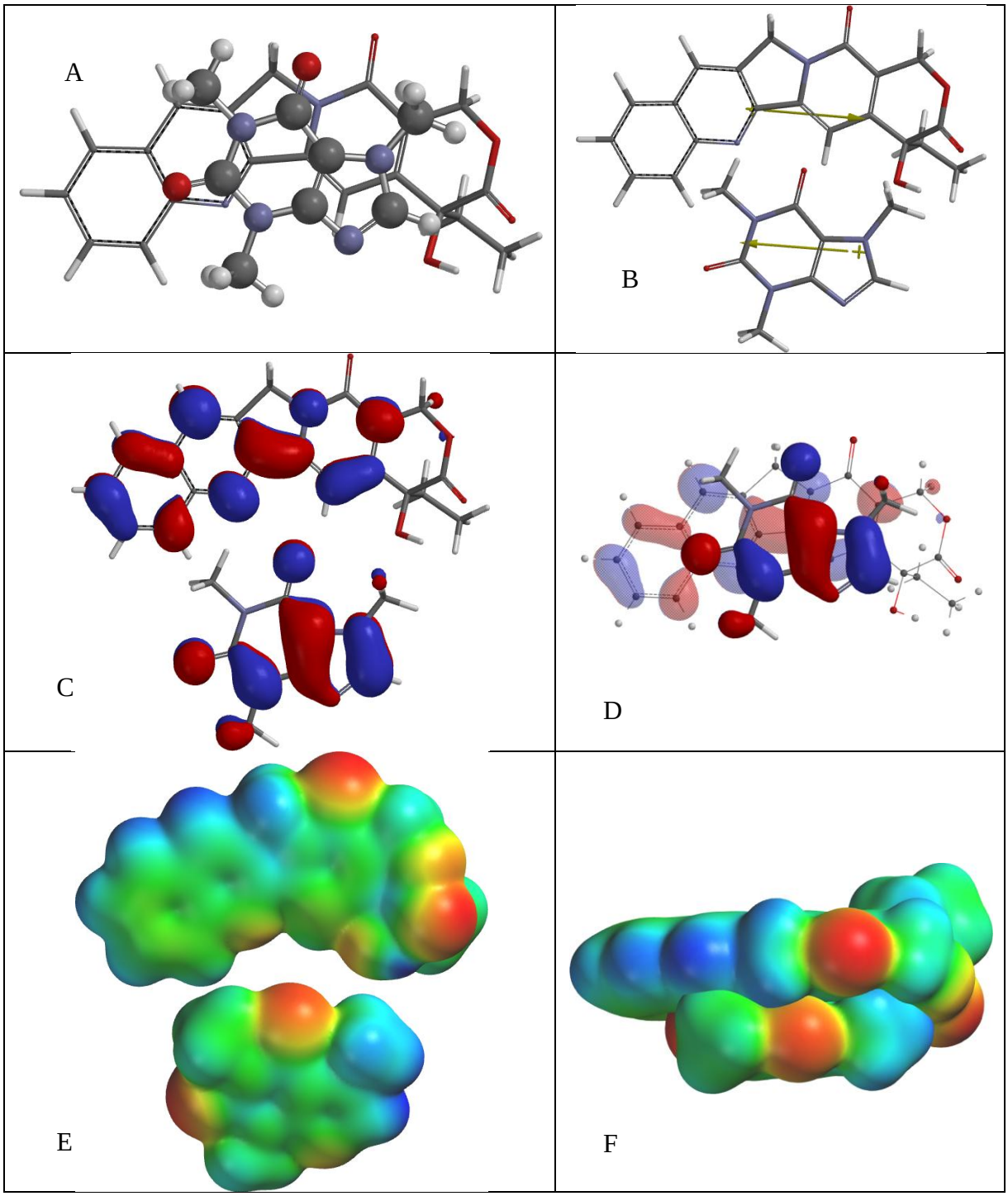

Figure 4.33. Fourth Orientation of the π – π Complex between Camptothecin and Caffeine. [(A) Face-to face orientation of caffeine (ball and spoke model) with camptothecin (tube model). (B) Molecular dipoles of camptothecin (top) and caffeine (bottom). (C) LUMO of camptothecin (top) and HOMO of caffeine (bottom). (D) Frontier molecular orbital overlap of caffeine with camptothecin. (E) Electrostatic potential maps of camptothecin (top) and caffeine (bottom). (F) Electrostatic potential map of the π – π complex between camptothecin and caffeine.]

For the orientation shown in Figure 4.30, camptothecin and caffeine exhibit good electrostatic potential, fair frontier molecular orbital alignment, and good dipole-dipole interactions as the dipoles are 90º to each other. For the orientation shown in Figure 4.31, camptothecin and caffeine exhibit good electrostatic potential, good frontier molecular orbital alignment, and good dipole-dipole interactions as the dipoles are close to 90º to each other. For the orientation shown in Figure 4.32, camptothecin and caffeine exhibit good electrostatic potential, good frontier molecular orbital alignment, but poor dipole-dipole interactions as the dipoles align with each other. This figure represents the lowest energy orientation between caffeine and camptothecin. For the orientation shown in Figure 4.33, camptothecin and caffeine exhibit good electrostatic potential, good frontier molecular orbital alignment, and good dipole-dipole interactions as the dipoles oppose each other.

4.3.6 Doxorubicin

The interaction energy of doxorubicin and caffeine was found to be -19.16 kcal/mol in the gas phase and -15.86 kcal/mol in aqueous solution. These values were found by adding the individual energies found separately for caffeine and for doxorubicin, then subtracting that value from energies derived from different orientations of the caffeine/doxorubicin pair. Out of four caffeine/doxorubicin orientations, all of the orientations had aspects about them that made them acceptable. However, the orientation (orientation 2) that showed the most probability for what is actually happening between the two molecules in aqueous solution exhibited good overlap of molecular orbitals (HOMO and LUMO), good electrostatic interactions and 90˚ dipole moments. The total

energies of the doxorubicin and caffeine molecules and their energy differences (interaction energies) are listed in Table 4.12.

Table 4.12: Interaction energies of doxorubicin and caffeine in different orientations.

	E_{vac} (kcal/mol)	E_{aq} (kcal/mol)
Caffeine	-426682.26	-426689.01
Doxorubicin	-1209477.91	-1209494.15
Sum of energies	-1636160.17	-1636183.16
Orientation 1	-1636179.27	-1636198.90
Interaction energy	-19.10	-15.74
Orientation 2 (lowest)	-1636179.33	-1636199.02
Interaction energy	-19.16	-15.86
Orientation 3	-1636176.18	-1636195.48
Interaction energy	-16.01	-12.32
Orientation 4	-1636178.82	-1636198.50
Interaction energy	-18.65	-15.34

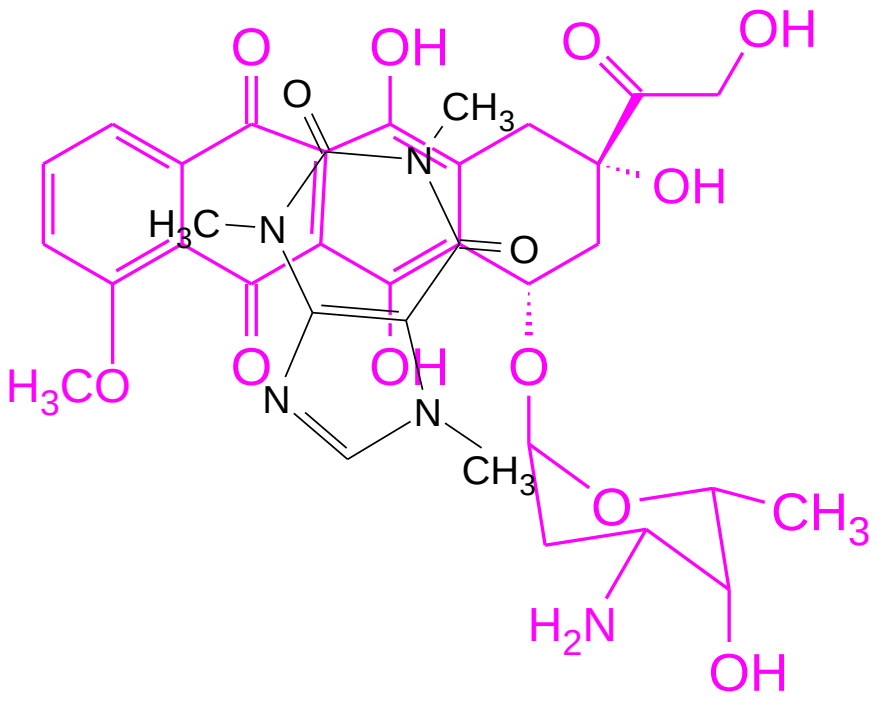

Figure 4.34: Most Probable Orientation of Doxorubicin and Caffeine

Figure 4.34 shows the most probable orientation (orientation two) of doxorubicin and caffeine represented as a line drawing with caffeine in black and doxorubicin in pink to give a better view of how the two molecules are overlaid onto each other. This orientation was chosen as the most probable because its three factors that agreed with another (the interactions listed above) gave it the best interaction energy in comparison with the other orientations attempted. Figures 4.35-4.38 illustrate the four orientations of doxorubicin and caffeine attempted.

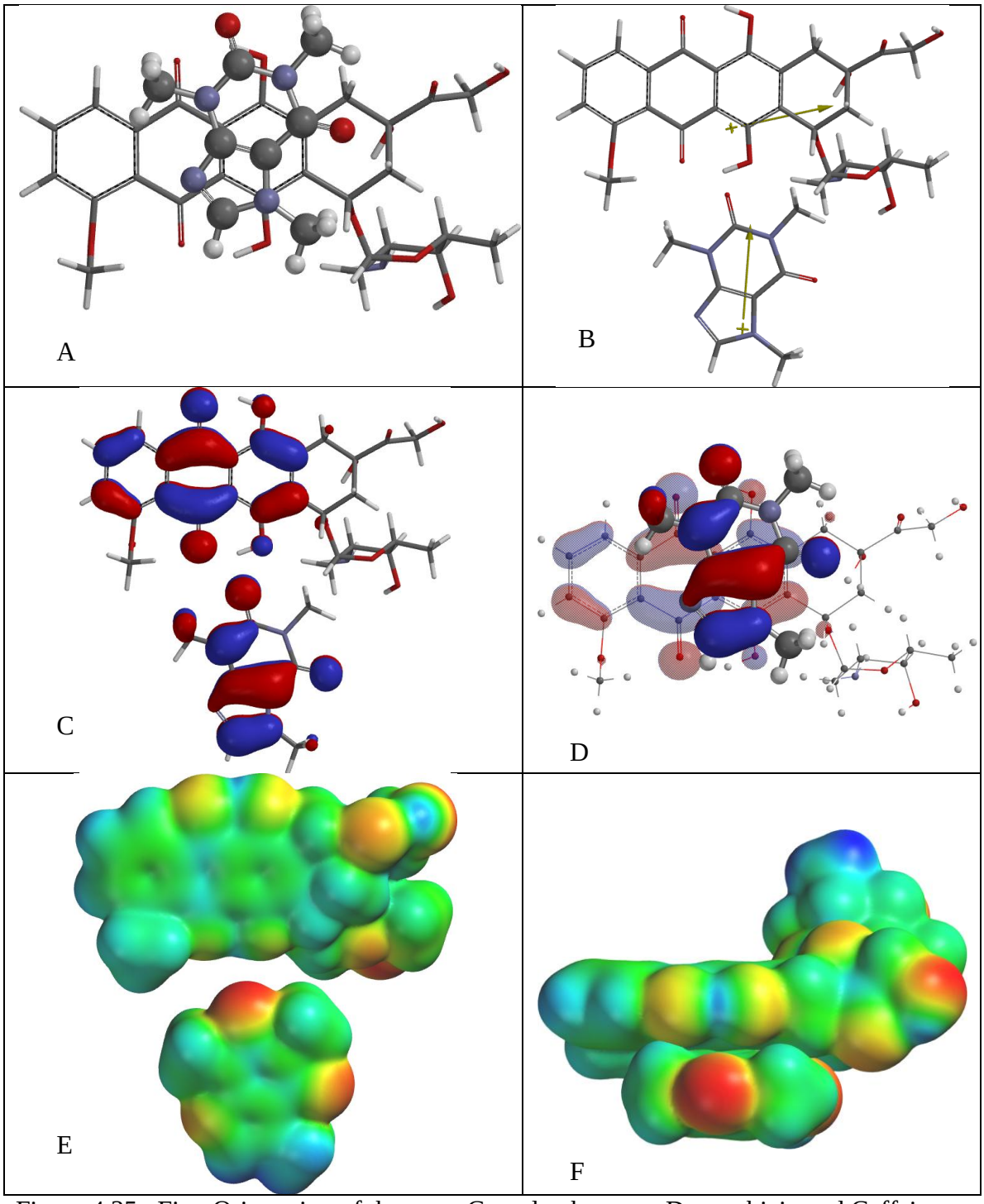

Figure 4.35. First Orientation of the π – π Complex between Doxorubicin and Caffeine. [(A) Face-to face orientation of caffeine (ball and spoke model) with doxorubicin (tube model). (B) Molecular dipoles of doxorubicin (top) and caffeine (bottom). (C) LUMO of doxorubicin (top) and HOMO of caffeine (bottom). (D) Frontier molecular orbital overlap of caffeine with doxorubicin. (E) Electrostatic potential maps of doxorubicin (top) and caffeine (bottom). (F) Electrostatic potential map of the π – π complex between doxorubicin and caffeine.]

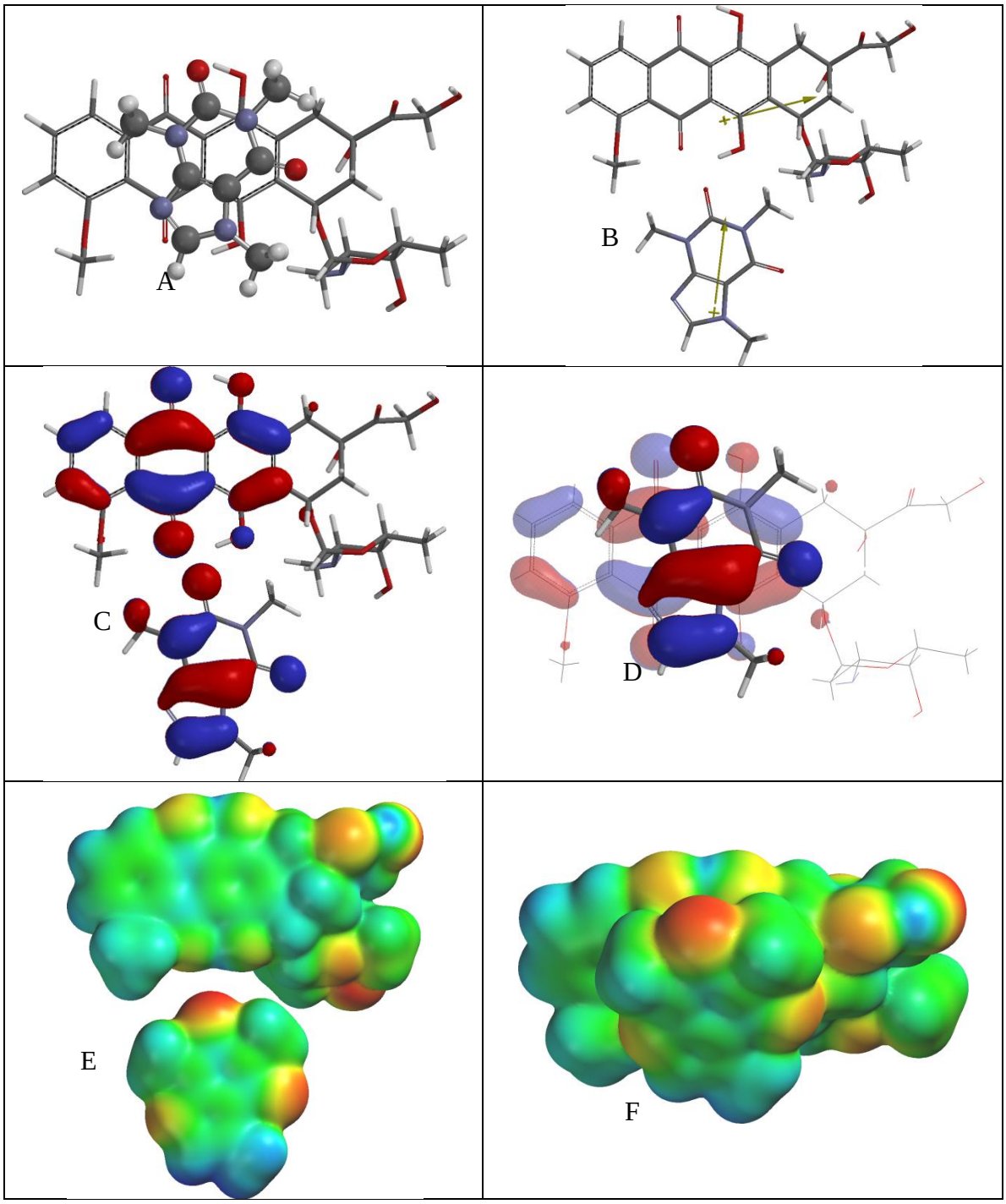

Figure 4.36. Lowest-Energy Orientation of the π – π Complex between Doxorubicin and Caffeine. [(A) Face-to face orientation of caffeine (ball and spoke model) in its lowest-energy orientation with doxorubicin (tube model). (B) Molecular dipoles of doxorubicin (top) and caffeine (bottom). (C) LUMO of doxorubicin (top) and HOMO of caffeine (bottom). (D) Frontier molecular orbital overlap of caffeine with doxorubicin in the lowest-energy orientation. (E) Electrostatic potential maps of doxorubicin (top) and caffeine (bottom). (F) Electrostatic potential map of the lowest-energy π – π complex between doxorubicin and caffeine.]

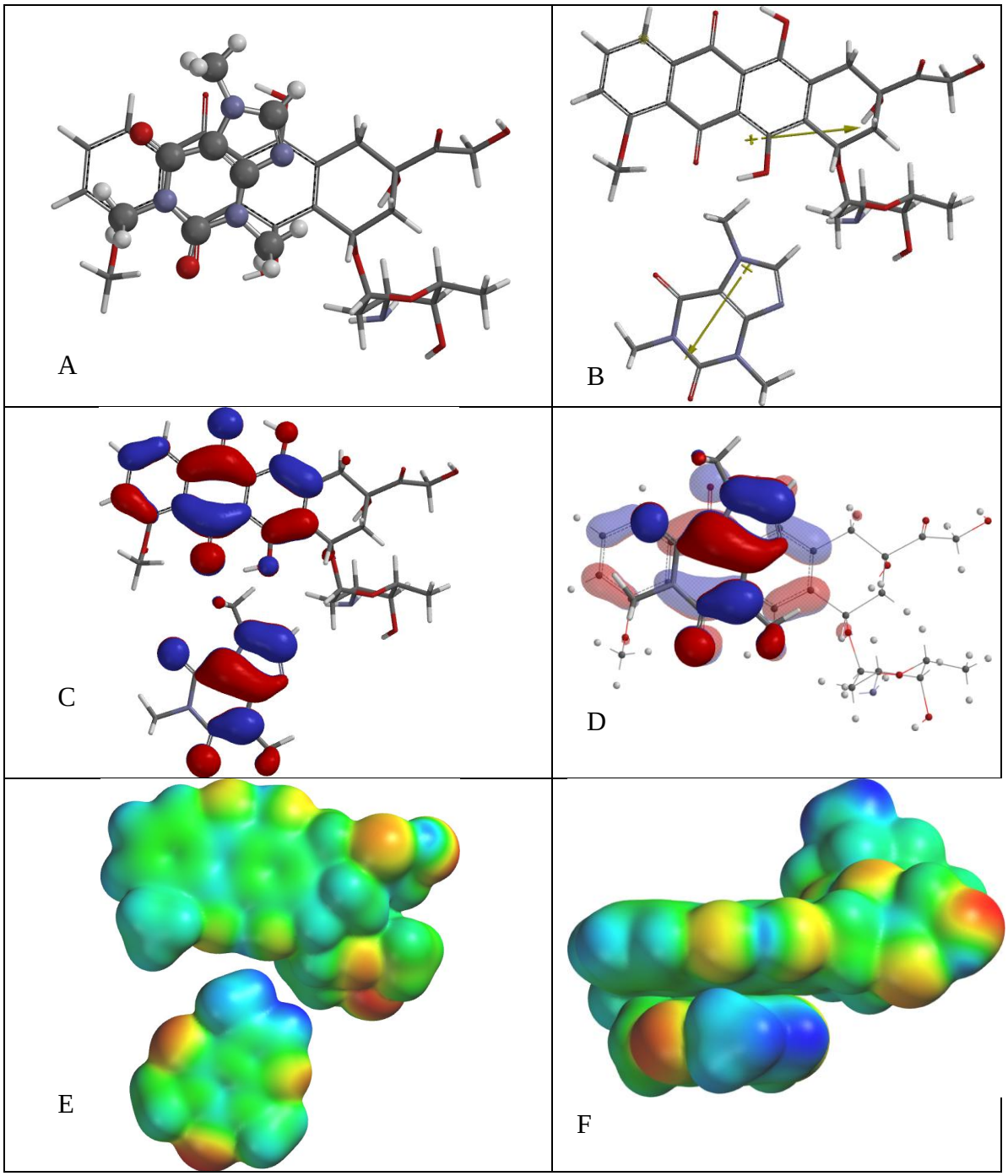

Figure 4.37. Third Orientation of the π – π Complex between Doxorubicin and Caffeine. [(A) Face-to face orientation of caffeine (ball and spoke model) with doxorubicin (tube model). (B) Molecular dipoles of doxorubicin (top) and caffeine (bottom). (C) LUMO of doxorubicin (top) and HOMO of caffeine (bottom). (D) Frontier molecular orbital overlap of caffeine with doxorubicin. (E) Electrostatic potential maps of doxorubicin (top) and caffeine (bottom). (F) Electrostatic potential map of the π – π complex between doxorubicin and caffeine.]

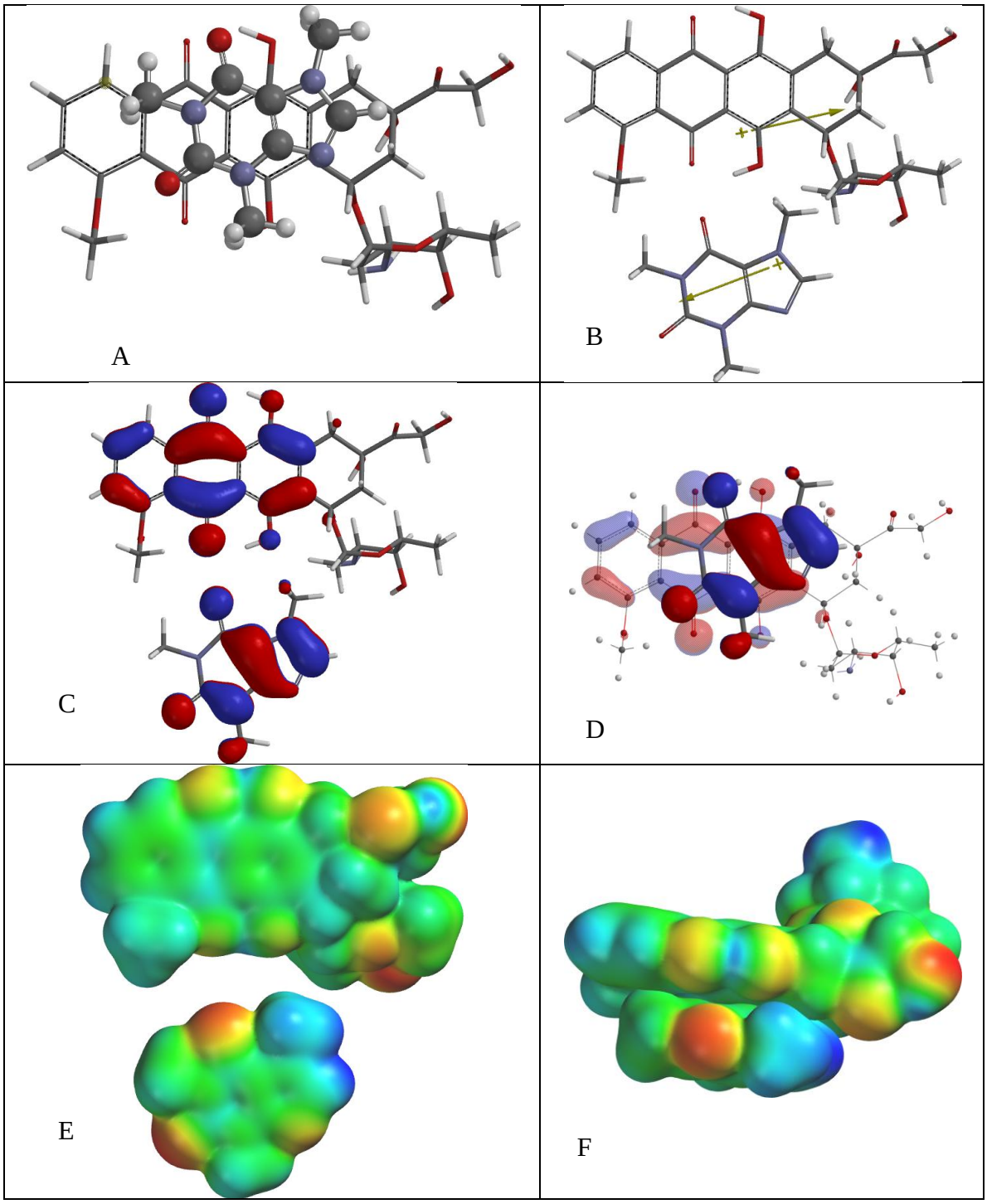

Figure 4.38. Fourth Orientation of the π – π Complex between Doxorubicin and Caffeine. [(A) Face-to face orientation of caffeine (ball and spoke model) with doxorubicin (tube model). (B) Molecular dipoles of doxorubicin (top) and caffeine (bottom). (C) LUMO of doxorubicin (top) and HOMO of caffeine (bottom). (D) Frontier molecular orbital overlap of caffeine with doxorubicin. (E) Electrostatic potential maps of doxorubicin (top) and caffeine (bottom). (F) Electrostatic potential map of the π – π complex between doxorubicin and caffeine.]

For the orientation shown in Figure 4.35, doxorubicin and caffeine exhibit good electrostatic potential, good frontier molecular orbital alignment, and good dipole-dipole interactions as the dipoles are 90º with each other. For the orientation shown in Figure 4.36, doxorubicin and caffeine exhibit good electrostatic potential, good frontier molecular orbital alignment, and good dipole-dipole interactions as the dipoles are 90º to each other. This figure represents the lowest energy orientation between caffeine and doxorubicin. For the orientation shown in Figure 4.37, doxorubicin and caffeine exhibit fair electrostatic potential, good frontier molecular orbital alignment, and excellent dipole-dipole interactions as the dipoles oppose each other. For the orientation shown in Figure 4.38, doxorubicin and caffeine exhibit good electrostatic potential, poor frontier molecular orbital alignment, and excellent dipole-dipole interactions as the dipoles oppose each other.

All of the compounds when docked with caffeine showed exothermic interaction energies which points to the method of bonding between the two molecules as being π–π interactions. This is consistent with the findings from another laboratory that previously conducted a simple quantum mechanics calculation not involving electron correlation as our study does, but still interestingly enough found that docked caffeine and doxorubicin and caffeine and mitoxantrone expressed exothermic energies with each calculation (Piosik, et al., 2002). When comparing the cytotoxicity data with the π–π interaction energies, the three compounds with the largest attenuation of cytotoxicity when bound to caffeine (berberine, ellipticine and camptothecin) had lower interaction energies than did the compounds with the lower attenuations of cytotoxicity (sanguinarine, chelerythrine and doxorubicin).

4.4 π-π Orientations: Molecular Orbital Overlap, Dipole-Dipole Interactions and Electrostatic Interactions

Several different forces play a role in the π–π interactions between two molecules, a few of which are overlapping of frontier molecular orbitals, dipole-dipole interactions and electrostatic interactions. An ideal orientation for the contact of two molecules would be for all of these interactions to be favorable for the best possible docking orientation.

4.4.1 Molecular Orbital Overlap

The overlap of molecular orbitals must be taken into account when two molecules come into contact with each other. Frontier molecular orbital theory describes the contact of two molecules in terms of the orbitals of the molecules that will be coming together and the occupation of electrons of each orbital. The molecules will react to each other based on how full of electrons these frontier orbitals are. These frontier molecular orbitals are referred to as the HOMO (highest occupied molecular orbital) and the LUMO (lowest unoccupied molecular orbital). Two orbitals that are mostly or fully filled will repel each other. If one of the orbitals from one molecule contacts an orbital from another molecule one of the said orbitals must be unoccupied for a complete π-π interaction to take place. Therefore, when the HOMO of one molecule interacts with the LUMO of another molecule, a π–π interaction can take place. Figure 4.39 illustrates caffeine and chelerythrine with good frontier molecular orbital overlap. In this orientation the orbitals agreed with each other, but the other interactions such as dipole-dipole and electrostatic interactions did not.

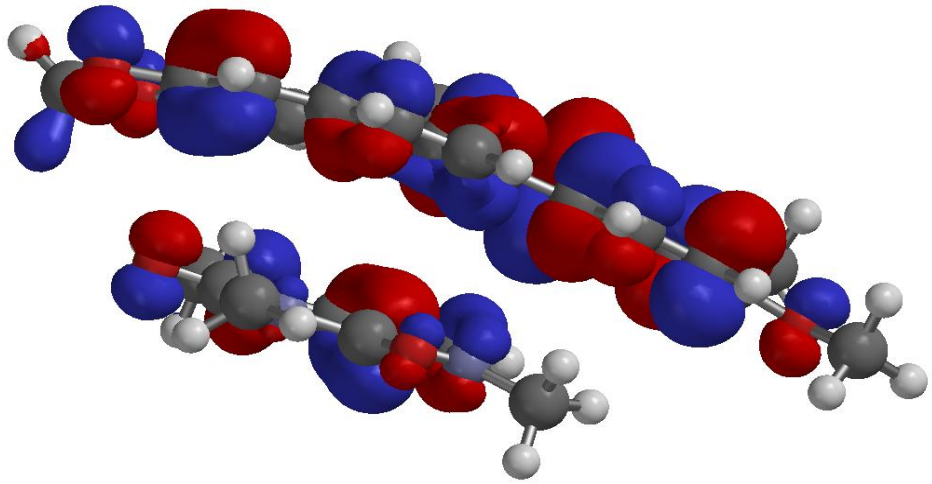

(a)

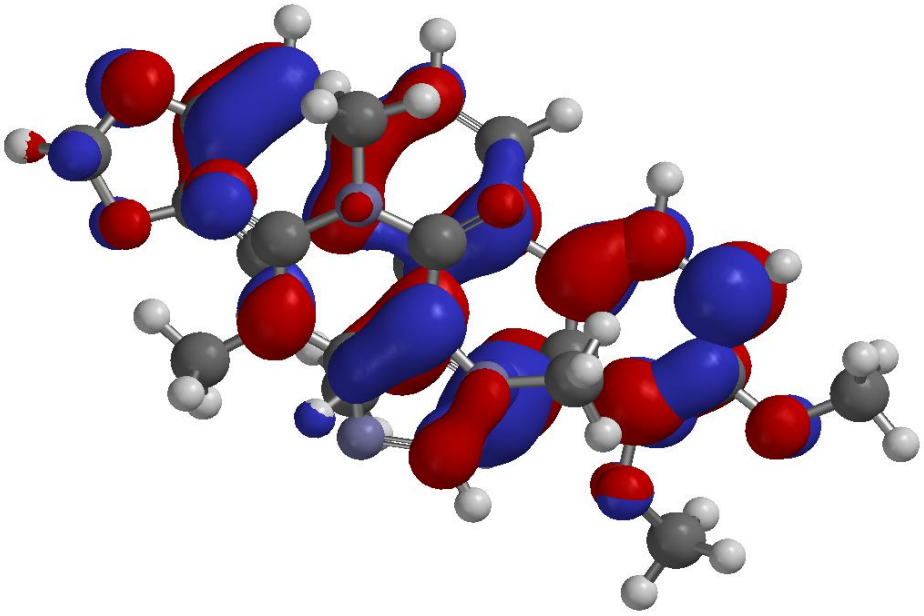

(b)

Figure 4.39: Frontier Molecular Orbital Alignment

Figure 4.39 (a) and (b) shows caffeine and chelerythrine in the same orientation and at a different angle. These figures represent caffeine and chelerythrine with the HOMO of caffeine and the LUMO of chelerythrine clearly shown. These non-covalent interactions of molecular orbital overlap are an important factor in the decision of whether or not two molecules can effectively come together in a π–π complex. Many biological molecules rely on molecular orbital overlap to allow certain processes such as protein folding and DNA transcription to occur (Anzellotti, et al., 2008). Accounting for HOMO and LUMO overlap is also very important in chemotherapeutic drug discovery techniques, as forming π–π interactions is the way that many of these drugs function.

4.4.2 Dipole-Dipole Interactions

Dipole-dipole interactions are another important aspect to consider when two molecules are docked together. These interactions refer to a permanent dipole within each molecule. The interactions between the two dipoles of the separate compounds allow for better interaction when they are opposing each other. This goes along with the simple concept that a more negative end of a molecule will attract the more positive end of another. Figure 4.40 shows caffeine and chelerythrine docked in a different orientation than is represented in Figure 4.39 with the dipole of caffeine shown (left) and the dipole of chelerythrine shown (right). In this orientation, chelerythrine and caffeine have opposing dipoles which give a great alignment for the docked molecules.

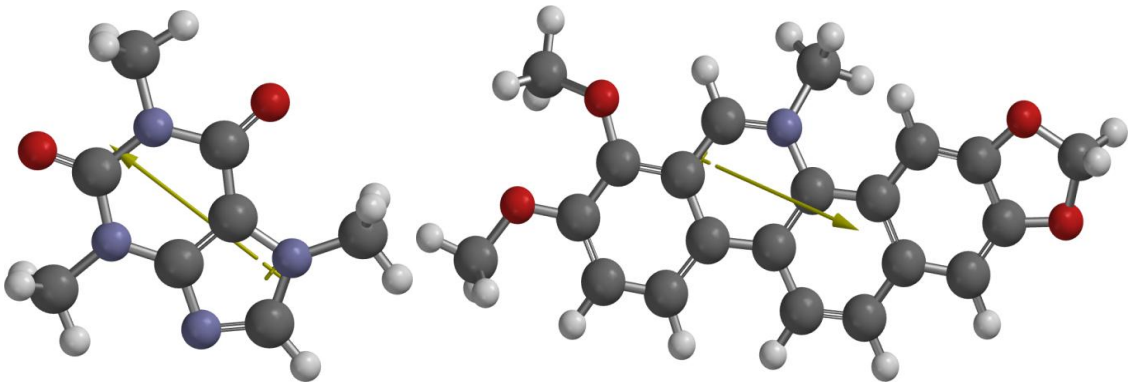

Figure 4.40: Opposing Dipoles of Caffeine and Chelerythrine

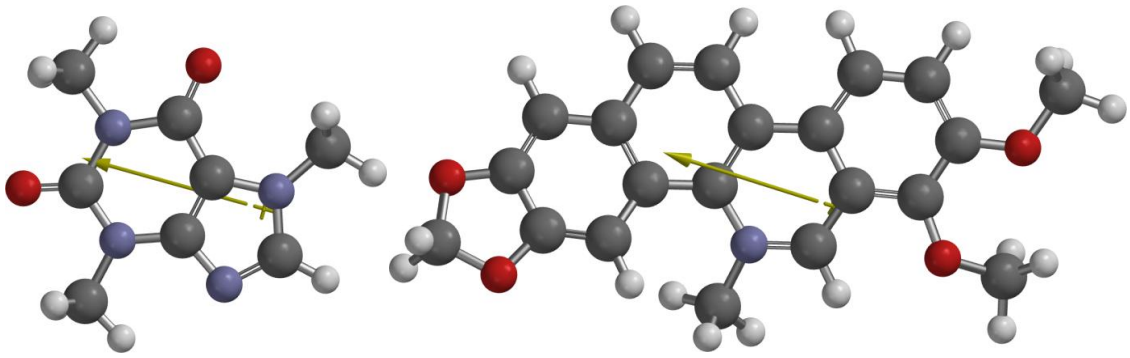

Figure 4.41: Aligning Dipoles of Caffeine and Chelerythrine

Figure 4.41 shows caffeine (left) and chelerythrine (right) in a different orientation than is represented in Figure 4.40 which presents with aligning dipoles, which is considered non-complementary to the docked molecules.

4.4.3 Electrostatic Interactions

Electrostatic interactions usually refer to permanent charges within the molecule and where within the molecule the electrons are most dense. Electrostatics must also be considered when determining the best orientation of two molecules. Generally, an electron-dense area of one molecule will have the most attraction for an area of low electron density of the other molecule.

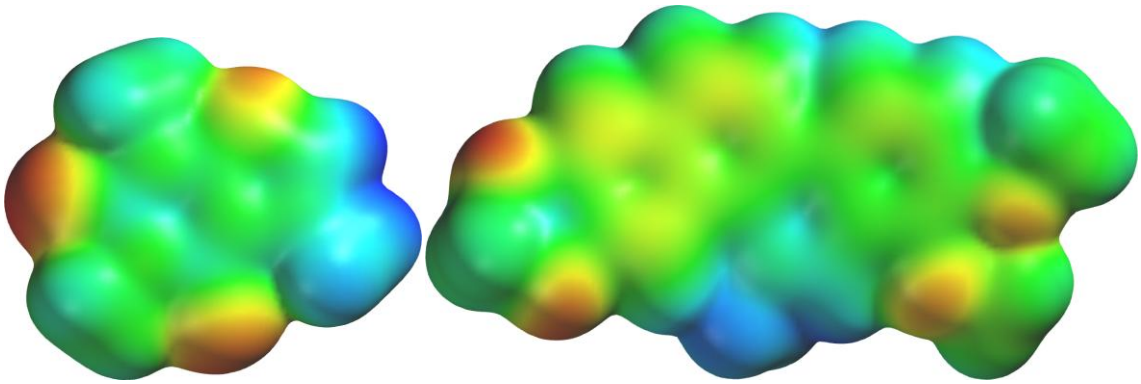

Figure 4.42: Caffeine (left) and Chelerythrine (right)

Figure 4.42 represents caffeine and chelerythrine with the electrostatic potential maps of each molecule shown. The blue color on the molecules represents the most electron-dense areas and the red color indicates less electron-dense areas. The most electron-dense areas of one molecule are more attracted to the less electron-dense areas of the other molecule.

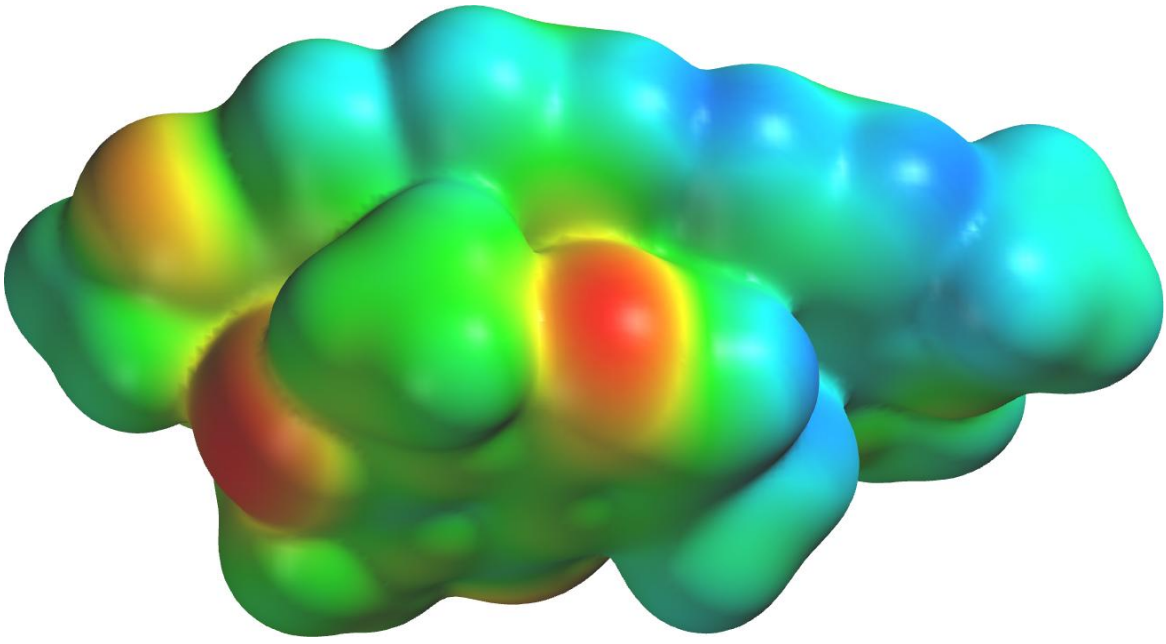

Figure 4.43: Electrostatic Potential Map of Docked Caffeine and Chelerythrine Molecules

Figure 4.43 represents the caffeine and chelerythrine molecules docked in a different orientation than shown in Figure 4.39. The docked molecule has been tilted forward slightly. The most electron-dense areas of one molecule are more attracted to the less electron-dense areas of the other molecule. The docked molecules of this orientation show good electrostatic interactions but non-complementary HOMO/LUMO interactions and poor dipole-dipole alignment.

CHAPTER FIVE

CONCLUSION

The isoquinoline alkaloids have been in medicinal use for many years for various ailments and diseases, although most recently for their cytotoxic properties and their potential for being used as anti-tumor drugs. The cytotoxicity data contained herein were conclusive in that all compounds tested (chelerythrine, sanguinarine, ellipticine, berberine, camptothecin and doxorubicin) were found to be cytotoxic as previously reported. Because of their planar aromatic structures, it has been hypothesized and tested in previous studies that the compounds used in this study have the capabilities to make π–π bonds with DNA bases and with other planar aromatic structures such as caffeine. In the presence of 1030 μM caffeine/media solution, the MCF-7 cells were not affected by the caffeine; however, cytotoxicity tests showed a definite attenuation in the efficacies of the drugs on the cells when in the presence of caffeine. This attenuation of cytotoxicity of each of the compounds tested points to a definite caffeine interference in the binding of the drug to the DNA in the cell. The molecular modeling studies contained herein also agreed with the cytotoxicity data in that all the interaction energies obtained from the calculations were exothermic and pointed to π–π interactions as the bonding mechanism for each docked caffeine/compound pair.

REFERENCES

Adhikari, A., Hossain, M., Maiti, M., and Kumar, G. 2008. Energetics of the Binding of Phototoxic and Cytotoxic Plant Alkaloid Sanguinarine to DNA: Isothermal Titration Calorimetric Studies. Journal of Molecular Structure. 889: 54-63.

Anzellotti, A., Bayse, C., and Farrell, N. 2008. Effects of Nucleobase Metalation on Frontier Molecular Orbitals: Potential Implications for π-Stacking Interactions with Tryptophan. Inorganic Chemistry. 47: 10425-10431.

Bai, L., Zhao, Z., Cai, Z., and Jiang, Z. 2006. DNA-binding Affinities and Sequence Selectivity of Quaternary Benzophenanthridine Alkaloids Sanguinarine, Chelerythrine, and Nitidine. Bioorganic and Medicinal Chemistry. 14: 5439-5445.

Bhadra, K., Maiti, M., and Kumar, G. 2007. Molecular Recognition of DNA by Small Molecules: AT Base Pair Specific Intercalative Binding of Cytotoxic Plant Alkaloid Palmatine. Biochimica et Biophysica Acta. 1770: 1071-1080.

Bhadra, K., Maiti, M., and Kumar, G. 2008. DNA-Binding Cytotoxic Alkaloids: Comparative Study of the Energetics of Binding of Berberine, Palmatine, and Coralyne. DNA and Cell Biology. 27: 675-685.

Bhadra, K,. and Kumar, G. 2010. Therapeutic Potential of Nucleic Acid-Binding Isoquinoline Alkaloids: Binding Aspects and Implications for Drug Design. Medicinal Research Reviews. DOI: 10.1002/med.20202.

Brana, M., Cacho, M., Gradillas, A., de-Pascual-Teresa, B., and Ramos, A. 2001. Intercalators as Anti-Cancer Drugs. Current Pharmaceutical Design. 7: 1745-1780.

Burghardt, I., May, V., Micha, D.A., and Bittner, E.R. 2009. Energy Transfer Dynamics in Biomaterial Systems. Springer Series in Chemical Physics. 93: 474-474.

Caballero-George, C., Vanderheyden, P., Solis, P., Gupta, M., Pieters, L., Vauquelin, G., and Vlietinck, A. 2003. *In vitro* Effect of Sanguinarine Alkaloid on Binding of [^{3}H]Candesartan to the Human Angiotensin AT_1 Receptor. European Journal of Pharmacology. 458: 257-262.

Canals, A., Purciolas, M., Aymami, J., and Coll, M. 2005. The Anticancer Agent Ellipticine Unwinds DNA by Intercalative Binding in an Orientation Parallel to Base Pairs. Acta Crystallographica Section D Biological Crystallography. 61: 1009-1012.

Chambers, C., Hawkins, G., Cramer, C., and Truhlar, D. 1996. Model for aqueous solvation based on class IV atomic charges and first solvation shell effects. J Phys Chem. 100: 16385-16398.

Chaturvedi, M., Kumar, A., Darnay, B., Chainy, G., Agarwal, S., and Aggarwal, B. 1997. Sanguinarine (Pseudochelerythrine) Is a Potent Inhibitor of NF-κB Activation, IκBα Phosphorylation, and Degradation. The Journal of Biological Chemistry. 272: 30129-30134.

Choi, Y., Choi, W., Hong, S., Kim, S., Kim, G., Lee, W., and Yoo, Y. 2009. Anti-invasive Activity of Sanguinarine through Modulation of Tight Junctions and Matrix Metalloproteinases Activities in MDA-MB-231 Human Breast Carcinoma Cells. Chemico-Biological Interactions. 179: 185-191.

Dabkowska, I., Gonzalez, H., Jurecka, P., and Hobza, P. 2005. Stabilization Energies of the Hydrogen Bonded and Stacked Structures of the Nucleic Acid Base Pairs in the Crystal Geometries of CG, AT, and AC DNA Steps and in the NMR Geometry of the 5'-d(GCGAAGC)-3' Hairpin: Complete Basis Set Calculations at the MP2 and CCSD(T) Levels. Journal of Physical Chemistry A. 109: 1131-1136.

Dexheimer, T., and Pommier, Y. 2008. DNA Cleavage Assay for the Identification of Topoisomerase I Inhibitors. Nature Protocols. 3: 1736-1750.

Dkhissi, A., and Blossey, R. 2007. Performance of DFT/MPWB1K for Stacking and H-Bonding Interactions. Chemical Physics Letters. 439: 35-39.

Evstigneev, M., Lantushenko, A., Evstigneev, V., Mykhina, Y., and Davies, D. 2008. Quantitation of the Molecular Mechanisms of Biological Synergism in a Mixture of DNA-acting Aromatic Drugs. Biophysical Chemistry. 132: 148-158.

Ferlin, M., Marzano, C., Gandin, V., Dall'Acqua, S., and Via, L. 2009. DNA Binding Ellipticine Analogues: Synthesis, Biological Evaluation, and Structure-Activity Relationships. ChemMedChem. 4: 363-377.

Fiethen, A., Jansen, G., Hesselmann, A., and Schutz, M. 2008. Stacking Energies for Average for B-DNA Structures from the Combined Density Functional Theory and Symmetry-Adapted Perturbation Theory Approach. Journal of the American Chemical Society. 130: 1802-1803.

Giri, P., and Kumar, G. 2008. Self-structure Induction in Single Stranded Poly(A) by Small Molecules: Studies on DNA Intercalators, Partial Intercalators and Groove Binding Molecules. Archives of Biochemistry and Biophysics. 474: 183-192.

Graf, T., Levine, K., Andrews, M., Perlmutter, J., Nielsen, S., Davis, J., Wani, M., and Oberlies, N. 2007. Variability in the Yield of Benzophenanthridine Alkaloids in Wildcrafted vs Cultivated Bloodroot (*Sanguinaria canadensis* L.). Journal of Agricultural and Food Chemistry. 55: 1205-1211.

Grycova, L., Dostal, J., and Marek, R. 2007. Quaternary Protoberberine Alkaloids. Phytochemistry. 68: 150-175.

Ho, Y., Yang, J., Lu, C., Chiang, J., Li, T., Lin, J., Lai, K., Liao, C., Lin, J., and Chung, J. 2009. Berberine Inhibits Human Tongue Squamous Carcinoma Cancer Tumor Growth in a Murine Xenograft Model. Phytomedicine. 16: 887-890.

Hobza, P., and Sponer, J. 2002. Toward True DNA Base-Stacking Energies: MP2, CCSD(T), and Complete Basis Set Calculations. Journal of the American Chemical Society. 124: 11802-11808.

Imanshahidi, M., and Hosseinzadeh, H. 2008. Pharmacological and Therapeutic Effects of *Berberis vulgaris* and its Active Constituent, Berberine. Phytotherapy Research. 22: 999-1012.

Jang, B., Park, J., Song, D., Baek, W., Yoo, S., Jung, K., Park, G., Lee, T., and Suh, S. 2009. Sanguinarine Induces Apoptosis in A549 Human Lung Cancer Cells Primarily via Cellular Glutathione Depletion. Toxicology in Vitro. 23: 281-287.

Jantova, S., Cipak, L., Cernakova, M., and Kostalova, D. 2003. Effect of Berberine on Proliferation, Cell Cycle and Apoptosis in HeLa and L1210 Cells. Journal of Pharmacy and Pharmacology. 55: 1143-1149.

Jemal, A., Siegel, R., Xu, J., and Ward, E. 2010. Cancer Statistics, 2010. CA: A Cancer Journal for Clinicians. 60: 277-300.

Lee, W., Kim, J., Kang, J., Oh, W., Jung, J., Kim, Y., Jung, H., Choi, J., and Lee, S. 2010. Palmatine Attenuates D-galactosamine/lipopolysaccharide-induced Fulminant Hepatic Failure in Mice. Food and Chemical Toxicology. 48: 222-228.

Le Deley, M., Suzan, F., Cutuli, B., Delaloge, S., Shamsaldin, A., Linassier, C., Clisant, S., de Vathaire, F., Fenaux, P., and Hill, C. 2007. Anthracyclines, Mitoxantrone, Radiotherapy, and Granulocyte Colony-Stimulating Factor: Risk Factors for Leukemia and Myelodysplastic Syndrome after Breast Cancer. Journal of Clinical Oncology. 25: 292- 300.

Letasiova, S., Jantova, S., Miko, M., Ovadekova, R., and Horvathova, M. 2006. Effect of Berberine on Proliferation, Biosynthesis of Macromolecules, Cell Cycle and Induction of Intercalation with DNA, dsDNA Damage and Apoptosis in Ehrlich ascites Carcinoma Cells. Journal of Pharmacy and Pharmacology. 58: 263-270.

Liu, Z., Liu, Q., Xu, B., Wu, J., Guo, C., Zhu, F., Yang, Q., Gao, G., Gong, Y., and Shao, C. 2009. Berberine Induces p53-dependent Cell Cycle Arrest and Apoptosis of Human Osteosarcoma Cells by Inflicting DNA Damage. Mutation Research. 662: 75-83.

Mackraj, I., Govender, T., and Gathiram, P. 2008. Sanguinarine. Cardiovascular Therapeutics. 26: 75-83.

Maiti, M., and Kumar, G. 2010. Polymorphic Nucleic Acid Binding of Bioactive Isoquinoline Alkaloids and Their Role in Cancer. Journal of Nucleic Acids. 2010: 1-23.

Matkar, S., Wrischnik, L., and Blumberg, U. 2008. Production of Hydrogen Peroxide and Redox Cycling can Explain how Sanguinarine and Chelerythrine Induce Rapid Apoptosis. Archives of Biochemistry and Biophysics. 477: 43-52.

Matkar, S., Wrischnik, L., and Hellman-Blumberg, U. 2008. Sanguinarine Causes DNA Damage and p53-independent Cell Death in Human Colon Cancer Cell Lines. Chemico-Biological Interactions. 172: 63-71.

Mukherjee, A., Lavery, R., Bagchi, B., and Hynes, J. 2008. Journal of the American Chemical Society 130: 9747-9755.

Nafisi, S., Manouchehri, F., Riahi, H., and Varavipour, M. 2008. Structural Features of DNA Interaction with Caffeine and Theophylline. Journal of Molecular Structure. 875: 392-399.

Nitiss, J. 2009. Targeting DNA Topoisomerase II in Cancer Chemotherapy. Nature Reviews Cancer. 9: 338-350.

Patro, B., Maity, B., and Chattopadhyay, S. 2010. Topoisomerase Inhibitor Coralyne Photosensitizes DNA, Leading to Elicitation of Chk2-dependent S-phase Checkpoint and p53-independent Apoptosis in Cancer Cells. Antioxidants and Redox Signaling. 12: 945-960.

Piosik, J., Zdunek, M., and Kapuscinski, J. 2002. The Modulation by Xanthines of the DNA-Damaging Effect of Polycyclic Aromatic Agents. Part II. The Stacking Complexes of Caffeine with Doxorubicin and Mitoxantrone. Biochemical Pharmacology. 63: 635-646.

Poljakova, J., Frei, E., Gomez, J., Aimova, D., Eckschlager, T., Hrabeta, J., and Stiborova, M. 2007. DNA Adduct Formation by the Anticancer Drug Ellipticine in Human Leukemia HL-60 and CCRF-CEM Cells. Cancer Letters. 252: 270-279.

Punchihewa, C., Carver, M., and Yang, D. 2009. DNA Sequence Selectivity of Human Topoisomerase I-mediated DNA Cleavage Induced by Camptothecin. Protein Science. 18: 1326-1331.

Reed, L., and Muench, H. 1938. A simple method of estimating fifty percent endpoints. The American Journal of Hygiene. 27: 493–497.

Rozmus, Glenn. 2005. *Ab Initio* Energy Calculations and Frontier Orbital Evaluation of Rhodomyrtoxin B with the Guanine-Cytosine DNA Base Pair. A Dissertation.

Sabisz, M., and Skladanowski, A. 2008. Modulation of Cellular Response to Anticancer Treatment by Caffeine: Inhibition of Cell Cycle Checkpoints, DNA Repair and More. Current Pharmaceutical Biotechnology. 9: 325-336.

Sanchez-Arreola, E., Hernandez-Molina, L., Sanchez-Salas, J., and Martinez-Espino, G. 2006. Alkaloids from *Bocconia frutescens* and Biological Activity of their Extracts. Pharmaceutical Biology. 44: 540-543.

Saturnino, C., Buonerba, M., Boatto, G., Pascale, M., Moltedo, O., De Napoli, L., Montesarchio, D., Lancelot, J., and Caprariis, P. 2003. Synthesis and Preliminary Biological Evaluation of a New Pyridocarbazole Derivative Covalently Linked to a Thymidine Nucleoside as a Potential Targeted Antitumoral Agent. Chemical and Pharmaceutical Bulletin. 51: 971-974.

Setzer, M. 2005. Drugs from the Cloudforest: The Phytomedicinal Potential of Tropical Cloudforest Plants from Monteverde, Costa Rica. A Thesis.

Shewach, D. 2009. Introduction to Cancer Chemotherapeutics. Chemical Reviews. 109: 2859-2861.

Sinnokrot, M., and Sherrill, C. 2006. High-Accuracy Quantum Mechanical Studies of π–π Interactions in Benzene Dimers. Journal of Physical Chemistry A. 110: 10656-10668

SPARTAN '08 for Windows; 2008. Wavefunction, Inc.: Irvine, CA, USA.

Su, Y., and Wei, X. Interaction of Chelerythrine Chloride in Acid Buffer with Calf-thymus DNA. 2006. Chinese Chemical Letters. 17: 691-694.

Swart, M., van der Wijst, T., Guerra, C., and Bickelhaupt, F. 2007. π–π Stacking Tackled with Density Functional Theory. Journal of Molecular Modeling. 13: 1245-1257.

Trnkova, L., Stiborova, M., Huska, D., Adam, V., Kizek, R., Eckshlager, T., and Hubalek, J. 2009. Electrochemical Biosensor for Investigation of Anticancer Drugs Interactions (Doxorubicin and Ellipticine) with DNA. Sensors, IEEE. 2009: 1200-1203.

Veldman, J., Murray, K., Hull, A., Garcia-C, J., Mungall, W., Rotman, G., Plosz, M., and McNamara, L. 2007. Chemical Defense and the Persistence of Pioneer Plant Seeds in the Soil of a Tropical Cloud Forest. Biotropica. 39: 87-93.

Vrba, J., Dolezel, P., Vicar, J., and Ulrichova, J. 2009. Cytotoxic Activity of Sanguinarine and Dihydrosanguinarine in human Promyelocytic Leukemia HL-60 cells. Toxicology in Vitro. 23: 580-588.

Wheeler, S., McNeil, A., Muller, P., Swager, T., and Houk, K. 2010. Probing Substituent Effects in Aryl-Aryl Interactions Using Stereoselective Diels-Alder Cycloadditions. Journal of the American Chemical Society. 132: 3304-3311.

Wong, B. 2008. Noncovalent Interactions in Supramolecular Complexes: A Study on Corannulene and the Double Concave Buckycatcher. Journal of Computational Chemistry. 30: 51-56.

Xia, A., Wu, H., Li, S., Zhu, S., Zhang, Y., Han, Q., and Yu, R. 2007. Study of the Interactions of Berberine and Daunorubicin with DNA Using Alternating Penalty Trilinear Decomposition Algorithm Combined with Excitation-Emission Matrix Fluorescence Data. Talanta. 73: 606-612.

Ying, V., Haverstick, K., Page, R., and Saltzman, W. 2007. Efficacy of Camptothecin and Polymer-Conjugated Camptothecin in Tumor Spheroids and Solid Tumors. Journal of Biomaterials Science, Polymer Edition. 18: 1283-1299.

Zar, J. 1996. Biostatistical Analysis. Prentice Hall, Upper Saddle River Road, New Jersey. 3: 123-128.

Zhao, Y., and Truhlar, D. 2006. A New Local Density Functional for Main-Group Thermochemistry, Transition Metal Bonding, Thermochemical Kinetics, and Non-covalent Interactions. The Journal of Chemical Physics. 125: 1-18.

Zhao, Y., and Truhlar, D. 2008. The M06 Suite of Density Functionals for Main Group Thermochemistry, Thermochemical Kinetics, Noncovalent Interactions, Excited States and Transition Elements: Two New Functionals and Systematic Testing of Four M06-class Functionals and 12 Other Functionals. Theoretical Chemistry Accounts: Theory, Computation, and Modeling. 120: 215-241.